

Final Report

Mechanisms of Particulate Toxicity: Effects on the Respiratory System

ARB Contract number: 96-310

Principal Investigator:

Kent E. Pinkerton, Ph.D.
Professor in Residence
Department of Anatomy, Physiology, and Cell Biology
School of Veterinary Medicine

Co-Investigators:

Alan R. Buckpitt, Ph.D.

Dallas M. Hyde, Ph.D.

Charles G. Plopper, Ph.D.

Prepared by:

Institute of Toxicology and Environmental Health,
Department of Anatomy, Physiology, and Cell Biology
Department of Molecular Biosciences,
California Regional Primate Research Center,
School of Veterinary Medicine,
University of California
Davis, CA 95616
December 2000

Prepared for the California Air Resources Board and the California Environmental Protection Agency.

Disclaimer

The statements and conclusions in this Report are those of the contractor and not necessarily those of the California Air Resources Board. The mention of commercial products, their source, or their use in connection with material reported herein is not to be construed as actual or implied endorsement of such products.

Acknowledgements

This Report was submitted in fulfillment of 96-310 Mechanisms of Particulate Toxicity: Effects on the Respiratory System by the Regents of the University of California under the sponsorship of the California Air Resources Board. Work was completed as of September 26, 2000.

Table of Contents

Title Page	i
Disclaimer	ii
Acknowledgements	iii
Table of Contents	iv
List of Figures	v
List of Tables	x
Abstract	xii
Executive summary	xiii
Body of report	
Introduction	1
Study Design	2
Measures of Particle-induced Respiratory Effects: A	5
Materials and Methods	6
Conditions of Exposure	
Measure 1: Cell Permeability	10
Measure 2: Measurement of Glutathione	10
Measure 3: Cell Proliferation/Morphometry	11
Measure 4: Particle Deposition/Fate	14
Measure 5: Bronchoalveolar Lavage	15
Results	16
Exposure Assessment	
Measure 1: Cell Permeability	31
Measure 2: GSH in Microdissected Airways	33
Measure 3: Cell Proliferation/Morphometry	43
Measure 4: Particle Deposition/Fate	55
Measure 5: Bronchoalveolar Lavage	67
Discussion	72
Summary and Conclusions	79
Recommendations	81
References	83
Glossary of Terms, Abbreviations, and Symbols	87
Appendix A	89
Appendix B	111

List of Figures

- Figure 1** For each PM exposure, mean total mass concentration compared to mean NH_4NO_3 concentration added to mean C concentration on the abscissa. The comparison is based on three of the aerosol analysis methods used during the exposures, gravimetry, ion chromatography and selective thermal oxidation (Fung, 1990).
- Figure 2** On top is an anion chromatogram (Model DX-120 ion chromatograph with PeakNet software, Dionex Corp., Sunnyvale, CA) of a high purity standard nitrate solution (EM Industries, Inc., Gibbstown, NJ). The bottom anion chromatogram is from a sample eluted from aerosol collected on a Supor[®]-800 filter (47 mm diameter, Pall Gelman Sciences, Ann Arbor, MI) from the chamber containing PM during a low concentration exposure. Conductivity in microsiemens is on the ordinate, and retention time is on the abscissa of the chromatograms. The chromatograms are nearly identical, indicating that the anionic species present in the PM aerosol was nitrate of high purity.
- Figure 3** PM samples for carbon analysis collected simultaneously on quartz fiber filters (QM-A, 47 mm diameter, Whatman, Inc., Clifton, NJ) from each of the two chambers containing the aerosol. Pairs for high, intermediate and low concentrations are from top to bottom with the carbon mass concentration handwritten on each filter container. Disks 3 mm in diameter were punched out of each filter for carbon analysis (Fung, 1990). Holes spanning the edge of a deposit were made to clean the punch mechanism before sample disks were removed.
- Figure 4** The top photograph is a light micrograph of the PM aerosol collected on a 0.2 μm pore size Nuclepore[®] filter (Whatman, Inc., Clifton, NJ). The bottom photograph is a scanning electron micrograph of a similar sample that was sputter coated with gold for stability in the electron beam.
- Figure 5** Confocal fluorescent laser scanning microscopy of the lung airways in an adult rat exposed to filtered air or to ammonium nitrate ($147 \pm 9 \mu\text{g}/\text{m}^3$) and carbon ($205 \pm 29 \mu\text{g}/\text{m}^3$). Epithelial cell permeability, identified as EtD-1 positive cells (red), line the surfaces of the airways at the level of the airway bifurcation. Few EtD-1 positive cells are present in the airway of a rat exposed to filtered air for three days. In contrast, the airway bifurcation contains numerous EtD-1 positive cells following PM exposure for three days.
- Figure 6** Reduced glutathione levels in dissected airways of male adult F344 rats exposed to filtered air, ozone, particles or particles plus ozone once for 6 hrs. Particle exposure conditions were targeted for the highest concentration ranges (ammonium nitrate $300 \mu\text{g}/\text{m}^3$; carbon $200 \mu\text{g}/\text{m}^3$). Values are the mean \pm SD for the following number of animals: filtered air (6), ozone (4), particles (6) and particles plus ozone (9).

- Figure 7** Glutathione levels in dissected airways of adult male F344 rats exposed for 6 hrs at the intermediate target particle dose (ammonium nitrate, 150 $\mu\text{g}/\text{m}^3$; carbon $\mu\text{g}/\text{m}^3$). Data are the mean of measurements on two animals per group.
- Figure 8** Glutathione levels in airways from adult male F344rats exposed to filtered air, ozone, particles or particles plus ozone. The intermediate target concentrations of particles were set at 150 $\mu\text{g}/\text{m}^3$ for ammonium nitrate and 100 $\mu\text{g}/\text{m}^3$ for carbon. Exposures were for 6 hr. All animals were pretreated with BSO prior to exposure. Values are the mean \pm SD for n=4 in each group.
- Figure 9** Glutathione levels in airways from adult male Sprague Dawley rats exposed to filtered air, ozone, particles or particles plus ozone. Exposures were 6 hr at the intermediate particle exposure level for 3 days with ammonium nitrate at 150 $\mu\text{g}/\text{m}^3$ and carbon at 100 $\mu\text{g}/\text{m}^3$. Values are the mean \pm SD for n=4 in each group.
- Figure 10** Glutathione levels in airways from adult male F344 rats exposed to filtered air or particles plus ozone. Particle concentrations were set at the intermediate range of 150 $\mu\text{g}/\text{m}^3$ for ammonium nitrate and 100 $\mu\text{g}/\text{m}^3$ for carbon. Values are the mean \pm SD for n=4 in each group
- Figure 11** Glutathione levels in airways from senescent 18 month old male F344 rats exposed to filtered air, to ozone, to particulates, or to particulates plus ozone for 3 days at intermediate particulate levels. These target concentrations were set at 150 $\mu\text{g}/\text{m}^3$ for ammonium nitrate and 100 $\mu\text{g}/\text{m}^3$ for carbon. ^aValues are the mean \pm SD for four animals in each group with the exception minor daughter and distal bronchiole segments of the particulate group. In these two instances, means and standard deviations exclude results of a single animal, which yielded values 183 and 93 in minor daughter and distal bronchiole, respectively. Protein values in these two analyses were abnormally low and could not be rerun.
- Figure 12** Glutathione levels in tracheobronchial airways of male and female neonatal F344 rats exposed from 3 days to filtered air, particles, ozone or a combination of filtered air and particles. Particulate concentrations were at the intermediate target concentrations of 150 $\mu\text{g}/\text{m}^3$ of ammonium nitrate and 100 $\mu\text{g}/\text{m}^3$ of carbon. Values are the mean \pm SD for n=4.
- Figure 13** Glutathione levels in airways of male and female neonatal F344 rats exposed for 3 days to atmospheres containing high levels of particulate matter (target concentrations: ammonium nitrate, 300 $\mu\text{g}/\text{m}^3$; carbon, 200 $\mu\text{g}/\text{m}^3$). Values are the mean \pm SD for n=5.
- Figure 14** Glutathione levels in lung subcompartments of male and female neonatal F344 rats exposed to atmospheres containing low levels of particles (target concentrations: ammonium nitrate, 75 $\mu\text{g}/\text{m}^3$; carbon, 50 $\mu\text{g}/\text{m}^3$). Values are the mean \pm SD for 6 animals.

- Figure 15** Low Concentration ($77 \mu\text{g}/\text{m}^3 \text{NH}_4\text{NO}_3$, $61 \mu\text{g}/\text{m}^3 \text{C}$) F344 Adult Male Rats Exposed 6 Hours for 1 Day
- Figure 16** Intermediate Concentration ($154 \mu\text{g}/\text{m}^3 \text{NH}_4\text{NO}_3$, $267 \mu\text{g}/\text{m}^3 \text{C}$) F344 Adult Male Rats Exposed 6 Hours for 1 Day.
- Figure 17** High Concentration ($310 \mu\text{g}/\text{m}^3 \text{NH}_4\text{NO}_3$, $230 \mu\text{g}/\text{m}^3 \text{C}$) F344 Adult Male Rats Exposed 6 Hours for 1 Day
- Figure 18** Intermediate Concentration ($166 \mu\text{g}/\text{m}^3 \text{NH}_4\text{NO}_3$, $116 \mu\text{g}/\text{m}^3 \text{C}$) F344 Adult Male Rats Exposed 6 Hours/Day for 3 Days
- Figure 19** Bar graph of BrdU labeling index (the percent of total cells labeled) for epithelial cells on airway bifurcations of adult male SD rats. Epithelial cells on the bifurcation were defined as cells within $200 \mu\text{m}$ of the apex of each bifurcation. For each animal, 3 to 5 bifurcations were counted for this analysis. The groups are FA (filtered air), O_3 (ozone), particulate matter (PM) and particulate matter plus ozone (PM + O_3). An asterisk denotes $p < 0.05$ compared with the FA group. The number of animals per exposure group is 6. All values are mean \pm SEM.
- Figure 20** Bar graph of BrdU labeling index for interstitial cells underlying airway bifurcations of adult male SD rats. Interstitial cells within airway bifurcations were defined as all cells underlying epithelial cells within $200 \mu\text{m}$ of the apex of each bifurcation. An average of 3 to 5 bifurcations was counted per animal for this analysis. The number of animals per exposure group is 6. All values are mean \pm SEM.
- Figure 21** Light micrographs of airway bifurcations from the lungs of adult male SD rats exposed to PM (A) or PM plus ozone (B). A number of epithelial cells as well as interstitial cells underlying the airway bifurcation are positive for the uptake of BrdU (A). Labeling of epithelial and interstitial cells with BrdU is evident as well as the labeling of a single endothelial cell lining a blood vessel (B).
- Figure 22** Bar graph of BrdU labeling index for epithelial cells along the walls of the airways, but not on bifurcation ridges of adult male SD rats. No significant differences in the labeling index were noted between groups. The number of animals per exposure group is 6. All values are mean \pm SEM.
- Figure 23** Bar graph of BrdU labeling index for epithelial cells lining terminal bronchioles of adult male SD rats. The groups are FA (filtered air), O_3 (ozone), particulate matter (PM) and particulate matter plus ozone (PM + O_3). An asterisk denotes $p < 0.05$ compared with the FA group. The number of animals per exposure group is 6. All values are mean \pm SEM.

- Figure 24** Bar graph of BrdU labeling index for interstitial cells within the wall of terminal bronchioles of adult male SD rats. The groups are FA (filtered air), O₃ (ozone), particulate matter (PM) and particulate matter plus ozone (PM +O₃). No significant differences were noted between groups. The number of animals per exposure group is 6. All values are mean \pm SEM.
- Figure 25** Bar graph of BrdU labeling index for cells of the proximal alveolar region in adult male SD rats. This region is defined as all parenchymal tissue within 400 μ m of the bronchiole-alveolar duct junction. Cell counting is for all cell types found within the region until a total of 1,000 cells is counted per animal. The number of animals per exposure group is 6. All values are mean \pm SEM.
- Figure 26** Intermediate Concentration (154 μ g/m³ NH₄NO₃, 116 μ g/m³ C) F344 Senescent Rats Exposed 6 Hours/Day for 3 Days.
- Figure 27** Low Concentration (76 μ g/m³ NH₄NO₃, 56 μ g/m³ C) F344 Rat Neonates Exposed 6 Hours/Day for 3 Days First & Third Weeks of Life.
- Figure 28** Intermediate Concentration (143 μ g/m³ NH₄NO₃, 119 μ g/m³ C) F344 Rat Neonates Exposed 6 Hours/Day for 3 Days First & Third Weeks of Life
- Figure 29** High Concentration (288 μ g/m³ NH₄NO₃, 243 μ g/m³ C) F344 Rat Neonates Exposed 6 Hours/Day for 3 Days First & Third Weeks of Life.
- Figure 30** Microdissected airway of the right infracardiac lobe.
- Figure 31** 0.5 μ m yellow-green fluorescent microspheres litter the airway surface.
- Figure 32** High magnification view of the airway bifurcation shown in Figure 31.
- Figure 33** 0.5 μ m yellow-green microspheres litter the bifurcation point of the airway.
- Figure 34** Diagram of airway locations within the right caudal lung lobe for examination of microsphere distribution.
- Figure 35** Images of the microdissected airway from two animals exposed to filtered air only followed by exposure to fluorescent. (A) shows the distribution pattern on bifurcation D immediately after exposure and (B) shows the same bifurcation 7 days after exposure.
- Figure 36** Microsphere distribution in the lungs of filtered air control animals. (A) Distribution of microspheres along the airways with increasing post exposure time. (B) Distribution of microspheres on bifurcations in the caudal lobe with increasing post exposure time. The overall reduction of microsphere abundance on airway bifurcations was significantly reduced with increasing post exposure time in the lungs of filtered air control animals.

- Figure 37** Fluorescent microspheres are preferentially deposited on airway bifurcations ridges as shown in this microdissected airway image.
- Figure 38** (A) Frequency of microspheres on major and minor daughter airway paths. (B) Frequency of microspheres on major and minor daughter airway paths.
- Figure 39** (A) Frequency of microspheres on axial airway path bifurcations. (B) Frequency of microspheres on axial airway path bifurcations. Microsphere abundance at airway bifurcations over time was significantly reduced in filtered air (FA) control animals, but not in animals previously exposed to PM and ozone.

List of Tables

- Table 1A.** Single 6-hour exposure of adult male Fischer 344 rats using three different target concentrations of ammonium nitrate (NH_4NO_3) and carbon (C).
- Table 1B.** Repeated 6-hour exposure for 3 days of healthy adult male Fischer 344 rats at the intermediate target concentration of ammonium nitrate (NH_4NO_3) and carbon (C).
- Table 2.** Repeated 6-hour exposure for 3 days of adult male Sprague Dawley rats at the Intermediate target concentrations of ammonium nitrate (NH_4NO_3) and carbon (C).
- Table 3.** Repeated 6-hour exposure for 3 days of senescent male Fischer 344 rats at the intermediate target concentration of ammonium nitrate (NH_4NO_3) and carbon (C).
- Table 4.** Repeated 6-hour exposure for 3 days at one week and three weeks of age in neonatal male and female Fischer 344 rats.
- Table 5.** Single 6-hour exposure of adult male Fischer 344 rats using three different target concentrations of ammonium nitrate (NH_4NO_3) and carbon (C).
- Table 6** Repeated 6-hour exposure for 3 days of adult male Sprague Dawley rats at the Intermediate target concentrations of ammonium nitrate (NH_4NO_3) and carbon (C).
- Table 7** Repeated 6-hour exposure for 3 days of healthy adult male Fischer 344 rats at the intermediate target concentration of ammonium nitrate (NH_4NO_3) and carbon (C).
- Table 8** Repeated 6-hour exposure for 3 days of senescent male Fischer 344 rats at the intermediate target concentration of ammonium nitrate (NH_4NO_3) and carbon (C).
- Table 9** Repeated 6-hour exposure for 3 days of young (neonatal) male and female Fischer 344 rats at three different target concentrations of ammonium nitrate (NH_4NO_3) and carbon (C).
- Table 10** Comparison of relative severity of injury following exposure to particulates, particulates + ozone, ozone alone or filtered air.
F344 Rats Adult, Senescent and Neonate; S-D Rats, Adult
- Table 11** Number of 0.5 μm fluorescent microspheres in the right cranial lobe (millions) of adult male F344 rats following exposure to NH_4NO_3 ($155 \mu\text{g}/\text{m}^3$), carbon ($260 \mu\text{g}/\text{m}^3$) and ozone (0.2 ppm)
- Table 12** Microsphere (1.0 μm diameter) Deposition/Retention/Clearance in F344 Senescent Male Rats following exposure to an intermediate level of NH_4NO_3 and carbon.

Table 13	Total Number of Microspheres in thousands from neonatal F344 rats
Table 14	Number of Microspheres in thousands per ml fixed tissue volume from neonatal F344 rats
Table 15	Bronchoalveolar lavage characteristics of recovered cells and fluids in male adult male Sprague Dawley Rats.
Table 16	Comparisons of Lung Lavage Cell Numbers, Viabilities, Differentials and Protein (“Intermediate” PM exposure, F344 Adult male Rats)
Table 17	Comparisons of Lung Lavage Cell Numbers, Viabilities, Differentials and Protein (“Intermediate” PM exposure, F344 Senescent male Rats)
Table 18	Bronchoalveolar Lavage: Male and Female F344 Rats Neonates Exposed 6 Hours/Day for 3 Days during the First & Third Weeks of Life to a Low PM Concentration (76 $\mu\text{g}/\text{m}^3$ NH_4NO_3 , 56 $\mu\text{g}/\text{m}^3$ C)
Table 19	Bronchoalveolar Lavage: Male and Female F344 Rats Neonates Exposed 6 Hours/Day for 3 Days during the First & Third Weeks of Life to an Intermediate PM Concentration (143 $\mu\text{g}/\text{m}^3$ NH_4NO_3 , 119 $\mu\text{g}/\text{m}^3$ C)
Table 20	Bronchoalveolar Lavage: Male and Female F344 Rats Neonates Exposed 6 Hours/Day for 3 Days during the First & Third Weeks of Life to a High PM Concentration (288 $\mu\text{g}/\text{m}^3$ NH_4NO_3 , 243 $\mu\text{g}/\text{m}^3$ C)

Abstract

Ambient exposure to particulate matter (PM) has been associated with a variety of adverse health effects primarily involving the cardiopulmonary system. However, the biological mechanisms to explain how exposure to PM exacerbates or directly causes adverse cardiopulmonary effects are unknown. This study was designed to determine if exposure to ammonium nitrate (NH_4NO_3) and carbon (C), two common components found in California PM, could be used to measure adverse biological changes in the respiratory tract of rats. Three different concentrations of NH_4NO_3 (300, 150 and $75 \mu\text{g}/\text{m}^3$) and C (200, 100 and $50 \mu\text{g}/\text{m}^3$) were used. Simultaneous exposure to NH_4NO_3 and C was done in the presence or absence of 0.2 ppm ozone for all experiments. Initial studies used a single 6-hour exposure period. Subsequent studies used a repeated exposure of 6 hours per day for 3 consecutive days. Adult male (9 week old), senescent male (22-24 months old), and young male and female (1 to 3 week old) Fischer 344 (F344) rats were used to determine PM exposure effects on cell permeability, glutathione levels and cell proliferation rates within the respiratory tract. Bronchoalveolar lavage (BAL) and fluorescent microspheres were also used to define particle effects and patterns of particle deposition in the lungs respectively. Adult male Sprague Dawley (SD) rats were also used in limited studies to determine potential strain differences as well as site-specific responses of the respiratory tract to particle exposure. F344 rats demonstrated a significant increase in cell proliferation of airway interstitial cells at the intermediate concentration of NH_4NO_3 and C in adult following a single day of exposure, but no changes in cellular permeability or glutathione levels. Repeated exposure to particles for 3 consecutive days in adult F344 rats did not demonstrate significant effects in any biological parameter measured in the respiratory tract. In contrast, male SD rats exposed to particles for 3 days demonstrated a significant increase in the number of cells recovered by BAL. In addition, the cell proliferation rates in SD rats for both epithelial and interstitial cells at airway bifurcations were significantly increased following 3 days of exposure to NH_4NO_3 and C. Significant particle and ozone effects were also noted for the cell proliferation rates within the proximal alveolar regions of these same adult male SD rats. These differences between rats could be strain dependent or due to differences in the target particle concentrations achieved in these experiments. Further studies in senescent F344 rats using a 3-day exposure regimen demonstrated a significant increase in BAL cell number recovered from the lungs, but no other significant changes in the respiratory tract. In young male and female F344 rats exposed to all three concentrations of particles, only the highest concentration of NH_4NO_3 and C was associated with significant elevations in the rate epithelial and interstitial cell proliferation within the terminal bronchioles following combined exposure to particles and 0.20 ppm ozone. These studies provide evidence for limited, but significant PM effects in the respiratory tract of healthy rats of all ages following short-term exposure to NH_4NO_3 and C. These findings further support the need for future studies to define the precise mechanisms of PM-induced lung injury and its potential interaction with ozone, even in healthy individuals.

Executive summary

Background

Health effects seen with ambient particle exposure continue to be a concern for numerous stakeholders including scientists, health experts, regulators, industry, and the general public. Epidemiological studies have consistently demonstrated adverse health effects to occur with exposure to airborne particle concentrations below the current national and international air quality standards. Sensitive individuals appear to be children, the elderly and those with pre-existing cardiopulmonary compromise. However, the precise mechanisms by which these individuals are at greater risk for morbidity and mortality are unclear. The purpose of this study was to examine the effects of acute exposure to NH_4NO_3 and carbon, components present in the particulate matter of California, in the lungs of young, adult, and senescent rats. We hypothesized that epithelial cells could serve as a direct measure of particle toxicity since they are the primary cells of the respiratory tract to exhibit adverse consequences of exposure to inhaled particles and gases. The response of epithelial cells of the airway bronchial tree and alveoli could function as a sensitive guide to identify patterns of injury due to particle deposition and/or particle-mediated effects observed within anatomically distinct regions of the lungs.

Methods

Young, adult, and old Fischer 344 rats were exposed to three different concentrations of NH_4NO_3 and carbon in the presence or absence of ozone. These three particle concentrations were designated as high ($300 \mu\text{g}/\text{m}^3$ NH_4NO_3 ; $200 \mu\text{g}/\text{m}^3$ carbon), intermediate ($150 \mu\text{g}/\text{m}^3$ NH_4NO_3 ; $100 \mu\text{g}/\text{m}^3$ carbon), and low ($75 \mu\text{g}/\text{m}^3$ NH_4NO_3 ; $50 \mu\text{g}/\text{m}^3$ carbon). Both genders (male and female) were examined in neonatal animals, while only male rats were examined in adult and senescent animals. Adult male Sprague Dawley rats were also examined in a limited series of experiments to determine the response of particulate exposure in a second strain of rats. Initial exposure to NH_4NO_3 and carbon was set for a single 6-hour exposure to determine effects on the respiratory system. Subsequent exposures were increased to 6 hours/day for 3 consecutive days. The desired target concentrations of NH_4NO_3 and ozone were achieved throughout the studies. However, problems occurred with carbon content and analysis for a number of the early studies with target levels greatly exceeded. Later experiments used an improved carbon analysis to assist in making the appropriate aerosol adjustments to come closer to the target concentrations of carbon intended.

Novel measures of cell permeability, glutathione, and cell proliferation were applied within site-specific regions of the respiratory tract. Bronchoalveolar lavage was used to determine changes in macrophage number and function. Particle deposition studies were used to better understand the relationship between particle deposition and biological responses in the respiratory tract of neonatal, adult and senescent rats.

Results

Single day exposure to NH_4NO_3 and carbon in adult male Fischer 344 rats was noted to significantly increase interstitial cell proliferation in the terminal bronchioles of the lungs in the

presence or absence of ozone. Only the intermediate concentration (154 $\mu\text{g}/\text{m}^3$ NH_4NO_3 and 267 $\mu\text{g}/\text{m}^3$ carbon) was associated with this effect, while lower (77 $\mu\text{g}/\text{m}^3$ NH_4NO_3 and 62 $\mu\text{g}/\text{m}^3$) or higher (310 $\mu\text{g}/\text{m}^3$ NH_4NO_3 and 236 $\mu\text{g}/\text{m}^3$ carbon) concentrations produced no effect. These studies were repeated in male adult (9 week old) SD rats using an exposure regimen of 6 hours/day for 3 consecutive days at the intermediate concentration of PM (140 $\mu\text{g}/\text{m}^3$ NH_4NO_3 and 195 $\mu\text{g}/\text{m}^3$ carbon). Lung cell effects were noted in the form of significant increases in cell proliferation at airway bifurcations and within the centriacinar regions following exposure to PM or PM plus ozone. Affected cells included both epithelial and interstitial cells at airway branch points. No significant differences in cell permeability or glutathione levels were noted following exposure, however, the number of alveolar macrophages recovered from the lungs following bronchoalveolar lavage was significantly increased in animals exposed to PM or PM plus ozone.

Further studies in Fischer 344 rats also used a repeated 3-day exposure regimen to expose male adult (9 week) and senescent (22 month) rats to intermediate target concentrations of PM (166 $\mu\text{g}/\text{m}^3$ NH_4NO_3 and 117 $\mu\text{g}/\text{m}^3$ carbon – adult rats; 154 $\mu\text{g}/\text{m}^3$ NH_4NO_3 and 116 $\mu\text{g}/\text{m}^3$ carbon – senescent rats). The effects of exposure to PM demonstrated no significant changes in cell permeability, glutathione levels, or rates of cell proliferation at bronchial bifurcations, terminal bronchioles or alveolar ducts for adult or senescent animals. This difference in effect in F344 rats compared with SD rats could be due to strain differences in sensitivity and/or due to the lower concentration of carbon attained during the 3-day exposure period. However, in the lungs of senescent rats the number of cells recovered following bronchoalveolar lavage was significantly increased following exposure to PM, a finding similar to that found in adult SD rats.

The final series of experiments conducted in male and female neonatal Fischer 344 rats examined the sequential effects of repeated 3-day exposure to PM following the first and third weeks of life at low (76 $\mu\text{g}/\text{m}^3$ NH_4NO_3 , 56 $\mu\text{g}/\text{m}^3$ carbon), intermediate (143 $\mu\text{g}/\text{m}^3$ NH_4NO_3 , 119 $\mu\text{g}/\text{m}^3$ carbon), and high (288 $\mu\text{g}/\text{m}^3$ NH_4NO_3 , 243 $\mu\text{g}/\text{m}^3$ carbon) concentrations of PM. This series of experiments demonstrated a significant increase in the proliferation of epithelial cells of the terminal bronchioles following exposure to the highest concentration of PM, alone or in combination with ozone. Repeated exposure to low and intermediate concentrations of PM was not associated with measurable effects in the lungs of neonatal rats.

Conclusions

Single and repeated 3-day exposure to NH_4NO_3 and carbon leads to alterations in the normal homeostasis of the lungs in neonatal, adult and senescent rats. These changes can occur either in the presence or absence of simultaneous exposure to ozone. PM-induced changes appear to be independent of age and dose. For neonatal animals only the highest concentration of particles yielded a significant increase in cell proliferation at the level of the terminal bronchiole. For adult and senescent animals these effects were noted at an intermediate concentration of particles primarily in the form of elevated numbers of cells recovered from the lungs by BAL. A single 6-hour period of exposure to particles in adult F344 rats failed to demonstrate an effect at a higher overall PM concentration (310 $\mu\text{g}/\text{m}^3$ NH_4NO_3 and 236 $\mu\text{g}/\text{m}^3$ carbon), compared with pulmonary effects measured at an overall lower PM concentration (154 $\mu\text{g}/\text{m}^3$ NH_4NO_3 and 267 $\mu\text{g}/\text{m}^3$ carbon). In general, alteration in the normal homeostasis of the lungs following exposure to airborne NH_4NO_3 /carbon particles appears to be triggered in the

healthy rat when the concentration of NH_4NO_3 reaches or exceeds $150 \mu\text{g}/\text{m}^3$ and the carbon concentration reaches or exceeds $195 \mu\text{g}/\text{m}^3$. These studies confirm that Fischer 344 and Sprague Dawley rats can serve as reasonable animal models to investigate the effects of PM on the respiratory tract. Mixtures of NH_4NO_3 and carbon, common components of California PM, evoke cellular changes in the lungs under conditions that could occur under high ambient concentrations in the state of California. These findings confirm that measures of biological effect can be used to determine short-term responses to PM exposure. These findings further support the need for additional studies in toxicology to better define the mechanisms of PM-related health effects. This study also emphasizes the importance of age- and dose-related effects to airborne particles as well as the importance of studying the long-term implications of chronic exposure to PM. The relevance to public health of this research lies in the fact that rats exposed for short-term to the two most common components found in California particulate matter (NH_4NO_3 and carbon) resulted in subtle, but significant respiratory effects in all ages studied. Therefore, it is also possible that human exposure to particles of composed of NH_4NO_3 and carbon could have similar consequences.

Introduction

Health effects seen with ambient particle exposure continue to be a concern for numerous stakeholders including scientists, health experts, regulators, industry, and the general public. This concern is largely founded on epidemiologic evidence which suggests that levels of particle air pollution below the current national and international air quality standards adversely effect morbidity and mortality (Dockery et al., 1993; Pope et al. 1991, 1993; Saldiva et al., 1995). Concerns have focused primarily on the young, the elderly, or those with pre-existing cardiovascular or pulmonary disease (Saldiva et al., 1995). Specific concerns regarding the health effects of particulate matter air pollution cover a variety of respiratory conditions over a wide range of ages. Concerns continue to point to epidemiological studies that suggest PM air pollution increases the number and incidence of asthma attacks, reduces lung function, aggravates bronchitis, increases respiratory infection, and can cause premature death.

The precise mechanisms by which individuals are at greater risk for morbidity and mortality are unclear. A number of questions arise from these epidemiological findings. A basic question yet to be resolved is whether particles at low ambient concentrations elicits direct toxic effects on the cells or organ systems with which they come into contact. If toxic effects do occur, what are the cellular mechanisms leading to injury and damage? If an inflammatory reaction is the basis for particle toxicity, how does exposure to PM initiate and/or aggravate such a response in the lungs? In a similar manner, could PM induce and/or promulgate an allergic response by way of an immune-mediated pathway triggered by the presence of particulate matter coming into contact with cells of the respiratory tract?

Several particle characteristics are also likely to play an important role in lung-induced injury. However, which characteristics are most important have yet to be definitively elucidated. Particle size, particle composition, as well as particle number and concentration are important considerations. Interaction of particles with other airborne pollutants may also be of concern to elicit injury to the lungs and other organ systems.

To address these concerns, we examined the effects of short-term exposure to low concentrations of particulate matter generated experimentally in an exposure chamber. The particulate matter selected for study is NH_4NO_3 and carbon. These are two major constituents of ambient particulate matter found in the state of California (Chow et al., 1992; Chow et al., 1993). NH_4NO_3 and carbon are released into the ambient air during combustion activity processes such as the burning of fossil fuel and vegetative burning agricultural field remnants and unplanned natural events such as forest fires. Although there are many other components of particulate matter that could be considered, these two constituents typically compose more than 50% of the total particulate matter found throughout the state of California. Therefore, both constituents are highly relevant and appropriate for studying health effects following exposure.

The hypothesis to be tested in this study focuses on respiratory tract toxicity of particles. Specifically, we hypothesized that epithelial cells can serve as a direct measure of particle toxicity since they are the primary cells of the respiratory tract to exhibit adverse consequences of exposure to inhaled particles and gases. If correct, the response of epithelial cells of the airway bronchial tree and alveoli could function as a sensitive guide to identify patterns of injury due to

particle deposition and/or particle-mediated effects observed within anatomically distinct regions of the lungs. From these studies we also wished to elucidate potential mechanism(s) by which systemic influences could be elicited from local responses initiated in the respiratory tract following particle exposure.

Over forty different cell types are present in the lungs. The composition of the epithelium of the respiratory tract varies as a function of airway generation and anatomical site and is completely different from epithelial cells of the gas exchange regions of the lungs. Using an aerosol of NH_4NO_3 and carbon in a closely controlled and monitored condition would allow questions of cellular response to be addressed in a systematic manner. The rat was chosen as a model because of the extensive information available for this species.

Clearly defined biological endpoints of cytotoxicity, cellular antioxidant level, cell proliferation, and macrophage function, as well as histopathology, were used at each level of the respiratory tract to establish the toxicity of well-characterized inhaled particles and gases in the lungs. The major cell types and anatomical sites for analysis included the epithelium, interstitium, and alveolar macrophages of the airways and lung parenchyma. Particle size and number are also likely to influence the effects they may produce on the airways and alveoli of the lungs. The combined studies from UC Davis and UC Irvine address these issues.

Study Design

Our study was designed to address the question of particle toxicity in the respiratory tract and whether increasing particle concentration increase the adverse effects of exposure to particles in the respiratory tract of rodents. Young, adult, and old animals would be used to test this hypothesis. Corollary studies at UC Irvine were designed to address the effects of particle size and number on the respiratory tract. NH_4NO_3 and carbon were chosen due to their relevance and prominence in California particulate matter. Studies to monitor particle composition in the state of California have demonstrated NH_4NO_3 and carbon to be two of the primary constituents found in ambient particulate matter, especially in the San Joaquin Valley (Chow et al. 1992; 1993).

A primary goal of the CARB-sponsored research projects at UC Davis and UC Irvine was to examine the potential mechanisms leading to respiratory tract toxicity following short-term exposure to PM. Cell injury, proliferation, inflammation, and toxicity were examined following short-term exposure to PM in young, adult and old rats to define the influence of particle concentration on adverse effects to the respiratory tract. Differences in age were used to explore whether young, adult and old rats respond in a different manner to inhaled particles. Fischer 344 rats were selected to study the issues of age based on the availability of senescent rats through the National Institutes of Aging supplied by Harlen Inc. (Indianapolis, IN). For a limited number of studies, adult male Sprague Dawley rats were used to compare interstrain differences in response to inhaled particles. In all instances, only healthy animals were used rather than attempting to create a compromised condition for the respiratory or cardiovascular systems in these animals. For studies using adult and senescent animals, only male rats were used. In contrast, for neonatal studies, both male and female rat pups were used.

The effects of PM on the respiratory tract were compared to the effects of ozone on the respiratory tract. Health effects associated with exposure to ambient air pollutants may be the result of the combined mixture of particles and gases. Therefore, we wished to examine the effects of PM and ozone alone on the respiratory tract as well as the effects of combined exposure to both pollutants. Experimental conditions to carefully control the inhalation of PM of defined composition in the presence or absence of ozone would allow us to directly examine the relative toxicity of PM to a specific concentration of ozone as well as potential interactive effects of PM with ozone, the major oxidant air pollutant.

For all studies, either Fischer 344 rats or Sprague Dawley rats were exposed to either: (1) filtered air (FA), (2) PM, (3) ozone, or (4) PM plus ozone. Exposure conditions over the period of the study were based on an exposure matrix and research design to identify biological endpoints using particle composition and particle concentration as the primary determinants of effects. Three distinct concentration ranges of NH_4NO_3 and carbon were selected for analysis. The concentrations selected span a range of values that are higher than ambient levels for each particle type encountered in the state of California, but that still fall in a concentration range that could be environmentally feasible. Little information is available regarding potential health effects associated with exposure to NH_4NO_3 . Exposure to carbon (C) black over a short time frame demonstrates minimal health effects. Therefore, although limited information is available on the potential health effects of NH_4NO_3 and C, since both particulates are measured in PM in California, they represented logical particle types for this study. Target concentrations for NH_4NO_3 were designated as high, intermediate and low levels. For NH_4NO_3 target concentrations were set at 300, 150 and 75 $\mu\text{g}/\text{m}^3$, respectively. Target concentrations of carbon were 200, 100 and 50 $\mu\text{g}/\text{m}^3$, respectively. For all studies, the average mass median aerodynamic diameter (MMAD) of the NH_4NO_3 /carbon particle matrix was 1.03 μm . All PM exposures were designed to simultaneously expose rats to NH_4NO_3 and carbon at either high, intermediate, or low concentrations. Although every effort was made to achieve each of these target concentrations over the course of the study, the actual concentrations of NH_4NO_3 and carbon covered a broader range. Despite these excursions from the desired concentrations, we will refer to each study in this report as low, intermediate, or high for the purposes of simplicity. The actual concentrations for each of the 39 total experiments performed over the course of this study can be found in the Appendix of this Report.

All exposure conditions were closely managed and coordinated with the project manager and staff at the California Air Resources Board and investigators at UC Davis and UC Irvine. A primary goal of CARB, UC Davis and UC Irvine as a collaborative research team was to determine exposure conditions that would best serve our understanding and elucidation of PM effects on the respiratory tract. Particle size and particle concentration represented the most critical factors driving our research. The effects of particle concentration on respiratory toxicity was studied by the UC Davis team, while the influence of particle size on respiratory toxicity was studied by the UC Irvine team. Quarterly teleconference meetings between UC Davis and UC Irvine with the Project Manager at CARB afforded us the opportunity to present, discuss and review each "research block" of planned experiments. For example, our initial studies examined the effects of a single 6-hour period of particle exposure on adverse lung effects. Since limited effects were noted, a repeated exposure regimen of exposure for 3 consecutive days was agreed upon to determine if the effects on the respiratory system would become evident. Conference

discussions were a critical part of the decision-making process in guiding future experiments. To review the findings of each set of experiments provided key input and a cohesive plan to provide the flexibility in research design to build upon each block of experiments. Rather than blindly pursuing a matrix of exposure scenarios, we were able to identify the most critical findings of each study to guide us to the next series of experiments.

Regular meetings with the CARB Project Manager and investigators at UC Davis and UC Irvine were instrumental in establishing study design throughout the course of the study. The source of carbon black for the UC Davis and UC Irvine studies was determined as a result of these meetings. A single type of carbon black particle was selected from Cabot Corporation for both the UC Davis and UC Irvine studies to better correlate the findings from each institution. The particle size used in aerosol experiments at UC Davis was instrumental in establishing the particle size studies at UC Irvine. Methods used to aerosolize particles at UC Davis for NH_4NO_3 and carbon were formulated through extensive discussions with our colleagues at UC Irvine. The meetings provided a dynamic approach for each inhalation study, built upon the discussion of results from previous experiments. Through these meetings, the following sequence of 5 research blocks emerged and was carried out during the period of the contract.

- (1) Single 6-hour exposures to PM in healthy adult Fischer 344 rats using three different concentrations of NH_4NO_3 and carbon. (These studies established whether adverse effects following particle could be detected.)
- (2) Repeated 6-hour exposures for 3 days to PM at only the intermediate concentration of NH_4NO_3 and carbon. These studies were done using healthy adult Sprague Dawley rats. (These studies were designed to establish potential interstrain differences with exposure to particles at a single concentration.)
- (3) Repeated 6-hour exposures for 3 days to PM in healthy adult Fischer rats at the intermediate concentration of NH_4NO_3 and carbon. (These studies were designed to determine if longer exposure to particles was associated with adverse effects in the respiratory system.)
- (4) Repeated 6-hour exposures for 3 days to PM in senescent Fischer rats at the intermediate concentration of NH_4NO_3 and carbon. These studies were done simultaneously with adult Fischer 344 rats to insure identical exposure conditions. (These studies were designed to determine if older rats were more adversely affected by particle exposure.)
- (5) Repeated 6-hour exposures for 3 days to PM in young (neonatal) Fischer 344 rats at three different concentrations of NH_4NO_3 and carbon. Exposures are done at the end of the first week of postnatal life and again following the end of three weeks of postnatal life. (These studies were designed to determine if young rats were more adversely affected by particle exposure during critical windows of lung development.)

Measures of particle-induced respiratory effects: A systematic testing approach

A systematic testing approach to define the effects of PM on the respiratory tract was used. Should particles inhaled into the lungs produce an adverse health effect, it was felt that alterations in one or more of a total of 5 measures would be seen, based on the toxic properties of the particle. These measures are assays for: (1) cellular permeability, (2) glutathione levels within site-specific lung regions, (3) cell proliferation within site-specific lung regions, (4) particle deposition, and (5) bronchoalveolar lavage.

Epithelial cell permeability and glutathione levels (GSH) are biomarkers of effects reflecting cellular injury and oxidative stress respectively. Measurement of GSH is a reflection of the redox status of the cells and is a primary factor in controlling the sensitivity of the cell to chemicals injured by inducing oxidative stress or by agents metabolized to electrophilic derivatives. Uptake of bromodeoxyuridine (BrdU) into cells reflect both the proliferation of cells in site-specific locations of the airways and lung parenchyma as well as a process of cell injury and repair occurring within these same sites. Particle deposition studies using fluorescent microspheres are designed to examine the distribution and fate of particles in the lungs. Bronchoalveolar lavage (BAL) is used to determine lung inflammatory response following exposure. To test our hypothesis that inhalation of particles induces epithelial damage, increases epithelial permeability, reduces glutathione levels, stimulates the recruitment of inflammatory cells, and leads to cell proliferation, these assays can be applied to both the airways and the lung parenchyma.

Since particles of NH_4NO_3 and carbon under the conditions generated in these studies are virtually impossible to see, selected studies completed in neonatal, adult and senescent Fischer 344 rats and adult Sprague Dawley rats used fluorescent microspheres to determine particle deposition (based on particle size or timing of exposure) and patterns of clearance from anatomically distinct regions of the lungs. These fluorescent microspheres were not designed to directly assess the effects of exposure to NH_4NO_3 and carbon, but rather to better understand particle deposition in the lungs of rats. In most instances, the size of these microspheres approximated the size of the NH_4NO_3 and carbon particles used in our studies.

The effect(s) inhaled particles may have on the airways and alveoli of the lungs depend on a number of factors, such as particle size, number, durability and relative toxicity. The focus of studies with fluorescent microspheres was to examine the feasibility of using particles of uniform size to determine the patterns and distributions of deposition and clearance from anatomically distinct regions in the lungs of F344 and SD rats. More specifically, fluorescent microspheres were used to (1) determine particle deposition and clearance following exposure to PM or filtered air in adult male F344 rats, (2) the influence of particle size on deposition and clearance in adult male SD rats, (3) particle deposition and clearance in senescent male F344 rats following PM exposure, and (4) particle deposition and clearance in male and female neonatal F344 rats.

Materials and Methods

A. Animals

Fischer 344 rats of three different ages were used for these experiments. All animals were obtained from Harlen, Inc. (Indianapolis, IN). Adult male Sprague-Dawley rats were also obtained from Harlen, Inc. (Indianapolis, IN) and used for a limited set of experiments to examine strain differences and to establish potential respiratory effects induced by particle exposure. Both strains of rats were maintained in chambers for 1 week prior to the onset of each study to permit acclimation. Two animals were randomly selected prior to each experiment for complete health screening and serology to confirm that the animals were free of disease and respiratory pathogens.

B. Characterization of particle exposures:

A total of 38 exposure experiments in rats were completed during the course of this three year study using aerosolized NH_4NO_3 and carbon at different concentrations. For all experiments, multiple exposures were done for each group. For example, 6 separate exposures were done using adult male F344 rats for a single day of exposure at the high concentration of particles. Please see the Appendix for the complete set of measured observations and characterization of each individual experiment. The general methods used to generate these exposure conditions are described in the following section.

C. Particle generation and characterization

Exposures of rats were conducted in four 4.2 m³ volume stainless steel and glass exposure chambers that were updated from a design originally described by Hinnert *et al.* (1968). This chamber design with square cross section (137 cm x 137 cm) and pyramidal top with tangential cylinder mixing inlet is perhaps the most widely used for animal inhalation exposure studies and can be appropriately termed a conventional design. These chambers have a well-documented capability of producing homogeneous distribution of aerosols and gases (Hinnert *et al.*, 1968; MacFarland, 1983). Distribution studies most representative of actual exposure conditions were those conducted by Hinnert *et al.* (1968) that evaluated retention of inhaled bacterial aerosols in the lungs of exposed mice. They demonstrated that uniform concentrations were produced at all cage positions on a given level in the chamber. In our facility the chambers were connected to a common air handling system in which the air supplied passed through two pre-filters, a HEPA filter and finally, an activated charcoal filter to remove most common air pollutants (such as acids, nitrates, and sulfates). Each chamber was operated at an air flow rate of 2.1 m³/min. The high rate of ventilation at 30 air changes per hour causes rapid chamber atmosphere equilibration and lowers the level of airborne contaminants from the animals housed within. For this series of exposures, chamber relative humidity was maintained at $42.2 \pm 10\%$ at a temperature of $23.8 \pm 0.5^\circ\text{C}$ (mean \pm SD for all exposures). Animals were housed in stainless steel open mesh cages specially designed for inhalation exposure. The cages were arrayed in a single layer; a small animal load relative to the chamber volume was used. Waste was flushed daily from the chambers. Animal care complied fully with the guidelines established by the Institute of Laboratory Animal Resources (1996). One chamber contained the

ammonium nitrate (NH_4NO_3) and carbon (C) particulate matter aerosol (PM) with ozone (O_3); one contained PM; one contained O_3 , and the remaining chamber contained only filtered air as a control atmosphere. The two chambers used for aerosol exposure were each fitted with an aerosol discharger and conditioning column as well as other items necessary for precisely controlled aerosol generation and characterization.

Atmosphere Generation and Characterization

PM aerosol exposure methods were adapted from those described by our collaborator, Dr. Michael T. Kleinman of UC Irvine, in Kleinman *et al.* (2000) Elemental carbon as carbon black called “Monarch[®] 120” was obtained from the Cabot Corporation (Billerica, MA). This carbon black consists of primary particles with a mean diameter of 75 nm in clusters with a smallest dispersible aggregate diameter of 150 to 200 nm (Cambrey, 1997). The carbon used for these studies was derived from a single manufacturing batch. A comprehensive gas chromatography-mass spectrometry analysis of this material was completed by Dr. Barbara Zielinska of the Desert Research Institute, Reno, NV. Samples were taken from two randomly selected 1 kg. containers out of 11 total containers. Analysis was performed to detect the presence and measure the concentrations of 84 polycyclic aromatic hydrocarbons and other contaminants that might compromise assessment of the contribution of the elemental carbon to toxicity during our exposure studies. Analysis revealed very low contaminant concentrations. Fluoranthene at 0.003% and pyrene at 0.011% were the major contaminants. Results from each of the two containers from the same manufacturing batch were within 1% agreement. We, therefore, concluded that this carbon was suitable for our studies. A copy of the results of this analysis is included in the Appendix.

The carbon was weighed and dispersed in dilute NH_4NO_3 (Analytical Reagent, Mallinckrodt Chemical, Inc., Paris, KY) solutions with an ultrasonic probe to form a slurry that was stirred for two to four days before use. This mixture was nebulized by using a modified compressed air nebulizer operated at approximately 4 liters/min. The nebulized droplets were diluted with the introduction of an equal flow rate of dry air in a radial dilutor and conveyed upward through a vertical conditioning column 198 cm long and 14.7 cm in diameter. The column contained a ^{85}Kr source to ionize the air and, therefore, reduce charge on the aerosol to near Boltzman equilibrium (Teague *et al.*, 1978). The conditioned aerosol was introduced into the mixing inlet of the exposure chamber where the PM was further diluted in a chamber flow rate of $2.1 \text{ m}^3/\text{min}$. NH_4NO_3 deliquesces at a relative humidity of 61.2 % at 25°C (Clegg *et al.*, 1998, 2001). Since the chamber relative humidity during these studies ($42.2 \pm 10 \%$ RH at $23.8 \pm 0.5^\circ \text{C}$, mean \pm SD) was well below this deliquescence point, the PM aerosol phase was solid particles composed of NH_4NO_3 salt residue and carbon. Slurry concentrations of NH_4NO_3 and carbon were selected to ultimately produce in the chamber an aerosol of the desired mass concentrations with a mass median aerodynamic diameter (MMAD) of about $1 \mu\text{m}$. Compressed air flow through each nebulizer was also adjusted slightly during exposure as a fine control of total mass concentration in each chamber containing the PM.

The carbon black particles are very hydrophobic and are very difficult to keep suspended in an aqueous solution. A major problem was preventing the loss of carbon from the slurry during a six hour exposure interval. The carbon particles tend to rapidly agglomerate, deposit on

and adhere to the wetted surfaces of nebulizers, pumps, reservoirs, tubing and other components in the system. The carbon adhered less to glass and PFA Teflon[®] in our system, and these materials were given preference. Obviously, losses from the slurry cause lower carbon content in the aerosol, and the build up of deposits can cause poor nebulizer performance. Therefore, the nebulizers were modified to permit a continuous flow of slurry through them, minimizing recirculation within. The slurry was pumped to the nebulizers from a common glass reservoir containing 3.5 liters, sufficient for a six-hour exposure interval in both chambers containing the aerosol. The slurry was constantly stirred to prevent the carbon from stratifying and accumulating at the bottom of the reservoir. Fresh liquid was provided to each nebulizer in excess of about 30 times the amount being nebulized. Excess slurry was continually pumped from each nebulizer to a waste vessel. Components were arranged so that tubing lengths were minimized. For supply a small internal tubing diameter about 1.6 mm was selected to maximize the velocity of the pumped liquid, and, therefore, reduce the contact time of the slurry with the pump and tubing.

Ozone was produced from medical grade oxygen by electric discharge ozonizers (Model IV, Erwin Sander Elektroapparatebau G.m.b.H., Uetze-Eltze, Germany) to avoid the generation nitrogen oxides. The operation of a corona ionizer using room air can lead to the buildup ammonium nitrate on the negative corona points and the potential release of submicron particles into the atmosphere (Hobbs et al., 1990). High purity medical oxygen eliminates the buildup of nitrogen salts on the corona discharge during the generation of ozone or the potential release of particles (Harris et al., 1982). Ozone was carried through Teflon[®] tubing to the mixing inlet of each chamber. Ozone concentrations during exposure were continuously monitored. The analyzer was connected to computer-controlled sampling valves set to sample each of the two ozone containing chambers every 4 minutes. All components in the sampling stream were made from Teflon[®]. A Teflo[™] filter (Pall Gelman Sciences, Ann Arbor, MI) was used to filter the air sampled by the analyzer to prevent aerosol contamination of the optics and other components in the sampling stream. Calibration of the analyzer was performed with the filter in place.

Measurements of exposure concentrations of NH₄NO₃, carbon and ozone were by standard methods used in ambient air monitoring. This ensures that the exposure data are fully comparable. Ion chromatography (Model DX-120 with PeakNet software, Dionex Corp., Sunnyvale, CA) was used to analyze NH₄NO₃ sampled on filters from the chambers, the same method used by the California Air Resources Board (CARB 1992). Carbon content of aerosol samples was determined by Dr. Kochy Fung of Atmospheric Assessment Associates, Inc., Calabasas, CA, by selective thermal oxidation and subsequent flame ionization detection (Fung, 1990). For ozone monitoring, a programmable multi-gas calibrator (Model 5008 with D&P, Dasibi Environmental Corporation, Glendale, CA) was calibrated and certified with a National Institute of Standards and Technology (NIST) standard reference photometer (serial number 4) located at the CARB. This calibrator was used to calibrate the ozone analyzer (Model 1003AH, Dasibi Environmental Corporation, Glendale, CA) used to continuously monitor exposure concentrations of ozone during these studies (EPA 1988).

Detailed characterization and monitoring were performed during each exposure. All air samples were drawn from the animal breathing zone of the chambers. Air sampling devices with probes were inserted through specially designed ports located on each side of the chamber in the

animal holding volume. For the two chambers containing PM, known volumes of air were drawn at constant flow rates through filters to determine mass concentrations and Mercer-type cascade impactors (Mercer et al., 1970) to determine aerodynamic size. During 6 hour exposures three samples for NH_4NO_3 analysis were collected on modified polysulfone membrane filters (Supor[®]-800, 47 mm diameter, Pall Gelman Sciences, Ann Arbor, MI) during each 2 hour segment of the interval. These samples were drawn for 60 min. at a flow rate of 19 liters/min. Within 1 hour after the sample was collected, deposited PM was extracted by adding aliquots of water and sonicating the filters for 60 min. Then nitrate was analyzed by ion chromatography. Simultaneously with the nitrate samples, three samples for carbon analysis were collected on quartz fiber filters (QM-A, 47 mm diameter, Whatman, Inc., Clifton, NJ). These samples were drawn for 60 min. at a flow rate of 22 liters/min. The carbon samples were sent to Dr. Fung for analysis (Fung, 1990). During 3 day, 6 hours per day exposures, the number of samples for NH_4NO_3 and for carbon were reduced to two samples per day for each analysis and were collected during each 3 hour half of the interval.

Samples for total mass concentration and aerodynamic size with cascade impactors required 5 hour sampling periods to collect sufficient amounts for analysis. Therefore, one total mass concentration determination was made for each daily interval. The PM was collected on preweighed Teflon[®] coated glass fiber filters (Pallflex[™], EMFAB, 47 mm diameter, Pall Gelman Sciences, Ann Arbor, MI). These samples were collected at 22 liters/min., and the filters were weighed immediately after the sampling period of approximately 5 hours. For aerodynamic size determinations one cascade impactor sample was drawn for each 6 hour exposure, and one or two were taken during the 3 day exposures. Air was drawn through the impactor at 0.9 liters/min. Glass coverslips were used on each of the seven cascade impactor stages and a Supor[™] membrane was used for the after filter. Each stage and after filter were analyzed by ion chromatography for the mass of nitrate collected. The resulting data were fitted with a log normal distribution to derive the mass median aerodynamic diameter (MMAD) and geometric standard deviation (σ_g) of the PM size distribution. A piezobalance aerosol mass monitor (Model 3511, Kanomax Japan, Inc., Osaka, Japan) was also used during these exposures. Hourly measurements were made with this mass monitor for each chamber containing aerosol. This instrument permitted a determination of total mass concentration after a two minute sampling period. It was used for adjustment of chamber mass concentrations during exposures and allowed rapid detection of problems with aerosol generation. Also, a few PM samples were collected on 0.2 μm pore size Nuclepore[®] filters (25 mm, Whatman, Inc., Clifton, NJ) during the study for examination by microscopy to see the general appearance of the particles.

For a limited number of exposures, selected rats were exposed for two hours to polychromatic red or yellow-green fluorescent microspheres with a uniform diameter of about 0.5 or 1 μm . The microspheres were coated with albumin before use. The animals were evaluated to measure deposition and clearance of the fluorescent test particles. Exposure of the adult and senescent rats to these microspheres was accomplished in a nose-only small animal exposure system. Each rat was held in a cylinder with a small opening at the head end through which the aerosol passed so that the nasal area was continuously exposed to a fresh supply of particles and air. Dams with litters were exposed in a small, 0.44 m^3 exposure chamber. The mass concentrations were measured by the increase in weight of a Pallflex[™] filter after

collecting the aerosol from a known volume of air. Exposures were conducted for two hours and resulted in an abundance of single particles deposited in the lungs of the rats during this period. These techniques and the morphological evaluation have previously been described in detail (Pinkerton et al., 1993).

F. Measure 1: Cell Permeability

The method used for this analysis was developed by the investigators at UC Davis to provide three-dimensional maps of acute cytotoxic injury patterns within the tracheobronchial airways of the lungs (Postlethwait et al., 2000; Van Winkle et al., 1999). The procedure was as follows. Immediately following exposure, the animals (Fisher 344 or Sprague-Dawley rats) were deeply anesthetized with pentobarbital, weighed and the tracheas exposed by midline dissection and a tracheal cannula inserted at the larynx. The lungs were collapsed and ethidium homodimer-1 (10 μ M in F-12 medium) was infused via the tracheal cannula and the lungs inflated with this solution for 10 minutes at body temperature. The lungs were lavaged once with F-12 medium, then fixed by inflation at 30 cm fluid pressure with glutaraldehyde/ paraformaldehyde (1% / 1%) for a minimum of 2 hours. Following pressure fixation, the trachea was ligated and the lungs stored in the same fixative until analysis. The airway tree of the right cardiac lobe was exposed by micro-dissection from the lobar bronchus to the terminal bronchioles along the axial path. The dissected preparations were then incubated with a second nuclear dye, YOPRO-1, to label all nuclei within the specimen. The position and density of ethidium homodimer-1-positive cells was evaluated by epi-fluorescence using either a stereomicroscope or a laser confocal microscope. The density was evaluated for the entire airway tree. All the animals in each experiment were ranked for level of severity of injury based on numbers and distributions of permeable, or injured, cells. The animals were then ranked based on overall extent of permeable cells compared to animals in other experiments.

Rankings were based on our experience with this approach as applied to a number of different injury models. Injury was ranked as most severe (Rank = 3) if permeable cells were everywhere throughout the airway tree or composed more than 40% of the cells at one site. In none of the animals in any of the experiments listed in Table 1 was the injury that severe. Injury was ranked as non-existent (Rank = 0) if permeable cells were not observable in most of the airway tree and, where present, represented (10 or fewer per airway segment) a small proportion of the epithelial cells. This designation in the past has been true for most filtered air (FA) control animals. However, based on our experience to date, control (unexposed) laboratory rats on average, regardless of strain, have more permeable cells in the airway epithelium than do the other species, (mouse, rhesus monkey) to which we have applied this technique.

G. Measure 2: Glutathione levels in Microdissected Airways

Cellular redox status is a primary factor in controlling the sensitivity of the cell to chemicals which injure the cell by inducing oxidative stress or by agents which are metabolized to electrophilic derivatives. One of the primary detoxication routes for both types of injury involves the utilization of the tripeptide, glutathione (see Meister, 1994 and Rahman et al., 1999 for review). The purpose of the studies described in this task was to determine whether

exposures to combinations of particles and oxidants (ozone) alter the reduced glutathione levels at specific sites within the lung.

Glutathione was measured in airways prepared by microdissection by a validated HPLC method published earlier (Lakritz et al., 1997). The method is highly sensitive and glutathione levels can be measured without derivatization with a relatively short run time (<15 min). The details of the analytical methodology have been published previously and the complete protocol utilized in these measurements is presented below. Briefly, airways, isolated by microdissection were homogenized in an acid buffer containing antioxidant. Protein was removed by centrifugation and an aliquot was injected directly onto a reversed phase column for GSH analysis. Standards were prepared with reduced glutathione in the same buffer solutions. For protein determinations, the protein pellet recovered from each sample by centrifugation was resuspended in 1N NaOH and was heated to 60° C to dissolve the protein and an aliquot was removed for determination of protein content by the method of Lowry et al., 1951. Data are expressed as nmoles metabolite/mg protein. For further details, please refer to the Appendix (Protocol for measurement of GSH in dissected airways).

Treatment of rats with Buthionine Sulfoximine:

In a few studies, rats were treated just prior to exposure with buthionine sulfoximine, an inhibitor of γ -glutamylcysteine synthase, the rate-limiting step in the enzymatic synthesis of glutathione. These studies were designed to determine if exposure to particles would be associated with a decrease in glutathione levels in the lungs, but not detected due to the rapid resynthesis of the glutathione. These studies were exploratory in nature and were limited in the number of animals tested.

H. Measure 3: Cell Proliferation/Morphometry

Bromodeoxyuridine (BrdU), a thymidine analog incorporated into DNA by cells undergoing DNA replication, is indicative of cell proliferation noted following cell injury (Rajini et al., 1993). Two different approaches were taken to express this measure, one in F344 rats and another in SD rats. For F344 rats, BrdU labeling was expressed as the number of positive cells per unit volume of the respective tissue compartment (epithelium or interstitium). For SD rats, cell labelling for BrdU was expressed as a proportion or fraction of the total cell number for each tissue compartment (epithelium or interstitium). Both techniques provide the same information to identify the relative rates of cell proliferation and are well-accepted methods to use. To perform this analysis in F344 rats, 30 μ m thick tissue sections were used with the optical dissector counting technique. The analysis in SD rats was done with 5 μ m thick sections using a cell labeling index approach.

In Vivo Cumulative Cell Labeling-Fisher 344 rats

A single osmotic minipump (ALZET pump Model 2ML1, nominal pumping rate 10 μ l/h; ALZA Corp., Palo Alto, CA) was placed subcutaneously between the shoulder blades of the anesthetized F344 rat 12 h prior to exposure. The pump was loaded with BrdU (Sigma, St. Louis, MO) dissolved in 0.01 N Sodium hydroxide. To ensure immediate release of BrdU, the pumps

were primed by immersion in 0.9% saline at 37°C 8 h prior to insertion. The duodenum served as a positive labeling control for each rat. The incorporated BrdU was detected using monoclonal antibody and immunocytochemical techniques as outlined by Hsu and co-workers (Hsu et al., 1981). Briefly, 30- μ m-thick paraffin sections were deparaffinize in three changes of xylene (5 min each) and rehydrated in a graded series of ethyl alcohol (100%–95%–75% distilled water, 5 min each). The tissue sections were then incubated in 2.5 N HCl for 30 min at 37°C to denature the DNA. We neutralized the acid by two borate buffer washes (5 min each) and a PBS wash (5 min). We incubated the sections in 3% hydrogen peroxide for 30 min to block the endogenous peroxidase activity, washed the sections for 10 min in PBS, and then incubated the sections in 5% NRS with 5% powdered milk for 1 h to block nonspecific binding. After blotting excess fluid, we incubated the sections with the primary mouse anti- BUdR (Dako Corp., Carpenteria, CA) diluted 1:50 in PBS with 5% powdered milk for 2 h. Tissue sections incubated with 5% powdered milk in PBS were used as negative controls. After washing with PBS, the sections were incubated for 60 min in biotinylated, rabbit antimouse immunoglobulin (Dako) diluted 1:200 in PBS with 5% NRS. We followed this procedure with two PBS washes and incubation of the sections in Vectastain ABC reagent (Vector Laboratories, Burlingame, CA) for 30 min. After two washes in PBS (5 min each), the sections were incubated in peroxidase substrate solution (7.5 μ l 30% hydrogen peroxide in 1.0 mg/ml diaminobenzidine in 0.1 M Tris-HCl buffer at pH 7.6) for 3 to 5 min. Finally, we rinsed the sections with PBS and then distilled water. Labeled nuclei appeared reddish-brown by light microscopy, and no counterstain was used.

In Vivo Cumulative Cell Labeling-Sprague Dawley rats

Implantation of osmotic minipumps containing BrdU was performed in an identical manner in SD rats as was done in F344 rats. One day prior to the onset of exposure, each rat was anesthetized and a 2 ml osmotic minipump (Alza, Palo Alto, CA, nominal pumping rate of 10 μ l/h) filled with a nucleotide analog, bromodeoxyuridine (BrdU, 30 mg/ml) was implanted subcutaneously on the back of each rat. Each animal was randomly assigned to one of four groups. Exposures were for 6 hrs/day for 3 days. The morning following the last day of exposure, animals were deeply anesthetized, the trachea cannulated and a solution of 1.0% paraformaldehyde, 0.1% glutaraldehyde instilled via the cannula at a hydrostatic pressure of 30 cm for 1 hr.

The right middle lobe was used for analysis in SD rats. The main axial airway of the lobe was bisected using a razor blade along its longitudinal path and embedded in Paraplast (Fischer, Pittsburgh, PA). Sections 5 μ m thick were cut using a microtome and placed on Superfrost Plus glass slides (Fischer, Pittsburgh, PA). Sections containing the longitudinal profile of the axial airway and its branchpoints were used for BrdU immunohistochemical staining using a monoclonal mouse antibody (anti- BrdU, Boehringer Mannheim, Indianapolis, IN). Sections were deparaffinized in 3 changes of xylene and rehydrated in decreasing concentrations of ethanol. To block endogenous peroxidase and to unmask antigenic sites, sections were treated in 3% hydrogen peroxide, followed by 0.1% pronase. To block nonspecific binding, 10 percent horse serum in physiologic buffered saline (PBS) was used. Tissues were incubated with anti-BrdU at a dilution of 1:100 for 1 hr at 37°C, washed with PBS and secondary antibody applied for 30 min in 5% horse serum and 5% rat serum. Visualization of positive cells was by the avidin-biotin complex method with commercially supplied reagent (Vector Laboratories,

Burlingame, CA). A negative control with substitution of the primary antibody was included to examine tissues for nonspecific reactions.

Morphometry of Cell Proliferation-F344 rats

Under low magnification, we examined 30- μm -thick sections and numbered the terminal bronchioles in a stratified manner on the slide, using NIH Image software. (NIH Image is public domain software available at <http://rsb.info.nih.gov/nih-image> and is authored by Wayne Rasband). Four terminal bronchioles were systematically sampled from the 10 to 20 terminal bronchioles sectioned per slide using a random start. We used an optical disector to count BrdU-positive epithelial and interstitial cells in terminal bronchioles, proximal alveolar ducts and bronchial bifurcations just proximal to the selected terminal bronchiole (Bolender et al., 1993). Stereologic techniques were used to determine the number of BrdU-positive cells per volume of epithelium or interstitium. Briefly, we estimated the number of cells per volume of epithelium using the following equation:

$$NV \text{ BrdU/epi} = N \text{ BrdU} / (A \text{ epi} * H \text{ epi})$$

where NV BrdU/epi is the number of BrdU-positive cells per volume of epithelium; NBrdU is the number of BrdU-positive cells counted in the 30- μm sections, excluding those that intersected the top of the section and two sides of the counting frame; Aepi is the area of epithelium in the counting frame; and Hepi is the height of the optical disector (usually 30 μm).

In a similar fashion, we estimated the number of cells per volume of interstitium using the following equation:

$$NV \text{ BrdU/int} = N \text{ BrdU} / (A \text{ int} * H \text{ int})$$

where NV BrdU/int is the number of BrdU-positive cells per volume of interstitium; NBrdU is the number of BrdU-positive cells counted in the 30- μm sections, excluding those that intersected the top of the section and two sides of the counting frame; Aint is the area of interstitium in the counting frame; and Hint is the height of the optical disector (usually 30 μm).

Morphometry of Cell Proliferation-SD rats

For SD rats, BrdU labeling was analyzed using 5- μm thick sections for (1) airway bifurcations (along the main axial pathway), (2) airway generations (i.e, airway walls along the main axial pathway), (3) terminal bronchioles and (4) the proximal alveolar region within 400 μm of the bronchiole-alveolar duct junction (BADJ) of randomly selected profiles arising along the main axial pathway of one of its minor daughter branches. The labeling index for airways on bifurcation ridges and along the main axial pathway, as well as for terminal bronchioles was determined for both epithelial and interstitial cells. The total number of epithelial and interstitial cells counted per animal was 1,000. For airway bifurcations, only epithelial cells and the underlying interstitial cells within 200 μm of the apex of the bifurcation ridge were counted as part of the bifurcation. Counting within the lung parenchyma was done for all cell types within random fields 400 μm or less from the BADJ. This region was identified by placement of a

pattern of concentric circles with a spacing interval of 100 μm over three randomly selected bronchiole-alveolar duct junction for each animal. Only parenchymal cells falling within 400 μm of the BADJ were counted.

A total of six Sprague Dawley rats / group were used to determine bromodeoxyuridine (BrdU) uptake in cells of the airways and proximal alveolar regions of the lungs. One day prior to the onset of exposure, each rat was anesthetized and a 2 ml osmotic minipump (Alza, Palo Alto, CA, nominal pumping rate of 10 $\mu\text{l/h}$) filled with a nucleotide analog, bromodeoxyuridine (BrdU, 30 mg/ml) was implanted subcutaneously on the back of each rat. Each animal was randomly assigned to one of four groups. Exposures were for 6 hrs/day for 3 days. The morning following the last day of exposure, animals were deeply anesthetized, the trachea cannulated and a solution of 1.0% paraformaldehyde, 0.1% glutaraldehyde instilled via the cannula at a hydrostatic pressure of 30 cm for 1 hr.

I. Measure 4: Particle Deposition/Fate

Preparation of microspheres

Yellow-green (YG) FluoresbriteTM and polychromatic red (PC-red) carboxylate microspheres from Polysciences, (Warrington, PA) were obtained in a 2.5% solids suspension. Nominal microsphere diameter for these studies was 1.0 μm . Microspheres were impregnated with a yellow-green fluorescent dye possessing a coumarin maximal excitation peak of 458 nm and a maximal emission peak at 540 nm. All microspheres were coated with albumin prior to aerosolization to reduce the loss of microspheres from the lungs during aldehyde fixation and processing of tissues. A thin coat of albumin served to crosslink this protein with other proteins of the lungs by glutaraldehyde and paraformaldehyde fixation (Hyat, 1989). A 1 ml suspension of microspheres was vortexed with 19 ml of distilled water containing 0.125% albumin for 1 minute, allowed to settle, and then vortexed a second time before centrifugation at 8,000 g for 10 minutes. The solution was decanted and the microspheres resuspended in distilled water containing 0.001% Zwittergent 3-08 surfactant solution (Calbiochem, San Deigo, CA). The microspheres were vortexed, centrifuged, and decanted to further remove residual albumin. The microspheres were resuspended a third time in distilled water with 0.001% Zwittergent 3-08 and sonicated to help break apart aggregates. This procedure resulted in a majority of single microspheres, although some aggregates still remained. Additional washing and sonication between centrifugation helped to further reduce microsphere clusters.

Aerosolization of microspheres

The final dilution of the microsphere suspension was calculated according to Raabe (Raabe, 1968). To yield 90% single particles after nebulization in our system, it was estimated that dilution of the original concentrated suspension by a ratio of 1:52 was required. The diluted suspension was placed in the reservoir of a Retec nebulizer (Model 7301, Cavitron, Englewood Cliffs, NJ). The nebulizer was immersed in an ice bath and the suspension was continuously stirred.

Air at 141 kg/cm^2 was supplied to the nebulizer to produce a flow rate of 5.4 l/min. The aerosol stream was diluted by adding 24.61 l/min of dry filtered air in a specifically designed mixer (In-Toz Products, Albuquerque, NM). The stream continued upward through a krypton-85 discharging and conditioning column (Teague et al., 1978), which was heated to maintain the exiting stream at 45°C . In this column the electrostatic charge of the aerosol was reduced to the Boltzmann equilibrium, and water was evaporated from the nebulized droplets to leave the microspheres.

J. Measure 5: Bronchoalveolar lavage

Following deep anesthesia, the trachea was cannulated and 35 ml/kg of sterile PBS, pH 7.4 was slowly instilled into the lungs with a syringe. The instilled fluid was recovered from the lungs with the same syringe. The lavage procedure was repeated to collect a total of 4 separate aliquots. Total cell number was determined using a hemacytometer and cell viability was determined by trypan blue exclusion. Cell differentials for each animal were determined from 200 μL cytopspin preparations stained with LeukoStat (Fisher Scientific, Pittsburgh, PA). A minimum of 500 cells was counted for each cytopspin slide preparation.

K. Statistical Methods

Data obtained for each task were analyzed using Dunnet's two-sided test to compare the control group with each treatment group. In some studies, one-way analysis of variance (ANOVA) was used. If significant differences were noted, Duncan's multiple range test was used to compare differences between treatment groups. For those studies (i.e., cell permeability) the relative rank (of permeable cell abundance) was compared between animals of different exposure groups (FA, ozone, PM, PM plus ozone) for a specific age, rat strain, and target particle concentration by Kruskal-Wallis nonparametric statistical rank test. A p value of less than 0.05 for this test was considered statistically significant.

Reduced glutathione levels were expressed as nmoles of glutathione per mg protein. Comparisons of glutathione concentrations between lung subcompartments and in lung subcompartments from air and exposed animals were done by a one-way analysis of variance (ANOVA). For analysis of BrdU labeling (cell proliferation/morphometry), post hoc tests were performed using Dunn's, the Bonferroni, or Student-Newman-Keuls's tests to determine significant differences between airway levels. For the analysis of data from bronchoalveolar lavage, analysis of variance was used to compare each treatment group to the control group. In limited instances where only one treatment group was compared to the control group, a student t-test was applied. A p value less than 0.05 for all tests was considered statistically significant.

Results

A. Characterization of aerosol and ozone exposure generation

The associated aerosol and ozone exposure data for each exposure have been tabulated and included in the Appendix to this report. Each exposure was assigned a consecutive code number, PM-1, PM-2, PM-3, etc. The two chambers containing PM were numbered EX6-1 and EX6-2 with the first chamber containing ozone as well. For the research, the intent was to study three PM concentrations that were called low, intermediate, and high. Target concentrations for the low PM exposures were $75 \mu\text{g}/\text{m}^3 \text{NH}_4\text{NO}_3 + 50 \mu\text{g}/\text{m}^3 \text{C}$, intermediate PM levels were intended to be $150 \mu\text{g}/\text{m}^3 \text{NH}_4\text{NO}_3 + 100 \mu\text{g}/\text{m}^3 \text{C}$ and high PM levels were $300 \mu\text{g}/\text{m}^3 \text{NH}_4\text{NO}_3 + 200 \mu\text{g}/\text{m}^3 \text{C}$. A single ozone concentration of 0.2 ppm was used for all exposures. Multiple measurements of a given parameter are expressed as mean \pm SD. NH_4NO_3 and elemental carbon concentrations are reported. The mass monitor data represents the most frequent (hourly) determination of PM concentration during exposure. The total mass concentration determination was a more direct measurement, but only one determination could be made for each exposure interval. Carbon by difference was calculated by subtracting the NH_4NO_3 concentration from the total mass concentration. This serves as an estimate of carbon concentration particularly for some of the early exposures when carbon analysis was problematic. Concentrations of NH_4NO_3 and carbon mixed in each slurry and the ratios of NH_4NO_3 to carbon are listed. A ratio is also given for NH_4NO_3 to carbon measured in the aerosol. Carbon loss in the system is reflected in a ratio in the aerosol smaller than what was in the slurry. Carbon stratification and concentration in the reservoir or nebulizer is reflected by a ratio greater in the aerosol than in the slurry. The aerodynamic size of the aerosol is listed. Finally, the ozone exposure concentration is given for chamber EX6-1. Since this tabulation was intended to primarily report aerosol characteristics, chamber EX6-3, containing the ozone alone atmosphere, was not included here.

The desired target concentrations of NH_4NO_3 and ozone were achieved through out these studies, even during the initial exposures when aerosol generation and some sampling techniques were under development. However, problems occurred with carbon content and analysis during some of the early exposures, primarily single 6-hour exposures at the intermediate PM concentration during which target levels were greatly exceeded. Later from exposure PM-13 on an improved carbon analysis by Dr. Kochy Fung (1990) was used and helped us make adjustments to come closer to the target concentrations intended.

Mean PM concentrations measured for each exposure from PM-13 on with three of the analytical methods used, gravimetry (total mass concentration), ion chromatography (NH_4NO_3) and selective thermal oxidation (C) (Fung, 1990) are compared on Figure 1. The linear regression line describing the relationship was $y = 1.0017x + 13.3378$, and the correlation coefficient was $r = 0.9841$. This is excellent agreement between three different analytical methods performed in two different laboratories. The intercept is only 10% of the lowest mass concentration point. The most likely causes could be slight moisture sorption as the total mass concentration samples were collected during the 5 hour sampling period or a small systematic weighing inaccuracy.

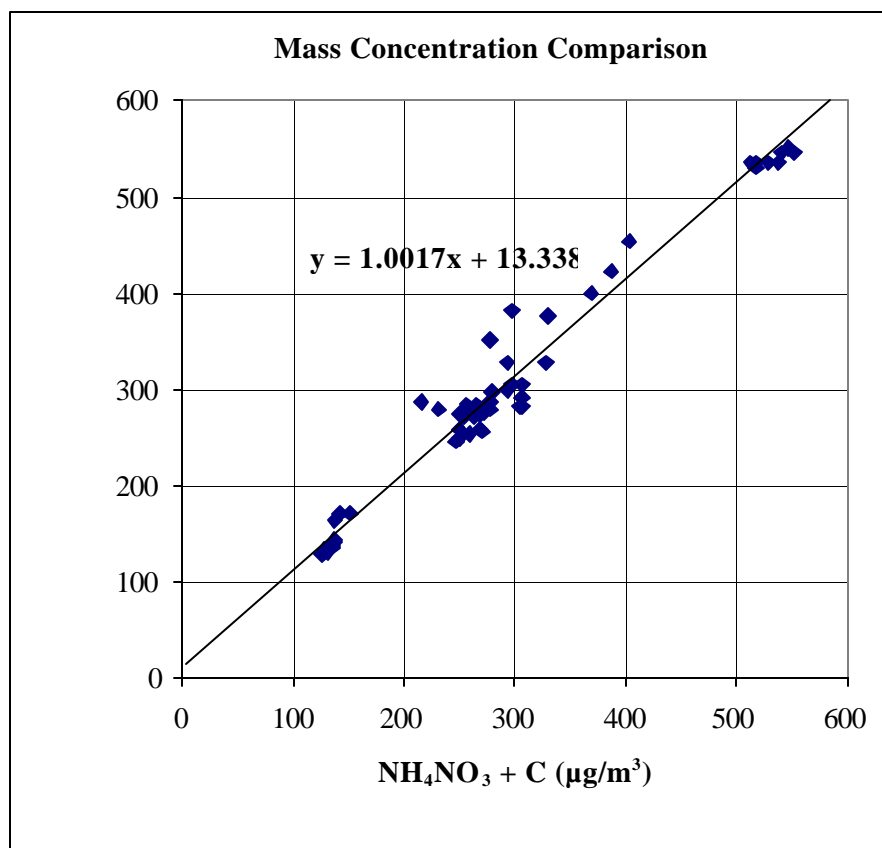


Figure 1. For each PM exposure, mean total mass concentration compared to mean NH_4NO_3 concentration added to mean C concentration on the abscissa. The comparison is based on three of the aerosol analysis methods used during the exposures, gravimetry, ion chromatography and selective thermal oxidation (Fung, 1990).

For nitrate analysis by ion chromatography, initial testing revealed that the modified polysulfone Supor™ filters were a better choice in our system than the Teflo™ filters that are more commonly used for ambient air monitoring. After extraction by the CARB procedure (undated) for Teflon® filters, they yielded about 9% less nitrate than the Supor™ filters. Ion chromatograms selected as typical examples from a low, intermediate and high PM concentration exposure are shown on Figure 2. Chromatograms of the nitrate calibration standards are equivalent to the chromatograms from the extracted PM samples, indicating that the anionic species present in the PM aerosol was nitrate of high purity. This equivalency to the nitrate standard was also evident in PM sampled from the chamber containing ozone. All deposited PM on filters or impactor stages was in a dry, solid phase as predicted since the chamber relative humidity ($42.2 \pm 10\%$ RH at $23.8 \pm 0.5^\circ\text{C}$, mean \pm SD for all exposures) was maintained below the deliquescence point of NH_4NO_3 (61.2% at 25°C) (Clegg et al., 1998, 2001). Nitrate loss is a frequent problem in ambient air sampling with acidified aerosols in the liquid phase. Nitric acid (HNO_3) can be formed, and this volatile acid is lost in the gas phase (Clegg et al., 1998, 2001). However, nitrate loss was not expected nor evident under our more controlled atmosphere generation conditions. NH_4NO_3 particles in the solid phase are not

volatile, exhibiting a very low vapor pressure (Clegg et al., 1998, 2001). In addition, our collaborator, Dr. Kleinman, generating aerosols at UC Irvine with the same chemical composition, tested nitrate loss during sampling by placing nylon filters behind the Teflon[®] filters he normally uses for collecting samples for nitrate analysis. He found no nitrate present on the Nylon filters that very effectively trap HNO₃ (Kleinman, 2001).

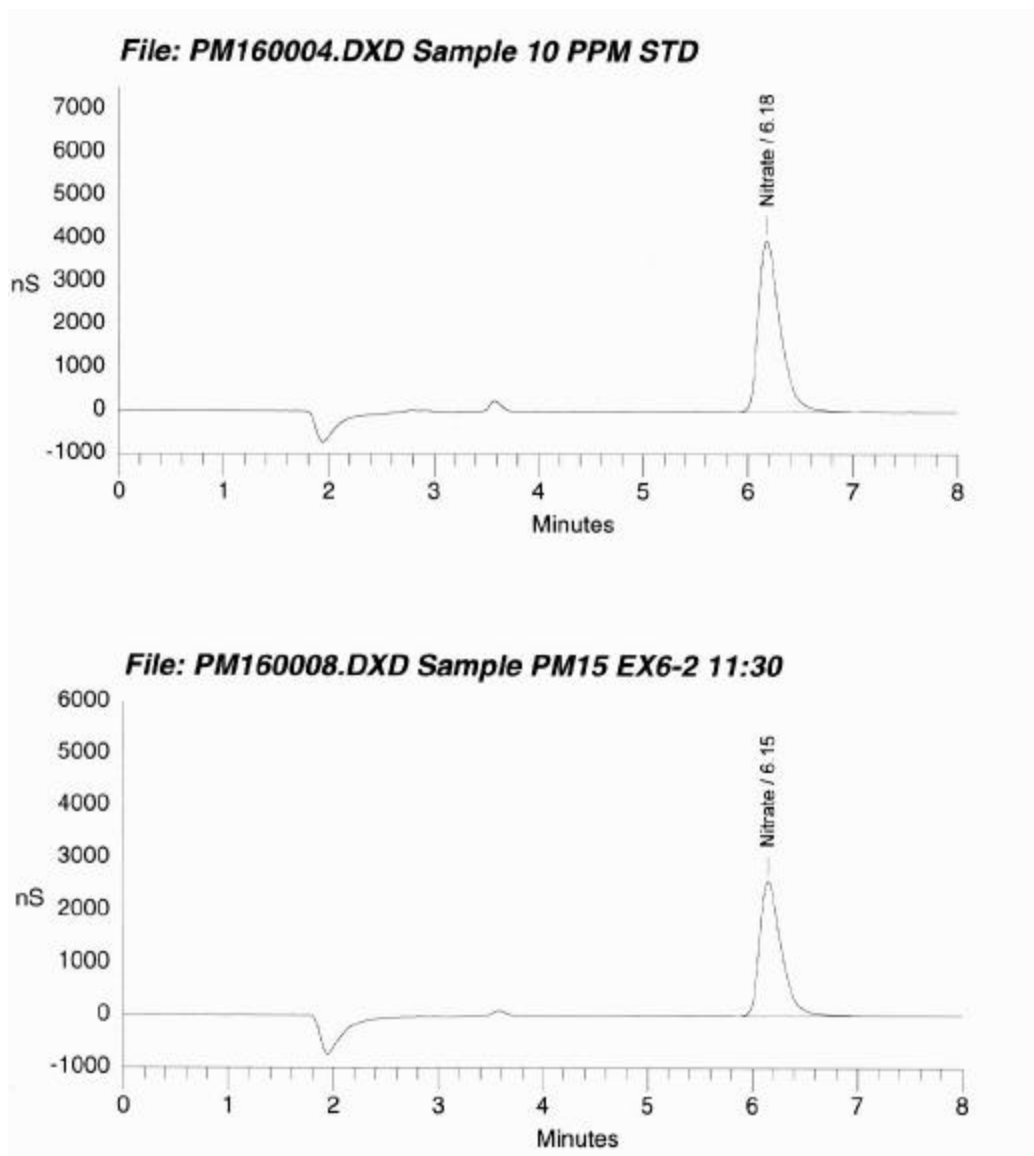


Figure 2. On top is an anion chromatogram (Model DX-120 ion chromatograph with PeakNet software, Dionex Corp., Sunnyvale, CA) of a high purity standard nitrate solution (EM Industries, Inc., Gibbstown, NJ). The bottom anion chromatogram is from a sample eluted from aerosol collected on a Supor[®]-800 filter (47 mm diameter, Pall Gelman Sciences, Ann Arbor, MI) from the chamber containing PM during a low concentration exposure. Conductivity in microsiemens is on the ordinate, and retention time is on the abscissa of the chromatograms. The chromatograms are nearly identical, indicating that the anionic species present in the PM aerosol was nitrate of high purity.

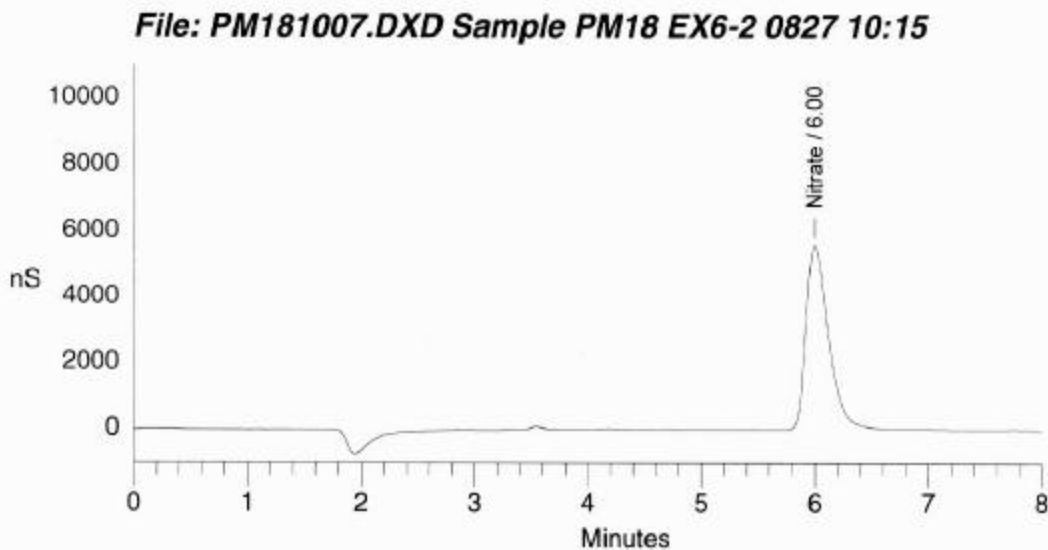
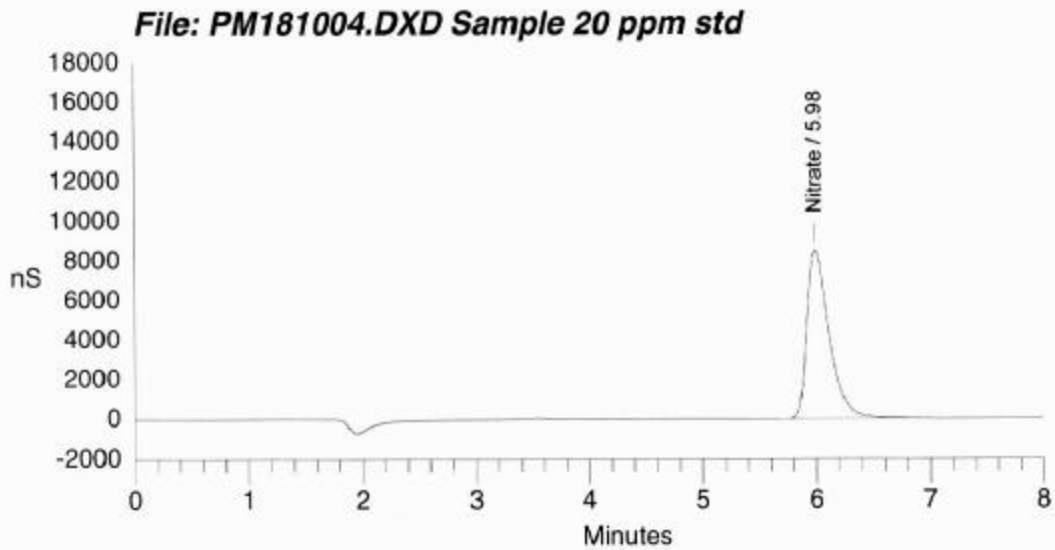


Figure 2. (Continued) The top anion chromatogram is of a standard nitrate solution at a concentration equivalent to the PM aerosol sample anion chromatogram below. The aerosol was collected from the chamber containing PM during an intermediate concentration exposure. Like the low concentration standard and sample, the chromatograms are equivalent.

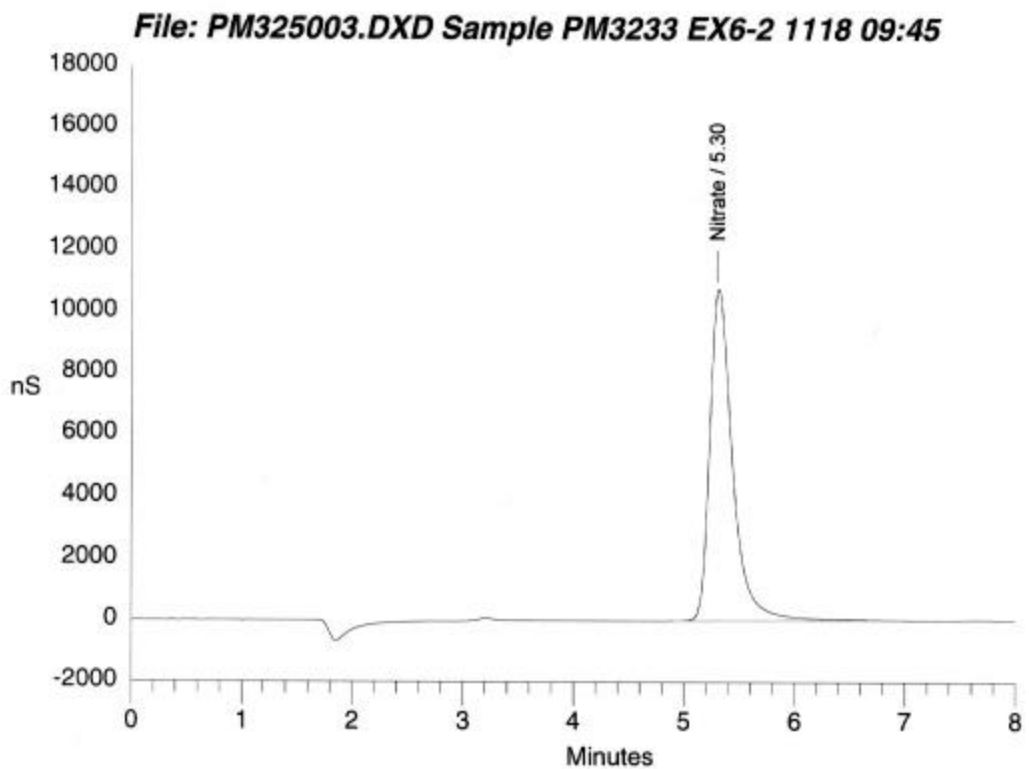
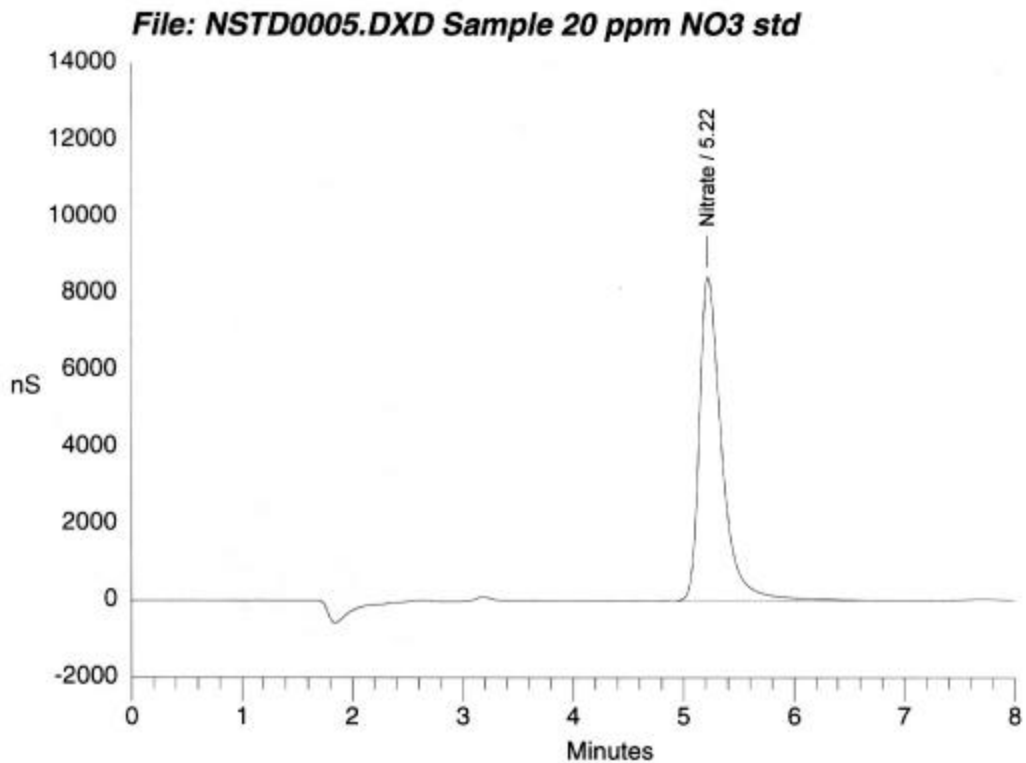


Figure 2. (Continued) This is a comparison of nitrate standard on the top with PM aerosol collected from the chamber containing PM during a high concentration exposure. Again, the anion chromatograms are equivalent.

Carbon was analyzed by Dr. Fung by his method of selective thermal oxidation that speciates elemental and organic carbon (Fung, 1990). As expected, elemental carbon was the predominant species present in the PM from the exposure atmospheres. The carbon analysis results are expressed as elemental carbon. Figure 3 is a photograph of quartz fiber filters on which PM aerosol was collected and analyzed for carbon content. Organic carbon was a ubiquitous contaminant. Relatively small amounts of organic carbon were detected in samples from the PM aerosol chambers, filtered air chamber and on filter blanks analyzed with the samples. The origin of any organic carbon in excess of what was found on the filter blanks was possibly the rodent diet or the rats themselves. During seven exposures, a total of 14 samples for carbon analysis were collected from the filtered air chamber. Elemental carbon from these was below the reliable detectable limit of the method and averaged less than 0.3% of that measured in the corresponding chambers containing the PM aerosol.

The target ozone concentration of 0.2 ppm was reached during each exposure with typical standard deviations 5% or less than the mean concentration. No ozone could be detected in the PM alone or filtered air atmospheres. The chamber filtration system is very effective for removing ambient ozone. Testing was conducted to see if reaction between ozone and the PM could be detected. The chamber was adjusted to a stable 0.20 ppm O₃. Then PM aerosol was generated and introduced into this chamber, in effect a gas phase titration of ozone and PM. No decrease in ozone concentration was evident. Over several hours the ozone concentration maintained the typical stability of ± 0.01 ppm with no adjustment required. During exposures no problems were encountered generating and monitoring stable ozone concentrations in the presence of PM. This was expected because the nitrate is in the highest oxidation state for oxides of nitrogen, and we would expect elemental carbon to be relatively inert under the conditions of these atmospheres. The photomicrographs of Figure 4 are particles imaged by light and scanning electron microscopy collected from about 12 liters of chamber air on Nuclepore[®] membrane filters (0.2 μ m pore size, 25 mm diameter, Whatman, Inc., Clifton, NJ). These were taken simply to view the general appearance of the PM collected.

The actual characterization of particle size distribution and aerodynamic behavior of particles for each experiment were determined. The actual mass of particles was determined gravimetrically by filter collection of known volumes of chamber air. Samples were taken from all levels of the chambers to demonstrate a consistent concentration of particles throughout the chamber for each experiment. Simultaneous measurement of particle mass was also done throughout each experiment using a piezobalance.

A cascade impactor with multiple stages was used to determine the mass median aerodynamic diameter (MMAD) and geometric standard deviation (s_g) of particles.

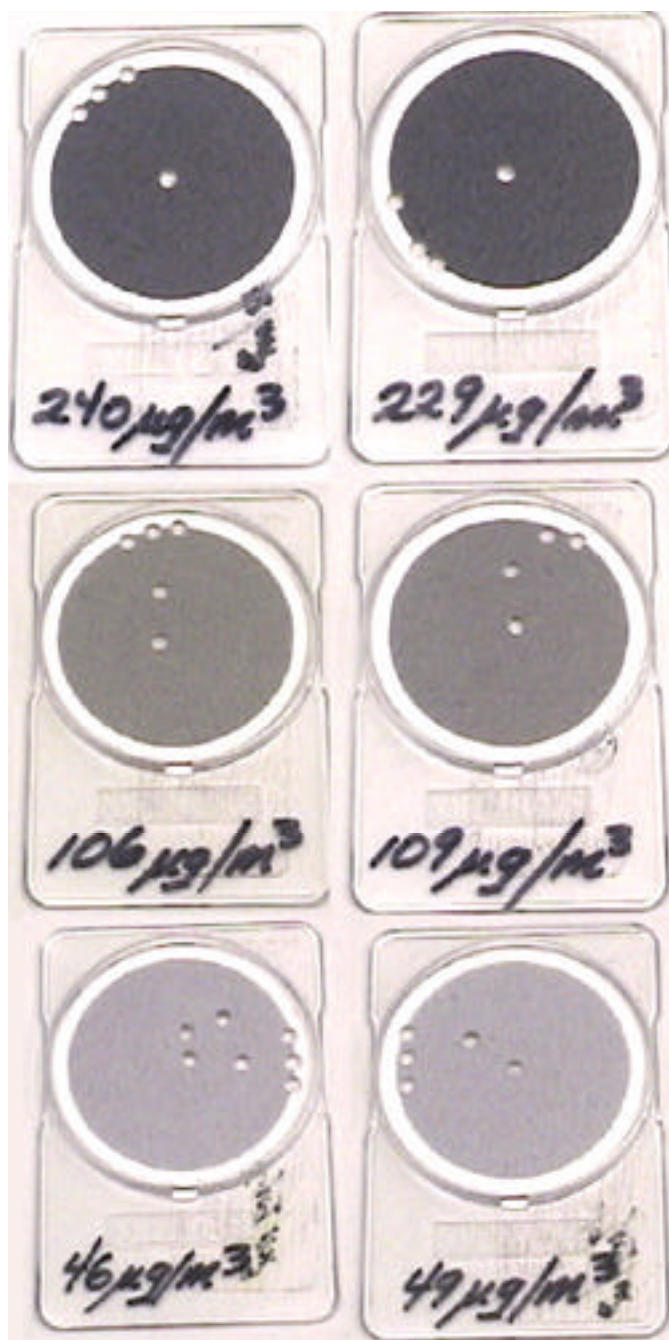


Figure 3. PM samples for carbon analysis collected simultaneously on quartz fiber filters (QM-A, 47 mm diameter, Whatman, Inc., Clifton, NJ) from each of the two chambers containing the aerosol. Pairs for high, intermediate and low concentrations are from top to bottom with the carbon mass concentration hand written on each filter container. Disks 3 mm in diameter were punched out of each filter for carbon analysis (Fung, 1990). Holes spanning the edge of a deposit were made to clean the punch mechanism before sample disks were removed.

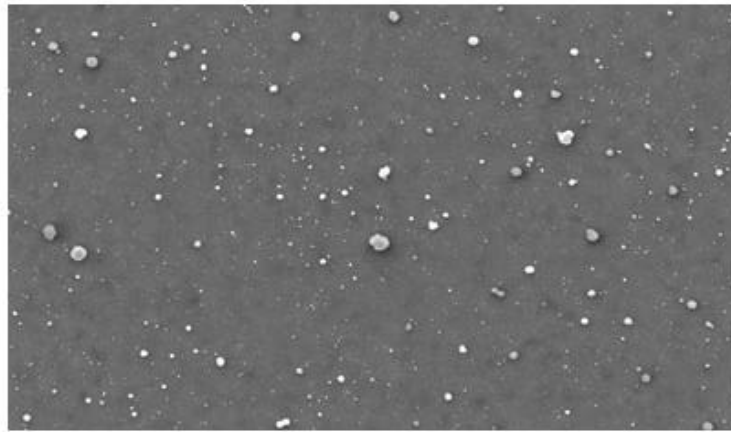
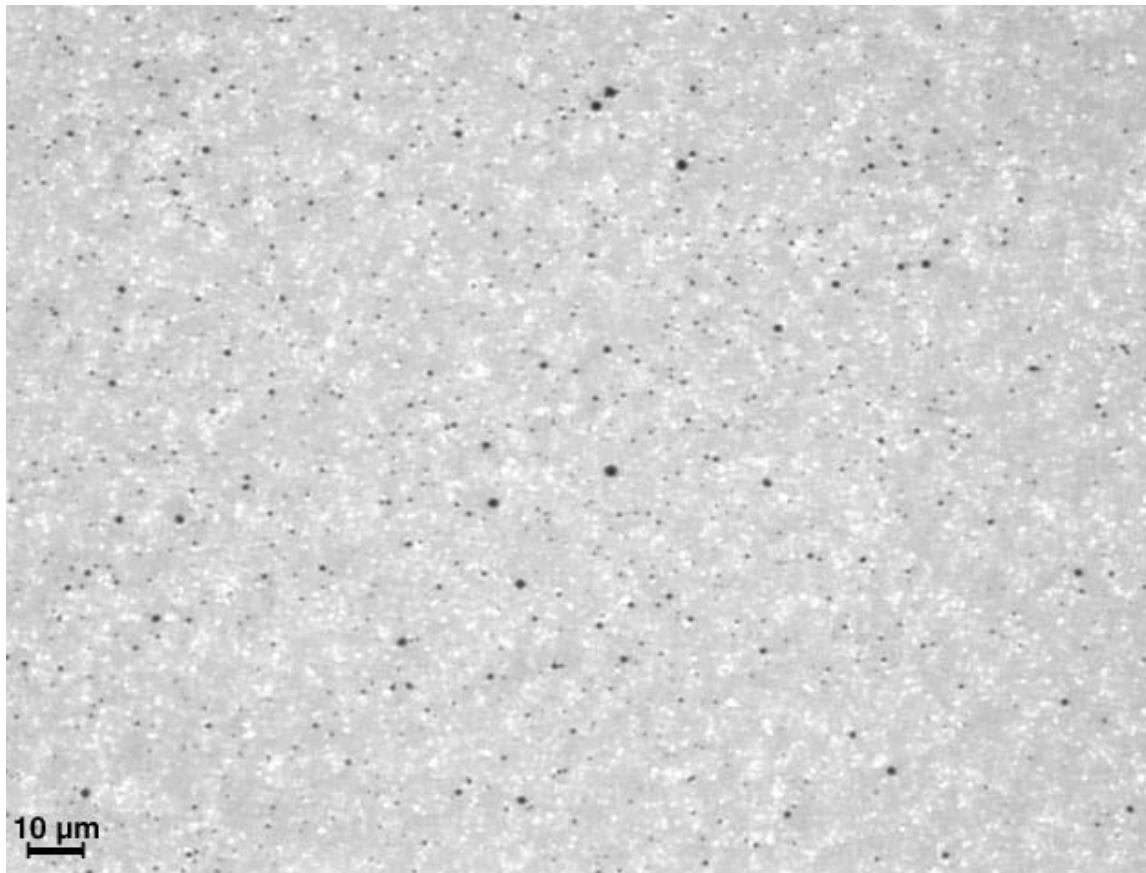


Figure 4. The top photograph is a light micrograph of the PM aerosol collected on a 0.2 μm pore size Nuclepore[®] filter (Whatman, Inc., Clifton, NJ). The bottom photograph is a scanning electron micrograph of a similar sample that was sputter coated with gold for stability in the electron beam.

B. Summary of exposure matrix for toxicology studies

Tables 1-4 provide a summary of all exposure conditions used and biological measures done to determine the effects of exposure to ammonium nitrate, carbon, and/or ozone in the lungs of Fischer 344 and Sprague Dawley rats. Tables 1A-B summarize all single and 3-day exposures in adult male Fischer 344 rats, Table 2 - all 3-day exposures in adult male Sprague Dawley rats, Table 3 - all 3-day exposures in senescent male Fischer 344 rats, and Table 4 - all 3-day exposures in male and female neonatal Fischer 344 rats.

TABLE 1A. SINGLE 6-HOUR EXPOSURE OF ADULT MALE FISCHER 344 RATS USING THREE DIFFERENT TARGET CONCENTRATIONS OF AMMONIUM NITRATE (NH₄NO₃) AND CARBON (C)

AGE	PARTICLE CONCENTRATION			O ₃	PARTICLE EXPOSURE	BIOLOGICAL MEASURES
	HIGH	INTERM	LOW			
ADULT	+	-	-	-	+	1, 2, 3
ADULT	-	+	-	-	+	1, 2, 3, 4
ADULT	-	-	+	-	+	3
ADULT	+	-	-	+	+	1, 2, 3
ADULT	-	+	-	+	+	1, 2, 3
ADULT	-	-	+	+	+	3
ADULT	-	-	-	+	+	1, 2, 3
ADULT	-	-	-	-	+	1, 2, 3, 4

- | | | |
|------------------------|---------------------------|-----------------------|
| 1. Cell Permeability | 2. Glutathione Level | 3. Cell Proliferation |
| 4. Particle Deposition | 5. Bronchoalveolar Lavage | |

TABLE 1B. REPEATED 6-HOUR EXPOSURE FOR 3 DAYS OF HEALTHY ADULT MALE FISCHER 344 RATS AT THE INTERMEDIATE TARGET CONCENTRATION OF AMMONIUM NITRATE (NH₄NO₃) AND CARBON (C).

AGE	PARTICLE CONCENTRATION			O ₃	PARTICLE EXPOSURE	BIOLOGICAL MEASURES
	HIGH	INTERM	LOW			
ADULT	-	+	-	-	+	1, 2, 3, 5
ADULT	-	+	-	+	+	1, 2, 3, 5
ADULT	-	-	-	+	+	1, 2, 3, 5
ADULT	-	-	-	-	+	1, 2, 3, 5

- | | | |
|------------------------|---------------------------|-----------------------|
| 1. Cell Permeability | 2. Glutathione Level | 3. Cell Proliferation |
| 4. Particle Deposition | 5. Bronchoalveolar Lavage | |

TABLE 2 REPEATED 6-HOUR EXPOSURE FOR 3 DAYS OF ADULT MALE SPRAGUE DAWLEY RATS AT THE INTERMEDIATE TARGET CONCENTRATIONS OF AMMONIUM NITRATE (NH₄NO₃) AND CARBON (C).

AGE	PARTICLE CONCENTRATION			O ₃	PARTICLE EXPOSURE 3 DAYS	BIOLOGICAL MEASURES
	HIGH	INTERM	LOW			
ADULT	-	+	-	-	+	1, 2, 3, 4, 5
ADULT	-	+	-	+	+	1, 2, 3
ADULT	-	-	-	+	+	1, 2, 3
ADULT	-	-	-	-	+	1, 2, 3, 5

1. Cell Permeability 2. Glutathione Level 3. Cell Proliferation
 4. Particle Deposition 5. Bronchoalveolar Lavage

TABLE 3. REPEATED 6-HOUR EXPOSURE FOR 3 DAYS OF SENESCENT MALE FISCHER 344 RATS AT THE INTERMEDIATE TARGET CONCENTRATION OF AMMONIUM NITRATE (NH₄NO₃) AND CARBON (C).

AGE	PARTICLE CONCENTRATION			O ₃	PARTICLE EXPOSURE 3 DAYS	BIOLOGICAL MEASURES
	HIGH	INTERM	LOW			
SENESCENT	-	+	-	-	+	1, 2, 3, 4, 5
SENESCENT	-	+	-	+	+	1, 2, 3
SENESCENT	-	-	-	+	+	1, 2, 3
SENESCENT	-	-	-	-	+	1, 2, 3, 5

1. Cell Permeability 2. Glutathione Level 3. Cell Proliferation
 4. Particle Deposition 5. Bronchoalveolar Lavage

TABLE 4 REPEATED 6-HOUR EXPOSURE FOR 3 DAYS AT ONE WEEK AND THREE WEEKS OF AGE IN NEONATAL MALE AND FEMALE FISCHER 344 RATS.

AGE	PARTICLE CONCENTRATION			O ₃	PARTICLE EXPOSURE 3 DAYS	BIOLOGICAL MEASURES
	HIGH	INTERM	LOW			
NEONATAL	+	-	-	-	+	1, 2, 3, 5
NEONATAL	-	+	-	-	+	1, 2, 3, 5
NEONATAL	-	-	+	-	+	1, 2, 3, 5
NEONATAL	+	-	-	+	+	1, 2, 3, 5
NEONATAL	-	+	-	+	+	1, 2, 3, 5
NEONATAL	-	-	+	+	+	1, 2, 3, 5
NEONATAL	-	-	-	+	+	1, 2, 3, 5
NEONATAL	-	-	-	-	+	1, 2, 3, 4, 5

1. Cell Permeability 2. Glutathione Level 3. Cell Proliferation
 4. Particle Deposition 5. Bronchoalveolar Lavage

C. Summary of exposure conditions for toxicology studies

The actual exposure concentrations attained for NH₄NO₃, carbon and ozone for each of the exposure conditions listed in Tables 1-4 are found in Tables 5-9. For actual NH₄NO₃, carbon and ozone concentrations generated in each chamber for each of the 38 experiments (PM1-39) completed, the reader is referred to the Appendix of this report.

Table 5. Single 6-hour exposure of adult male Fischer 344 rats using three different target concentrations of ammonium nitrate (NH₄NO₃) and carbon (C).

<u>Chamber 1: (PM)</u>	<u>Target</u>	<u>Actual</u>	<u>Particle Size</u>	
	<u>Concentration</u>	<u>Concentration</u> *	<u>MMAD (μm)</u>	<u>σ_g</u>
	<u>High</u>			
NH ₄ NO ₃ (μg/m ³)	300	300 ± 44	0.92	2.22
C (μg/m ³)	200	211 ± 112		
	<u>Intermediate</u>			
NH ₄ NO ₃ (μg/m ³)	150	153 ± 30	0.94	2.04
C (μg/m ³)	100	274 ± 40		
	<u>Low</u>			
NH ₄ NO ₃ (μg/m ³)	75	76 ± 6	1.09	1.90
C (μg/m ³)	50	63 ± 9		
<u>Chamber 2: (PM + O₃)</u>				
	<u>High</u>			
NH ₄ NO ₃ (μg/m ³)	300	319 ± 80	0.88	2.10
C (μg/m ³)	200	260 ± 197		
O ₃ (ppm)	0.20	0.20 ± 0.01	--	--
	<u>Intermediate</u>			
NH ₄ NO ₃ (μg/m ³)	150	155 ± 39	0.99	2.00
C (μg/m ³)	100	260 ± 42		
O ₃ (ppm)	0.20	0.20 ± 0.01		
	<u>Low</u>			
NH ₄ NO ₃ (μg/m ³)	75	78 ± 2	1.08	2.00
C (μg/m ³)	50	60 ± 1		
O ₃ (ppm)	0.20	0.2 ± 0	--	--
<u>Chamber 3: (O₃)</u>				
O ₃ (ppm)	0.20	0.20 ± 0.01	--	--
NH ₄ NO ₃ (μg/m ³)	0	0	--	--
C (μg/m ³)	0	0	--	--
<u>Chamber 4: (FA)</u>				
Filtered Air (%)	100	100	--	--
NH ₄ NO ₃ (μg/m ³)	0	0	--	--
C (μg/m ³)	0	0	--	--
O ₃ (ppm)	0	0	--	--

* Actual concentrations are mean ± standard deviation.

Particle size for each experiment was determined and expressed as mass median aerodynamic diameter (MMAD) and geometric standard deviation (σ_g) to reflect the relative heterogeneity of particle size for each experiment.

Table 6. Repeated 6-hour exposure for 3 days of adult male Sprague Dawley rats at the Intermediate target concentrations of ammonium nitrate (NH₄NO₃) and carbon (C).

	<u>Target</u>	<u>Actual</u>	<u>Particle Size</u>	
	<u>Concentration</u>	<u>Concentration</u> *	MMAD (μm)	σ_g
<u>Chamber 1: (PM)</u>				
NH ₄ NO ₃ ($\mu\text{g}/\text{m}^3$)	150	147 \pm 9	1.03	2.07
C ($\mu\text{g}/\text{m}^3$)	100	205 \pm 29		
<u>Chamber 2: (PM + O₃)</u>				
NH ₄ NO ₃ ($\mu\text{g}/\text{m}^3$)	150	136 \pm 11	1.08	2.00
C ($\mu\text{g}/\text{m}^3$)	100	182 \pm 49		
O ₃ (ppm)	0.20	0.20 \pm 0.01	--	--
<u>Chamber 3: (O₃)</u>				
O ₃ (ppm)	0.20	0.20 \pm 0.01	--	--
NH ₄ NO ₃ ($\mu\text{g}/\text{m}^3$)	0	0	--	--
C ($\mu\text{g}/\text{m}^3$)	0	0	--	--
<u>Chamber 4: (FA)</u>				
Filtered Air (%)	100	100	--	--
NH ₄ NO ₃ ($\mu\text{g}/\text{m}^3$)	0	0	--	--
C ($\mu\text{g}/\text{m}^3$)	0	0	--	--
O ₃ (ppm)	0	0	--	--

* Actual concentrations are mean \pm standard deviation.

Table 7. Repeated 6-hour exposure for 3 days of healthy adult male Fischer 344 rats at the intermediate target concentration of ammonium nitrate (NH₄NO₃) and carbon (C).

	<u>Target</u>	<u>Actual</u>	<u>Particle Size</u>	
	<u>Concentration</u>	<u>Concentration</u> *	MMAD (μm)	σ _g
<u>Chamber 1: (PM)</u>				
NH ₄ NO ₃ (μg/m ³)	150	169 ± 13	0.86	2.38
C (μg/m ³)	100	116 ± 16		
<u>Chamber 2: (PM + O₃)</u>				
NH ₄ NO ₃ (μg/m ³)	150	163 ± 16	0.96	2.43
C (μg/m ³)	100	117 ± 18		
O ₃ (ppm)	0.20	0.19 ± 0.01	--	--
<u>Chamber 3: (O₃)</u>				
O ₃ (ppm)	0.20	0.20 ± 0.01	--	--
NH ₄ NO ₃ (μg/m ³)	0	0	--	--
C (μg/m ³)	0	0	--	--
<u>Chamber 4: (FA)</u>				
Filtered Air (%)	100	100	--	--
NH ₄ NO ₃ (μg/m ³)	0	0	--	--
C (μg/m ³)	0	0	--	--
O ₃ (ppm)	0	0	--	--

* Actual concentrations are mean ± standard deviation.

Table 8. Repeated 6-hour exposure for 3 days of senescent male Fischer 344 rats at the intermediate target concentration of ammonium nitrate (NH₄NO₃) and carbon (C).

<u>Chamber 1: (PM)</u>	<u>Target</u>	<u>Actual</u>	<u>Particle Size</u>	
	<u>Concentration</u>	<u>Concentration</u> *	<u>MMAD (μm)</u>	<u>σ_g</u>
NH ₄ NO ₃ (μg/m ³)	150	157 ± 13	0.98	2.41
C (μg/m ³)	100	118 ± 9		
<u>Chamber 2: (PM + O₃)</u>				
NH ₄ NO ₃ (μg/m ³)	150	151 ± 15	1.10	2.40
C (μg/m ³)	100	114 ± 15		
O ₃ (ppm)	0.20	0.19 ± 0.01	--	--
<u>Chamber 3: (O₃)</u>				
O ₃ (ppm)	0.20	0.20 ± 0.01	--	--
NH ₄ NO ₃ (μg/m ³)	0	0	--	--
C (μg/m ³)	0	0	--	--
<u>Chamber 4: (FA)</u>				
Filtered Air (%)	100	100	--	--
NH ₄ NO ₃ (μg/m ³)	0	0	--	--
C (μg/m ³)	0	0	--	--
O ₃ (ppm)	0	0	--	--

* Actual concentrations are mean ± standard deviation.

Table 9. Repeated 6-hour exposure for 3 days of young (neonatal) male and female Fischer 344 rats at three different target concentrations of ammonium nitrate (NH₄NO₃) and carbon (C).

<u>Chamber 1: (PM)</u>	<u>Target</u>	<u>Actual</u>	<u>Particle Size</u>	
	<u>Concentration</u>	<u>Concentration</u> *	<u>MMAD (μm)</u>	<u>σ_g</u>
	<u>High</u>			
NH ₄ NO ₃ (μg/m ³)	300	285 ± 10	1.18	2.65
C (μg/m ³)	200	245 ± 8		
	<u>Intermediate</u>			
NH ₄ NO ₃ (μg/m ³)	150	142 ± 9	1.23	2.33
C (μg/m ³)	100	118 ± 18		
	<u>Low</u>			
NH ₄ NO ₃ (μg/m ³)	75	77 ± 2	0.97	2.00
C (μg/m ³)	50	56 ± 1		
<u>Chamber 2: (PM + O₃)</u>				
	<u>High</u>			
NH ₄ NO ₃ (μg/m ³)	300	292 ± 11	1.10	2.33
C (μg/m ³)	200	242 ± 4		
O ₃ (ppm)	0.20	0.19 ± 0.01	--	--
	<u>Intermediate</u>			
NH ₄ NO ₃ (μg/m ³)	150	145 ± 9	1.19	2.33
C (μg/m ³)	100	121 ± 17		
O ₃ (ppm)	0.20	0.20 ± 0.01	--	--
	<u>Low</u>			
NH ₄ NO ₃ (μg/m ³)	75	76 ± 2	0.98	2.05
C (μg/m ³)	50	56 ± 4		
O ₃ (ppm)	0.20	0.20 ± 0.01	--	--
<u>Chamber 3: (O₃)</u>				
O ₃ (ppm)	0.20	0.20 ± 0.01	--	--
NH ₄ NO ₃ (μg/m ³)	0	0	--	--
C (μg/m ³)	0	0	--	--
<u>Chamber 4: (FA)</u>				
Filtered Air (%)	100	100	--	--
NH ₄ NO ₃ (μg/m ³)	0	0	--	--
C (μg/m ³)	0	0	--	--
O ₃ (ppm)	0	0	--	--

* Actual concentrations are mean ± standard deviation.

B. Measure 1: Cell Permeability

The purpose of this task was to establish whether particulate exposure with or without co-exposure to ozone alters the level of cell injury based on loss of membrane integrity. Table 10 summarizes our evaluation of the extent and distribution of permeable cells.

Table 10. Comparison of relative severity of injury following exposure to particulates, particulates + ozone, ozone alone or filtered air. F344 Rats Adult, Senescent and Neonate; S-D Rats, Adult

Group (N)	Exposure	Strain	Dose	Relative Severity of Injury (scale of 0-3)			
				P	P+O ₃	O ₃	FA
Adult (24)	6 hrs for 1 day	F344	Intermediate	1.83	1.75	1.67	1.83
(26)	6 hrs for 1 day	F344	High	1.86	1.93	1.00	1.86
(8)	6 hrs for 3 days	F344	Intermediate	2.00	1.25	0.75	0.25
(20)	6 hrs for 3 days	S-D	Intermediate	0.90	1.20	0.80	1.00
Senescent (15)	6 hrs for 3 days	F344	Intermediate	1.38	1.13	0.50	0.40
Neonate (32)	6 hrs for 3 days	F344	Low	1.44	1.81	1.31	1.63
(32)	6 hrs for 3 days	F344	Intermediate	0.81	0.56	0.88	1.00
(23)	6 hrs for 3 days	F344	High	0.90	1.58	0.58	0.92

P = particulates

P + O₃ = particulates + ozone

O₃ = ozone

FA = filtered air

F344 = Fisher 344 rats

S-D = Sprague-Dawley rats

No significant differences were noted by Krusal-Wallace nonparametric ranking test.

Adult, 1-day, F344, intermediate dose. There was no major difference in the distribution, or relative density of permeable cells in the proximal middle or distal airways of rats exposed to intermediate dose particulates with or without ozone (Table 10).

Adult, 1-day, F344, high dose. As with the intermediate dose animals there was no difference in the distribution or density of permeable cells between the four exposure groups. The least severe level of injury was actually found within the ozone alone group, but there was no clear distinguishable difference between the four exposure groups (Table 10).

Adult, 3-day, F344, intermediate dose. There was an apparent difference between the three exposure groups and the filtered animals in the relative level and distribution of permeable cells. However, these differences were not statistically significant. The particulate group had the highest level of severity and the filtered air group the lowest level (Table 10 and Figure 5).

Unfortunately, a limited number of animals were available for this analysis at the intermediate dose.

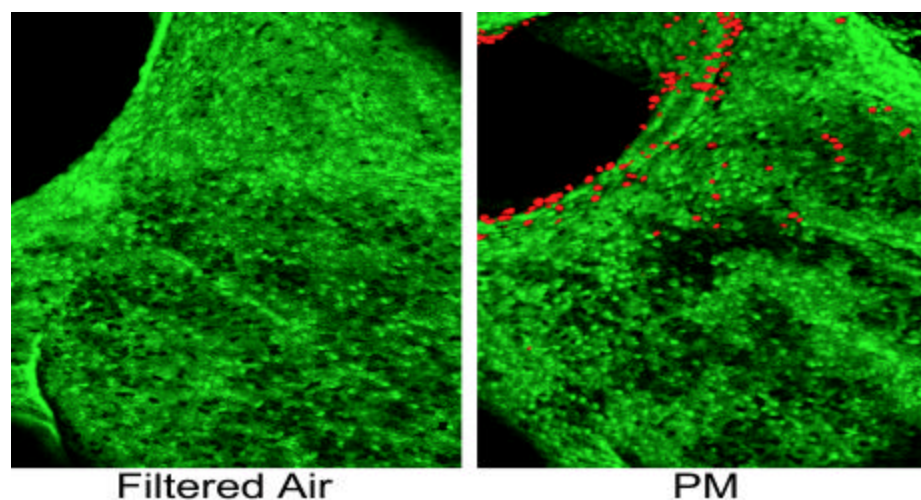


Figure 5 Confocal fluorescent laser scanning microscopy of the lung airways of an adult rat exposed to filtered air or to ammonium nitrate ($147 \pm 9 \mu\text{g}/\text{m}^3$) and carbon ($205 \pm 29 \mu\text{g}/\text{m}^3$) 6 h/day for 3 days. Epithelial cell permeability, identified as EtD-1 positive cells (red), line the surfaces of the airways at the level of the airway bifurcation. Few EtD-1 positive cells are present in the airway of a rat exposed to filtered air for three days. In contrast, the airway bifurcation contains numerous EtD-1 positive cells following PM exposure for three days.

Adult, 3-day, S-D, intermediate dose. There was no difference in the severity or distribution of permeable cells between the three exposure groups and the filtered air animals (Table 10).

Senescent, 3-day, F344, intermediate dose. There appeared to be differences between exposure groups in the level of permeable cells based both on density and distribution (Table 10). The group with the highest level of severity was the particulate exposed group. There was no difference between the ozone and the filtered air group, but both exhibited less severity than the particulate or particulate + ozone groups. Limited numbers of animals were available for this study.

Neonate, 3-day, F344, low dose. There was no difference in the density or distribution of permeable cells between the three exposure groups and the filtered air animals (Table 10).

Neonate, 3-day, F344, intermediate dose. The level of density of permeable cells and the distribution was less in all exposure groups and the filtered air animals than it was for the low dose exposed animals (Table 10). There was no clear difference between exposure groups, but the particulate + ozone group showed the least severity.

Neonate, 3-day, F344, high dose. There were no clear differences in the intensity or the extent of permeable cells within the airways of the three exposure groups compared to filtered air controls (Table 10). The only group that had a highly elevated level of cellular injury was the particulate + ozone group, however due to the high degree of inter-group variability for this measurement, a statistically significant difference was not observed with this group and the filtered air animals.

C. Measure 2: GSH in Microdissected Airways

Cellular redox status is a primary factor in controlling the sensitivity of the cell to chemicals which injure the cell by inducing oxidative stress or by agents which are metabolized to electrophilic derivatives. One of the primary detoxication routes for both types of injury involves the utilization of the tripeptide, glutathione (see Meister, 1994 and Rahman et al., 1999 for review). The results of the studies described in this task were used to determine whether exposures to combinations of particles and oxidants (ozone) alter the reduced glutathione levels at specific sites within the lung.

Single 6-hour exposures at high particulate levels in Fischer 344 rats

A total of 6 experiments were performed in rats exposed to filtered air, ozone alone, NH_4NO_3 plus carbon aerosol, and NH_4NO_3 plus carbon aerosol plus ozone (Table 10). Rats were killed immediately after the exposure and airways, isolated by microdissection, were processed for determination of reduced glutathione concentrations by high pressure liquid chromatography (HPLC) with electrochemical detection.

Our past experience in the measurement of glutathione in defined airways is that the levels of this tripeptide may vary from animal to animal. The levels we observed for F344 rats (Figure 6) are similar to those levels measured previously in Sprague Dawley rats. The data presented in Figure 6 are compiled from all exposures conducted at high concentrations of NH_4NO_3 and carbon with 0.2 ppm O_3 for 6 hours. Glutathione levels varied from approximately 5 nmoles/mg protein in the trachea to slightly over 10 nmoles/mg protein in distal airways. None of the exposure conditions resulted in a statistically significant change in reduced glutathione levels compared with filtered air control animals.

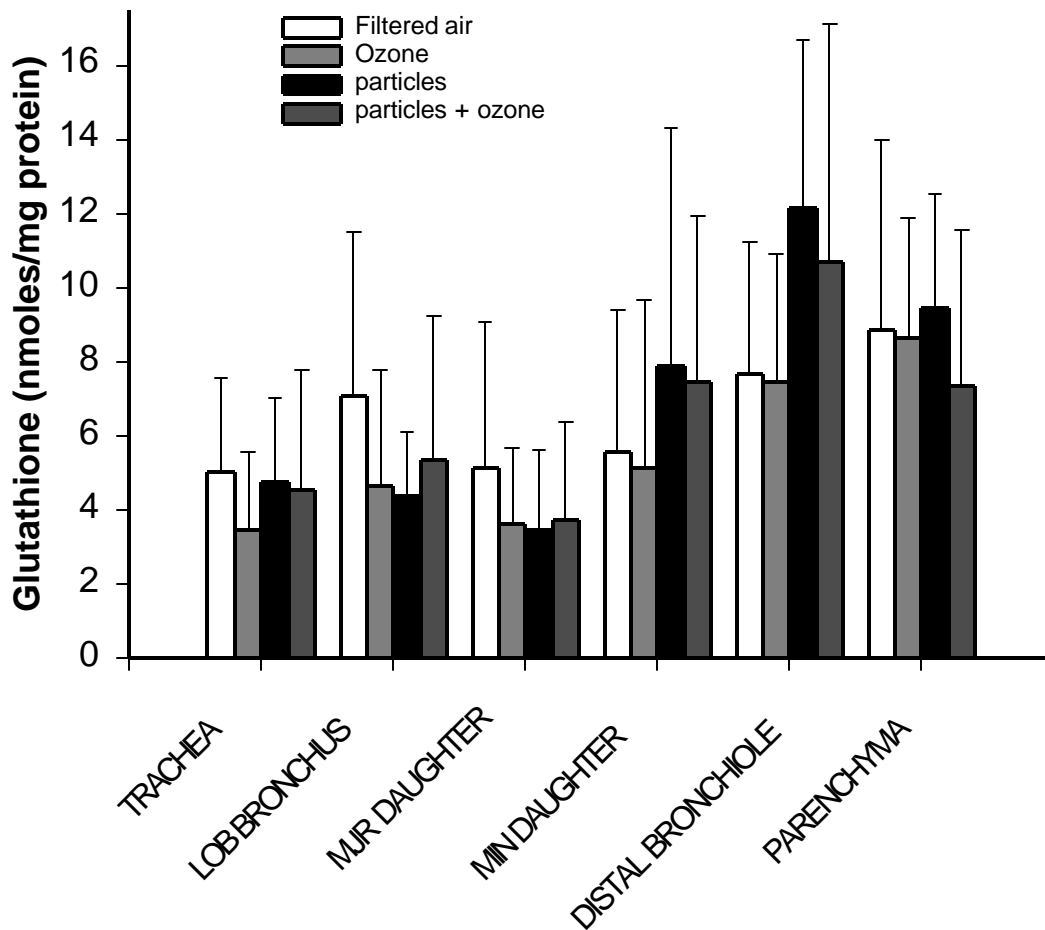


Figure 6 Glutathione levels in dissected airways of male adult F344 rats exposed to filtered air, ozone, particles or particles plus ozone once for 6 hrs. Particle exposure conditions were targeted for the highest particle concentration ranges. The actual concentrations generated were $310 \mu\text{g}/\text{m}^3$; NH_4NO_3 and $235 \mu\text{g}/\text{m}^3$ carbon. Values are the mean \pm SD for the following number of animals: filtered air (6), ozone (4), particles (6) and particles plus ozone (9).

Single 6-hour exposures at intermediate particulate levels in Fischer 344 rats

Although we observed no significant effects on glutathione levels in dissected airways of rats exposed to high particulate levels, we considered that it might be possible to observe effects at lower particulate levels. Accordingly, rats were exposed to filtered air, ozone, particles and particles plus ozone for 6 hours. Sampling was performed immediately after exposure for measurement of glutathione levels. The results of analysis for two animals are illustrated in Figure 7. The high GSH value in the lobar bronchus of particle only exposed animals is due to a data point which appears to be excessively high. Since there were no identifiable reasons for excluding this point, it was averaged. Based on these preliminary findings and the results of the high dose exposure, we were concerned that we were not seeing any treatment related effects due to the plasticity of glutathione levels in the lung.

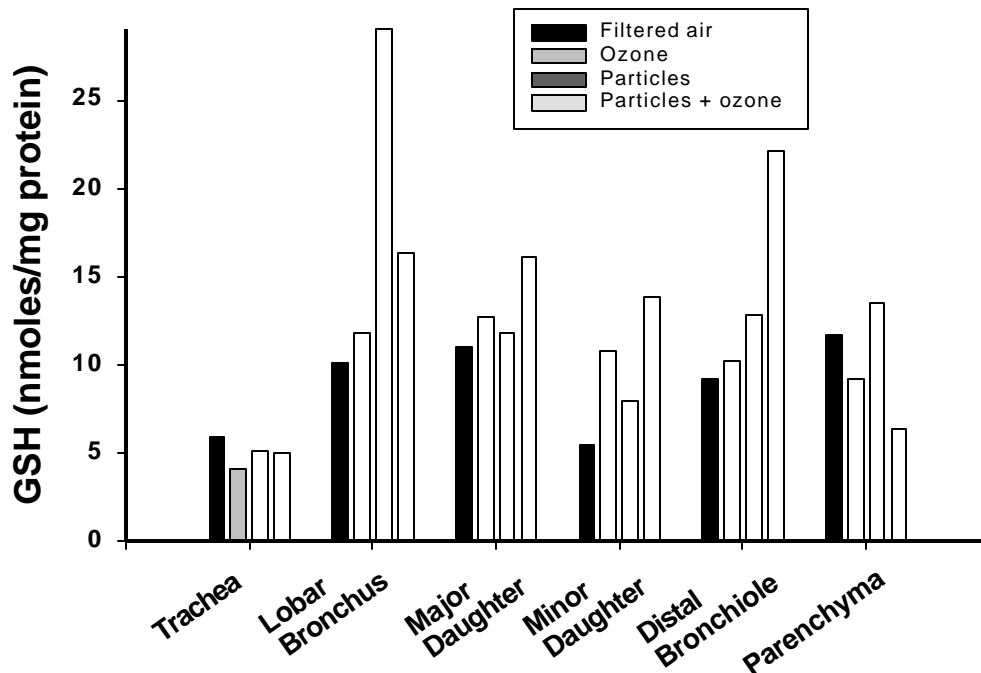


Figure 7 Glutathione levels in dissected airways of adult male F344 rats pretreated with BSO and subsequently exposed for 6 hrs at the intermediate target particle dose. The actual concentrations were $154 \mu\text{g}/\text{m}^3$, NH_4NO_3 , and $265 \mu\text{g}/\text{m}^3$ carbon. Data are the mean of measurements for two animals per group.

Although the normal turnover of glutathione in the lung is relatively slow, it appears that when the lung is challenged with a glutathione depletor, rapid resynthesis can occur. This raised the possibility that, in the 6 hour time period during exposure, sufficient glutathione synthesis was occurring to replace stores lost during as a result of exposure. This possibility is supported by our earlier work demonstrating rapid repletion of glutathione in both mouse and monkey dissected airways (Duan et al., 1996). Accordingly, to determine if glutathione levels could be affected by particle exposure when glutathione synthesis is blocked, we conducted four studies to determine whether differences in glutathione levels are apparent in exposed animals where glutathione synthesis is blocked. For this we have utilized buthionine sulfoximine (BSO), an irreversible inhibitor of glutathione synthetase (Griffith and Meister, 1979). This compound was administered intraperitoneally to all groups of rats at a dose of 800 mg/kg, just prior to the start of the exposure. Rats were killed immediately after the exposure and airways, isolated by microdissection, were processed for determination of reduced glutathione concentrations by HPLC with electrochemical detection. Prior to beginning this study, we conducted limited preliminary work to show that administration of BSO prior to the start of the exposure did not result in decreased airway levels of glutathione.

Additional studies were performed to increase the numbers of animals in each group to four pre-treated with BSO to determine whether glutathione levels would be significantly altered following particle or particle plus ozone exposure. The data showing glutathione levels in dissected airways of rats pretreated with BSO just prior to the start of the exposure to filtered air, ozone, particles and ozone plus particles is presented in Figure 8. The data indicate considerable inter-animal variability in measurements and no statistical, significant differences in glutathione levels between groups.

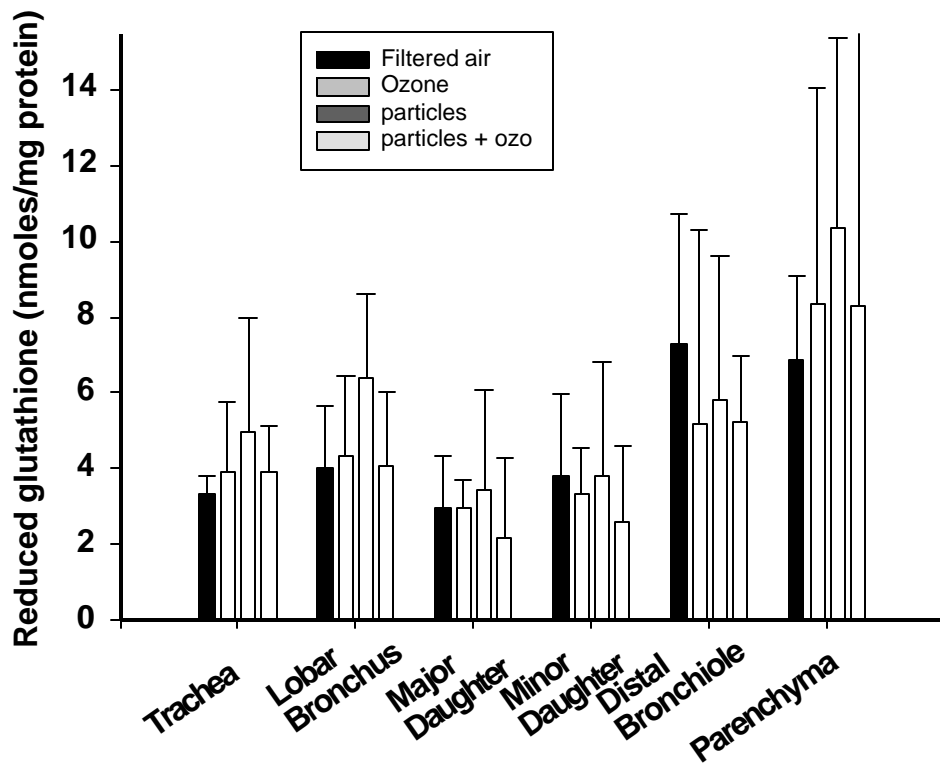


Figure 8 Glutathione levels in airways from adult male F344rats exposed to filtered air, and the intermediate target particle concentrations. The actual concentrations attained were $155 \mu\text{g}/\text{m}^3$, NH_4NO_3 and $265 \mu\text{g}/\text{m}^3$ carbon. Exposures were for 6 hr. All animals were pretreated with BSO prior to exposure. Values are the mean \pm SD for $n=4$ in each group. No statistically significant differences were noted between treatment groups and the control animals.

Multiple 6-hour exposures at intermediate particle concentrations in Sprague Dawley Rats

To determine whether multiple exposures to particles with or without oxidant gas exposure are capable of depleting reduced glutathione, rats were exposed to the intermediate particle exposure level for 6 hrs/day for 3 days. Samples were removed for analysis of glutathione at the end of the exposure period. The data in Figure 9 indicate that there were no significant differences between exposure groups. Note that, even if there were subtle differences in glutathione levels in these exposure groups, they would likely be masked by the high variability in the glutathione levels observed in all of these studies. This variability may result from several factors but is likely not related to the analytical methodology employed. Previous validation of the methods showed that coefficients of variation were generally less than 10% at the concentrations noted in the studies described here.

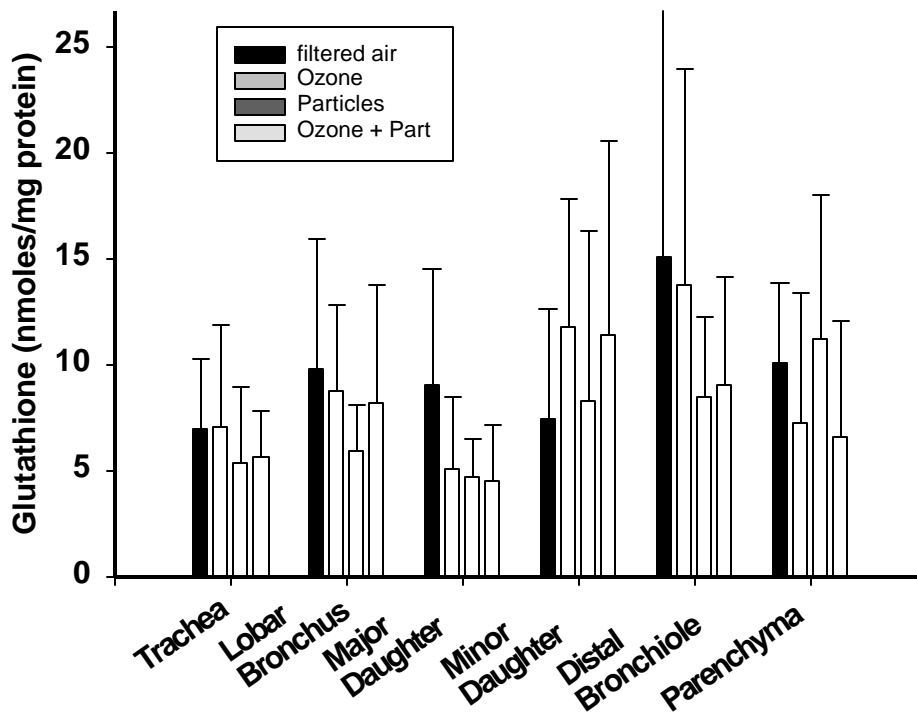


Figure 9 Glutathione levels in airways from adult male Sprague Dawley rats exposed to filtered air, ozone, particles or particles plus ozone. Exposures were 6 hr at the intermediate particle exposure levels for 3 days. (Actual concentrations were 142 $\mu\text{g}/\text{m}^3$, NH_4NO_3 and 190 $\mu\text{g}/\text{m}^3$ carbon.) Values are the mean \pm SD for n=4 in each group.

Age-related differences in pulmonary glutathione and in response to oxidant gases and particles: Single exposures

Studies to determine differences in particle-induced responses in healthy adult and senescent rats were conducted in collaboration with the Air Pollution Health Effects Laboratory at UC Irvine. More specifically, the purpose of these studies was to determine whether there are differences in glutathione levels in microdissected airways of young adult compared to senescent animals and to explore the possibility that the redox status of the lungs of senescent animals was more sensitive to exposure to oxidant gases and/or particles. Accordingly, groups of 9 week old and 24 month old male F344 rats (n=4/group) were exposed to filtered air or to ozone plus NH₄NO₃ plus carbon aerosol at the intermediate target concentration for 3 days. The results are presented in Figure 10.

Statistically significant differences were not observed in glutathione levels in microdissected airways from 9 week old compared to 24 month old rats (filtered air controls). The levels of glutathione were virtually identical in airways of filtered air compared to ozone plus NH₄NO₃/carbon aerosol in both the 9 week and 24 month old F344 rats (Figure 10).

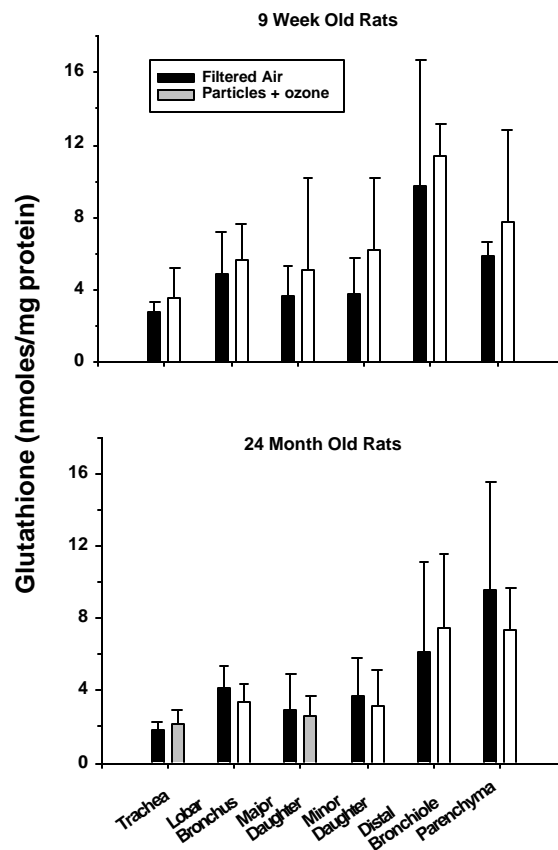


Figure 10 Glutathione levels in airways from adult (9 week old) male and senescent (24 months old) F344 rats exposed to filtered air or particles plus ozone. Particle concentrations were set at the intermediate target levels. (Actual concentrations in adults were 166 $\mu\text{g}/\text{m}^3$ NH₄NO₃ and 116 $\mu\text{g}/\text{m}^3$ for carbon while in senescent rats concentrations were 154 $\mu\text{g}/\text{m}^3$ NH₄NO₃ and 116 $\mu\text{g}/\text{m}^3$ for carbon. Values are the mean \pm SD for n=4 in each group.

These studies suggest that any changes resulting from oxidant gas plus particle exposures are not dramatic and that the variability between animals is sufficient to preclude any statistical differences. Glutathione levels in the lung are capable of rebounding rapidly and it is possible, at the exposure levels used in these studies, that the lung subcompartments are capable of supplying sufficient quantities of glutathione through synthesis to maintain the levels at those observed in filtered air controls.

Age-related differences in pulmonary glutathione and in response to oxidant gases and particles: Multiple exposures (3 days x 6 hr/day) at different particulate exposure concentrations

As described in other sections of this report, one of the purposes of this study was to determine whether either very young or very old animals responded to exposure in a unique fashion. Accordingly, senescent male F344 rats were exposed using the standard 3 day x 6 hr/day protocol (NH_4NO_3 $153 \mu\text{g}/\text{m}^3$, carbon $116 \mu\text{g}/\text{m}^3$ ozone, 0.2 ppm) (Table 8). It appears that the glutathione levels in the controls were slightly higher than those observed in earlier experiments. Since glutathione is highly susceptible to a number of outside influences, this variation could be due to several factors including diet. Comparison of the data among groups reveals no treatment-related differences (Figure 11).

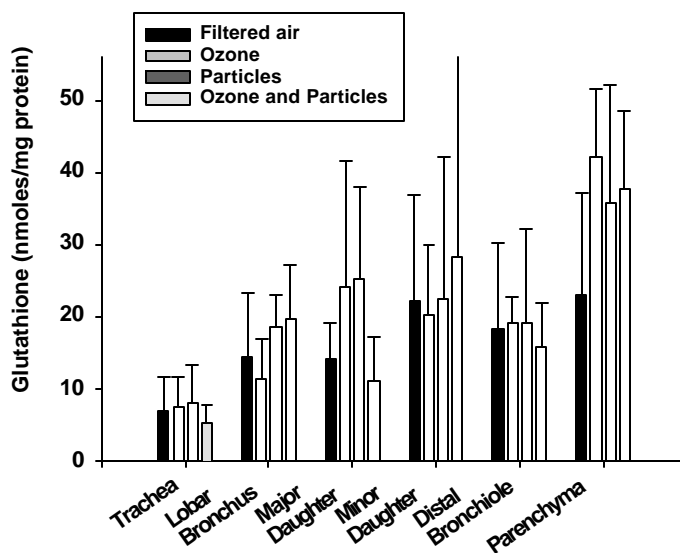


Figure 11 Glutathione levels in airways from male senescent F344 rats exposed to filtered air, to ozone, to particulates or to particulates plus ozone for 3 days at intermediate particulate levels. Actual concentrations were $142 \mu\text{g}/\text{m}^3$ NH_4NO_3 and $190 \mu\text{g}/\text{m}^3$ carbon. Values are the mean \pm SD for four animals in each group with the exception minor daughter and distal bronchiole segments of the particulate group. In these two instances, means and standard deviations exclude results of a single animal with values of 183 and 93 nmoles/mg protein in minor daughter and distal bronchiole, respectively. Protein values in these two analyses were abnormally low and could not be rerun.

Groups of neonatal rats were exposed to filtered air, ozone, particulates or ozone plus particulate using the standard 3 day protocol. Exposures were conducted at intermediate (Figure 12), high (Figure 13) or low particulate levels (Figure 14). The data in Figure 12 were derived from defined airway segments. In this small an animal, the procedure of microdissection became sufficiently time consuming so that we had concerns about the loss of glutathione which might occur during the dissection. Accordingly, in all subsequent experiments, lungs were divided into trachea, airways and parenchyma. As was the case with all of the other data in this study, there appeared to be no treatment related effects of any of the exposures on reduced glutathione levels.

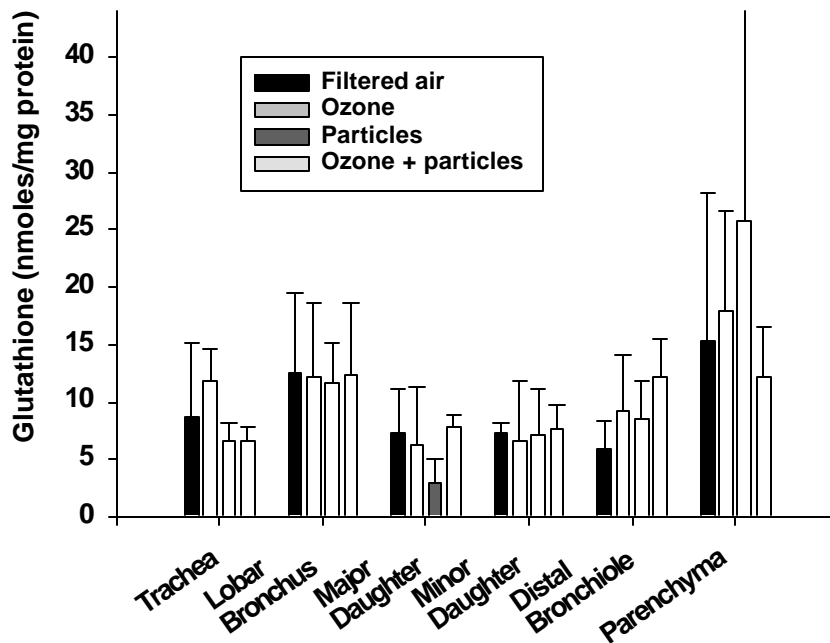


Figure 12 Glutathione levels in tracheobronchial airways of male and female neonatal F344 rats exposed from 3 days to filtered air, particles, ozone or a combination of filtered air and particles. Particulate concentrations were set at the intermediate target concentrations. (Actual concentrations were $143 \mu\text{g}/\text{m}^3 \text{NH}_4\text{NO}_3$ and $119 \mu\text{g}/\text{m}^3$ carbon. Values are the mean \pm SD for n=4.

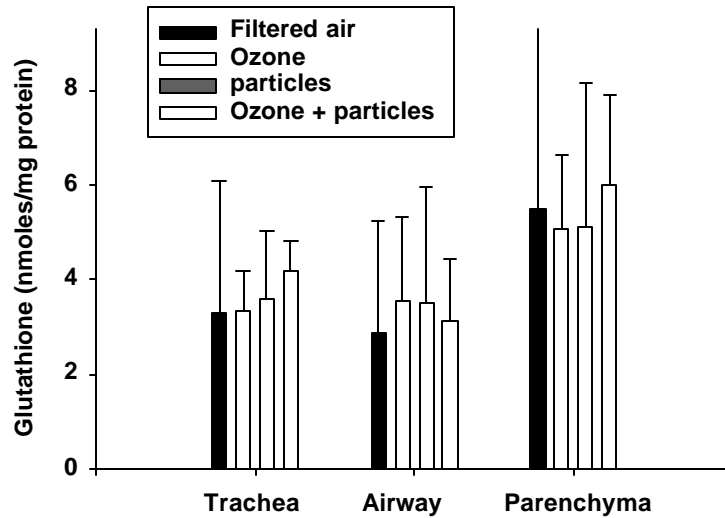


Figure 13 Glutathione levels in airways of male and female neonatal F344 rats exposed for 3 days to atmospheres containing the highest target levels of particulate matter (Actual concentrations were $288 \mu\text{g}/\text{m}^3$ NH_4NO_3 , $243 \mu\text{g}/\text{m}^3$ carbon.) Values are the mean \pm SD for n=5.

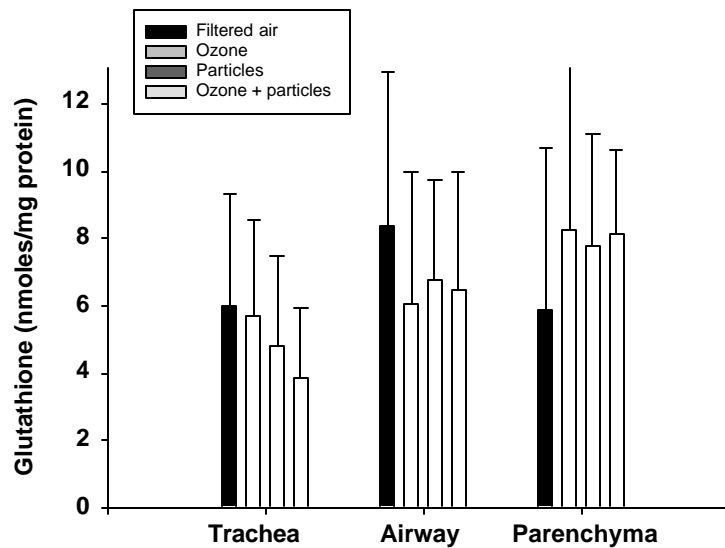


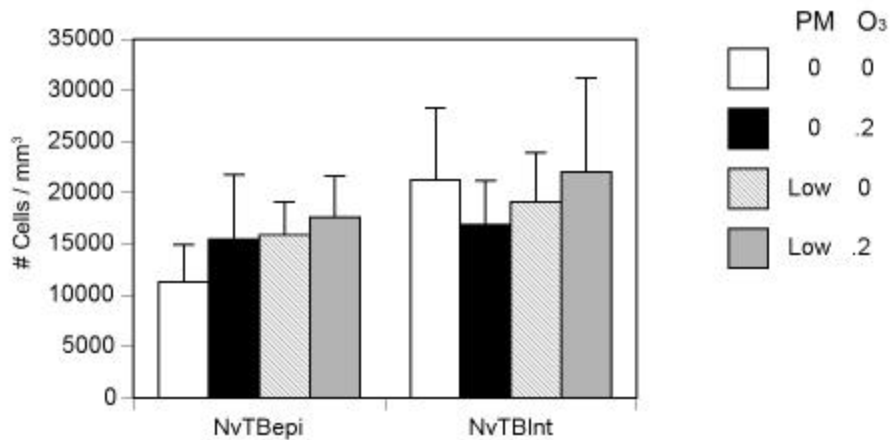
Figure 14 Glutathione levels in lung subcompartments of male and female neonatal F344 rats exposed to atmospheres containing the lowest target levels of particles (Actual concentrations were NH_4NO_3 , $77 \mu\text{g}/\text{m}^3$; and carbon, $56 \mu\text{g}/\text{m}^3$). Values are the mean \pm SD for 6 animals.

D. Measure 3: Cell Proliferation/Morphometry

Cell proliferation measures were designed to serve as indicators of the effects of inhaled particles under different conditions of exposure, concentrations and duration of exposure. Since cell proliferation is a reflection of cell injury and repair, BrdU uptake in cells undergoing DNA synthesis could be an of an adverse particle effect within specific regions of the lungs. Initial studies were done using a single 6 hour exposure to establish a potential dose response in adult male F344 rats.

Short-term exposures of 6 hours to NH_4NO_3 and carbon (PM) alone and PM with ozone (0.2 ppm) followed by 18 h in filtered air were done at low (Figure 15), intermediate (Figure 16) and high (Figure 17) PM concentrations. Although all PM- and ozone-exposed rats showed increased labeling as compared with filtered air control rats, only the intermediate dose of PM showed significantly more labeled cells in the interstitial compartment of terminal bronchioles for PM and PM + ozone exposure groups.

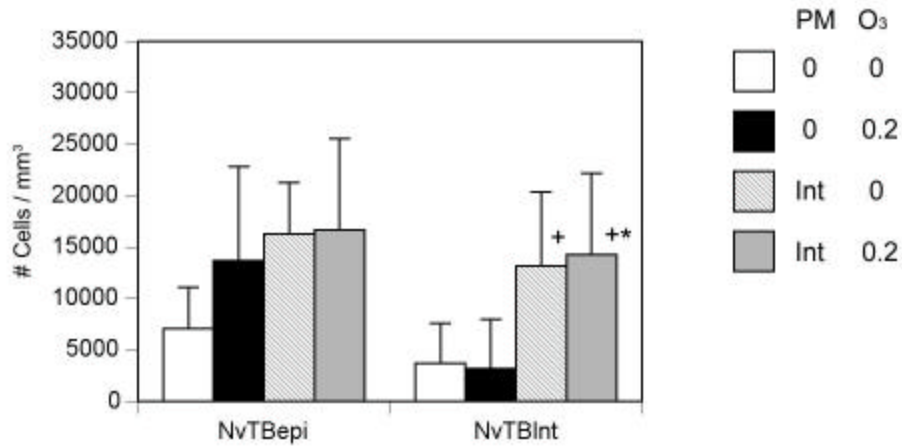
Figure 15. Low Concentration ($77 \mu\text{g}/\text{m}^3 \text{NH}_4\text{NO}_3$, $61 \mu\text{g}/\text{m}^3 \text{C}$)



F344 Adult Male Rats Exposed 6 Hours for 1 Day

Number of animals per exposure group was six. No significant were noted between groups. Abbreviations are $N_v \text{TB}_{\text{EPI}}$ = number of BrdU-labeled terminal bronchiolar epithelial cells per mm^3 of epithelium and $N_v \text{TB}_{\text{INT}}$ = the number of BrdU-labeled terminal bronchiolar interstitial cells per mm^3 of interstitium. All values are the mean of \pm SEM.

**Figure 16. Intermediate Concentration ($154 \mu\text{g}/\text{m}^3 \text{NH}_4\text{NO}_3$, $267 \mu\text{g}/\text{m}^3 \text{C}$)
F344 Adult Male Rats Exposed 6 Hours for 1 Day**



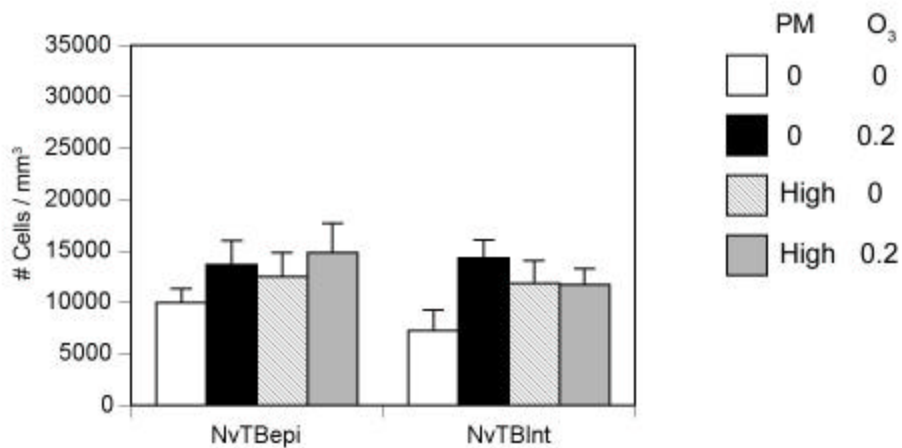
*Significant difference ($P < 0.05$) between groups by ANOVA.

⁺ Significantly different ($P < 0.05$) than 0,0 group (filtered air controls) by Bonferroni test.

Number of animals per exposure group was six.

Abbreviations are $N_V \text{TB}_{\text{EPI}}$ = number of BrdU-labeled terminal bronchiolar epithelial cells per mm^3 of epithelium and $N_V \text{TB}_{\text{INT}}$ = the number of BrdU-labeled terminal bronchiolar interstitial cells per mm^3 of interstitium. All values are the mean \pm SEM.

**Figure 17. High Concentration ($310 \mu\text{g}/\text{m}^3 \text{NH}_4\text{NO}_3$, $230 \mu\text{g}/\text{m}^3 \text{C}$)
F344 Adult Male Rats Exposed 6 Hours for 1 Day**



Number of animals per exposure group was six. No significant differences were noted between groups.

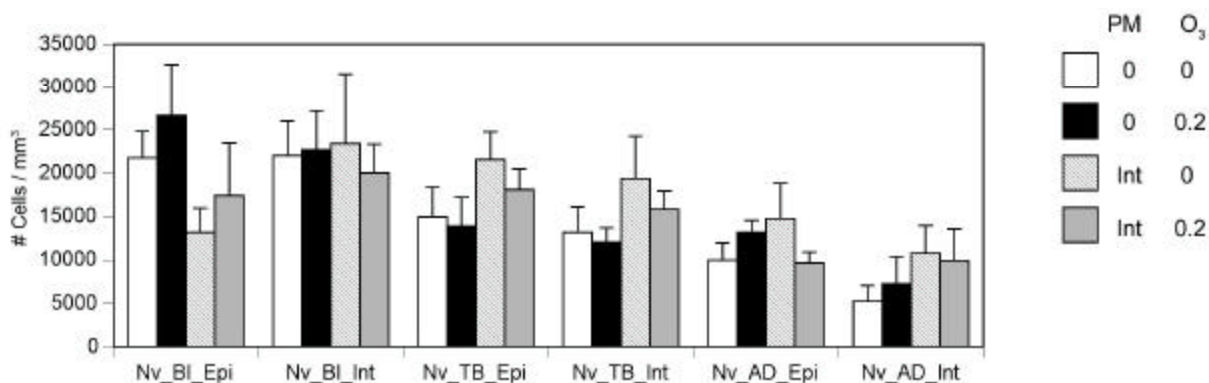
Abbreviations are $N_V TB_{EPI}$ = number of BrdU-labeled terminal bronchiolar epithelial cells per mm^3 of epithelium and $N_V TB_{INT}$ = the number of BrdU-labeled terminal bronchiolar interstitial cells per mm^3 of interstitium. All values are the mean \pm SEM.

Repeated 3-day exposure regimen to particles in adult male F344 rats.

Based on the results of a single day (6 hour) exposure in adult male F344 rats to inhaled particles, the intermediate concentration of NH_4NO_3 and carbon, particle particles was selected for repeated exposure for 6 hours per day for 3 consecutive days. This decision was made upon the significant effects of exposure for a single day in F344 rats on the interstitial compartment of the terminal bronchioles. In this next study we wished to determine if 3 days of repeated particulate exposure in F344 rats would augment the effects observed following a single day of exposure.

The results of these studies are shown in Figure 18. In this study airway bifurcations (N_v BI), terminal bronchioles (TB), and alveolar ducts (AD) were examined.

Figure 18. Intermediate Concentration ($166 \mu g/m^3 NH_4NO_3$, $116 \mu g/m^3 C$) F344 Adult Male Rats Exposed 6 Hours/Day for 3 Days



The number of animals per exposure group was 6. All values are the mean \pm SEM. No significant differences were noted between groups.

Abbreviations are $N_V BI_{EPI}$ = number of BrdU-labeled epithelial cells at bronchial bifurcations per mm^3 of epithelium, $N_V BI_{INT}$ = the number of BrdU-labeled interstitial cells at bronchial bifurcations per mm^3 of interstitium, $N_V TB_{EPI}$ = number of BrdU-labeled terminal bronchiolar epithelial cells per mm^3 of epithelium, $N_V TB_{INT}$ = the number of BrdU-labeled terminal bronchiolar interstitial cells per mm^3 of interstitium, $N_V AD_{EPI}$ = number of BrdU-labeled alveolar duct epithelial cells per mm^3 of epithelium and $N_V AD_{INT}$ = number of BrdU-labeled interstitial cells in alveolar ducts per mm^3 of interstitium.

Repeated 3-day exposure regimen to particles in adult male SD rats.

Although the goal of our study was to work with the F344 rat to measure PM effects in young, adult and senescent animals, we were interested in determining whether another strain of rat may respond in a different manner to the effects of particle exposure. Therefore, adult male Sprague Dawley rats were used to expose rats to the intermediate concentration of particles for 6 hours/day for 3 consecutive days. However, a different approach to examine BrdU uptake into cells was used. Sections 5 μm thick were used rather than sections 30 μm thick. Rather than expressing the number of BrdU positive cells per mm^3 of each respective tissue compartment (i.e., epithelium and interstitium), the BrdU labeling was expressed as a labeling index or the proportion of positive cells to total cells for each compartment (i.e., epithelium and interstitium). Both methods are valid measures of cell proliferation. Since studies in SD rats would be limited, we wished to use this approach to more precisely define anatomical sites of the lung using 5 μm rather than 30 μm thick sections. This method used in SD rats should not be construed to be a better or inferior procedure, compared to that method used in F344 rats. Differences in values between treatment groups derived by either method should be considered as significant. Although the method of expressing BrdU uptake into cells is different for the studies done in SD rats and F344 rats, both are measures of the relative rate of cell proliferation (BrdU uptake into cells) in the lungs.

Studies in SD rats were done using an intermediate concentration of NH_4NO_3 and carbon particles (actual mean concentrations were 140 $\mu\text{g}/\text{m}^3$ NH_4NO_3 and 194 $\mu\text{g}/\text{m}^3$ carbon). Labeling with BrdU was examined for both epithelial cells and interstitial cells at (1) airway bifurcations, (2) along airway wall generations, (3) within the terminal bronchiole, and (4) within the proximal alveolar region (defined as the first 400 microns beyond the bronchiole-alveolar duct junction).

The BrdU labeling index for epithelial cells found on airway bifurcations is given in Figure 19. The labeling index for interstitial cells underlying these same airway bifurcation ridges is found in Figure 20. The pattern of epithelial and interstitial cell labeling of airway bifurcations from the lungs of animals exposed to PM plus ozone is illustrated in Figures 21A-B. The average number of bifurcation ridges counted per animal to obtain a minimum of 1,000 cells ranged between 6 to 10 profiles.

Epithelial cell labeling of airway bifurcations

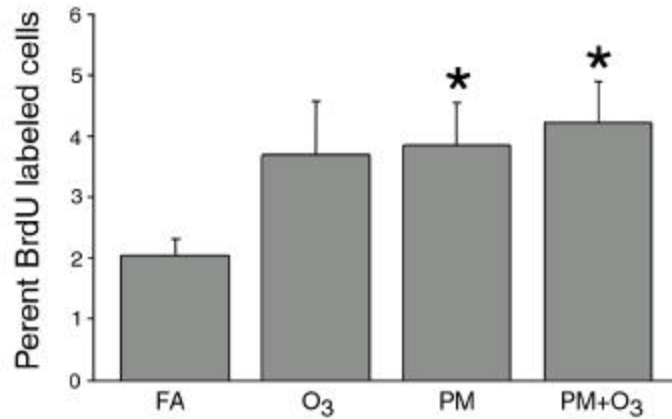


Figure 19 Bar graph of BrdU labeling index (the percent of total cells labeled) for epithelial cells on airway bifurcations of adult male SD rats. Epithelial cells on the bifurcation were defined as cells within 200 μm of the apex of each bifurcation. For each animal, 3 to 5 bifurcations were counted for this analysis. The groups are FA (filtered air), O₃ (ozone), particulate matter (PM) and particulate matter plus ozone (PM +O₃). An asterisk denotes $p < 0.05$ compared with the FA group. The number of animals per exposure group was 6. All values are the mean \pm SEM.

Interstitial cell labeling of airway bifurcations

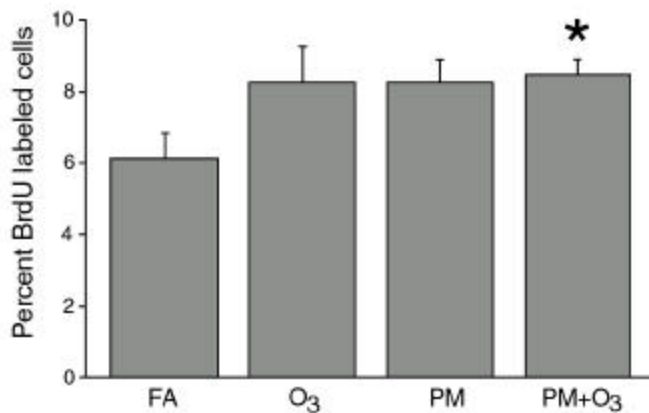
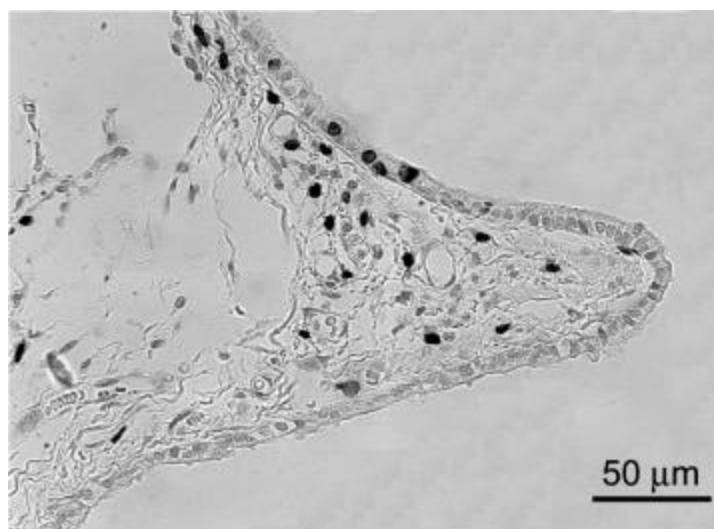


Figure 20 Bar graph of BrdU labeling index for interstitial cells underlying airway bifurcations of adult male SD rats. Interstitial cells within airway bifurcations were defined as all cells underlying epithelial cells within 200 μm of the apex of each bifurcation. An average of 3 to 5 bifurcations was counted per animal for this analysis. The number of animals per exposure group was 6. All values are the mean \pm SEM.

(A)



(B)

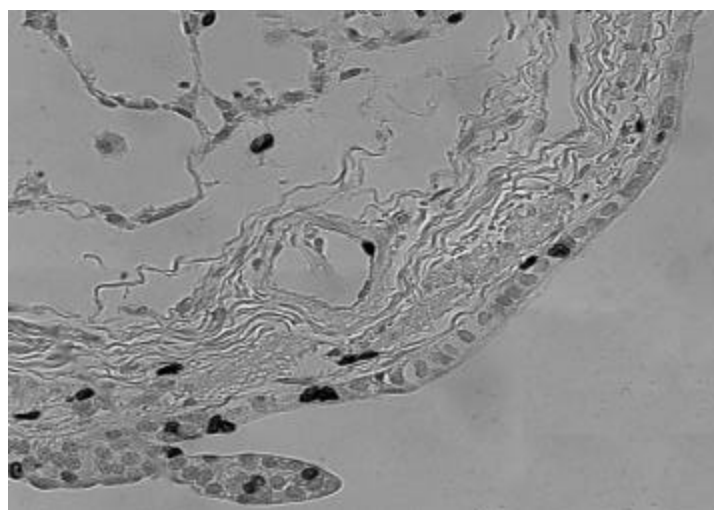


Figure 21. Light micrographs of airway bifurcations from the lungs of adult male SD rats exposed to PM (A) or PM plus ozone (B). A number of epithelial cells as well as interstitial cells underlying the airway bifurcation are positive for the uptake of BrdU (A). Labeling of epithelial and interstitial cells with BrdU is evident as well as the labeling of a single endothelial cell lining a blood vessel (B).

The epithelial labeling index along the walls of the axial pathway is shown in Figure 22. No statistically significant differences were found between the filtered air control group and any of the three treatment groups. Epithelial labeling of the terminal bronchioles is shown in Figure 23. The corresponding interstitial cell labeling index for the same sites is shown in Figure 24. An average of 3 terminal bronchioles per animal were counted to derive the labeling index. Animals exposed only to ozone demonstrated a significant increase in epithelial labeling of the terminal

bronchioles compared with terminal bronchioles observed in the lungs filtered air control animals. No significant difference was noted, however, in interstitial cell labeling of animals exposed to ozone compared with control.

Epithelial cell labeling of airways

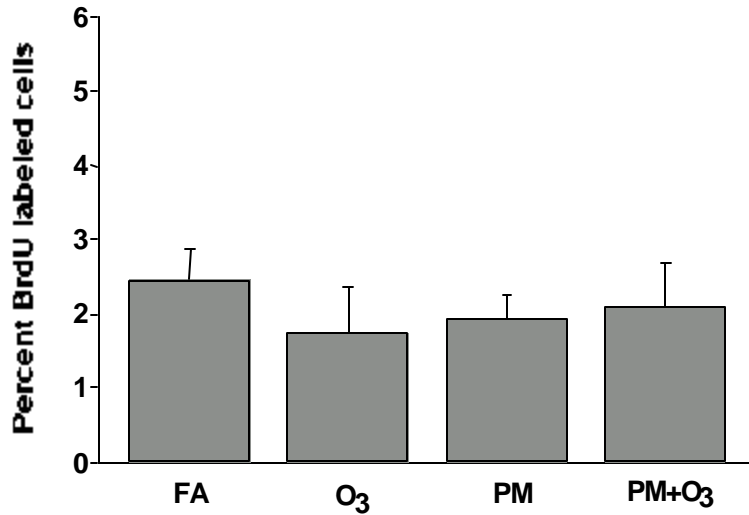


Figure 22 Bar graph of BrdU labeling index for epithelial cells along the walls of the airways, but not on bifurcation ridges of adult male SD rats. No significant differences in the labeling index were noted between groups. The number of animals per exposure group was 6. All values are the mean \pm SEM.

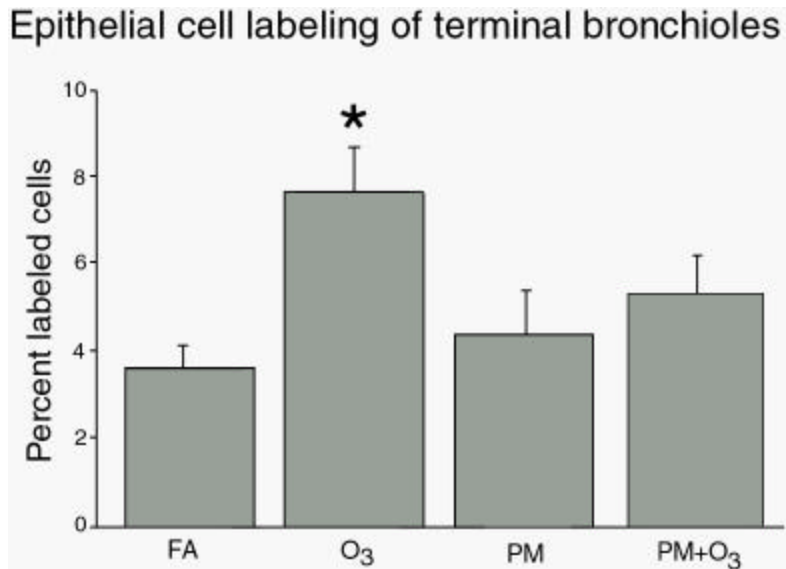


Figure 23 Bar graph of BrdU labeling index for epithelial cells lining terminal bronchioles of adult male SD rats. The groups are FA (filtered air), O₃ (ozone), particulate matter (PM) and particulate matter plus ozone (PM +O₃). An asterisk denotes $p < 0.05$ compared with the FA group. The number of animals per exposure group was 6. All values are the mean \pm SEM.

Interstitial cell labeling of terminal bronchioles

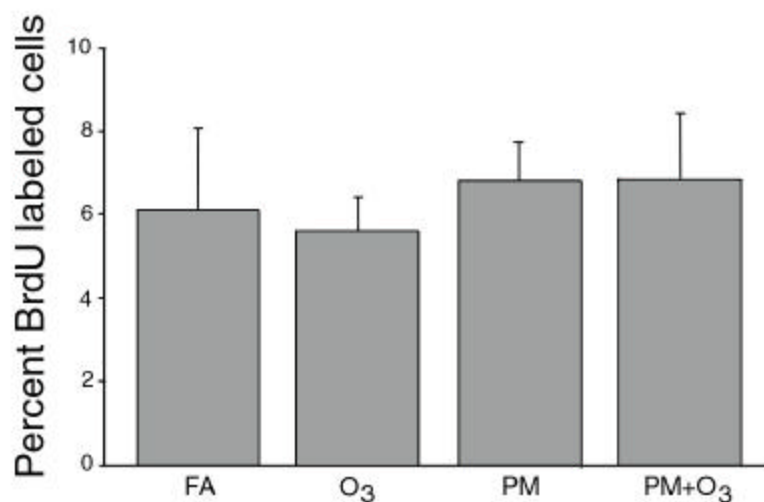


Figure 24 Bar graph of BrdU labeling index for interstitial cells within the wall of terminal bronchioles of adult male SD rats. The groups are FA (filtered air), O₃ (ozone), particulate matter (PM) and particulate matter plus ozone (PM +O₃). No significant differences were noted between groups. The number of animals per exposure group was 6. All values are the mean \pm SEM.

The final anatomical site for analysis, the proximal alveolar region within 400 μ m of the bronchiole-alveolar duct junction, demonstrated a striking increase in total cell labeling within the proximal alveolar region for animals exposed to ozone, PM, or PM plus ozone compared with control (Figure 25). Proximal alveolar tissue arising from an average of 3 terminal bronchioles per animal was used for these measurements.

Cell labeling of the proximal alveolar region

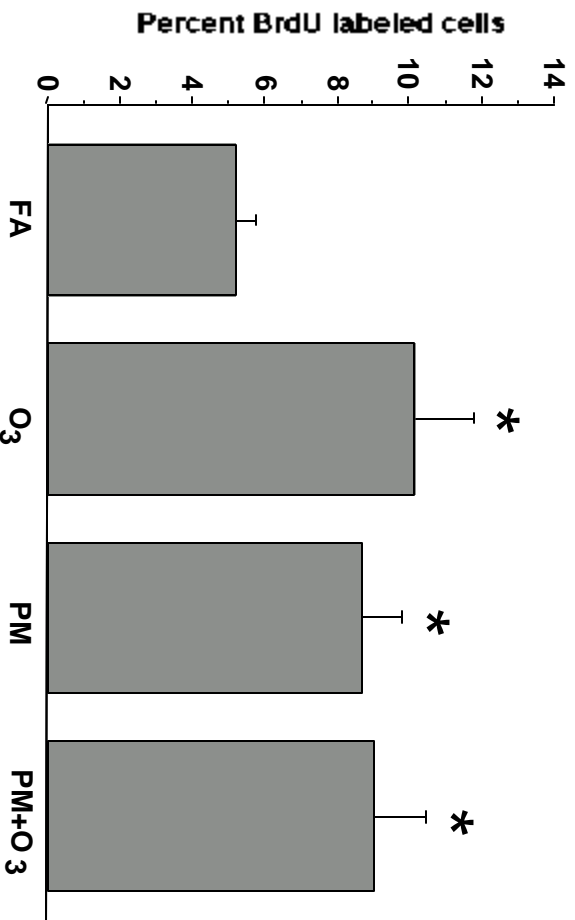
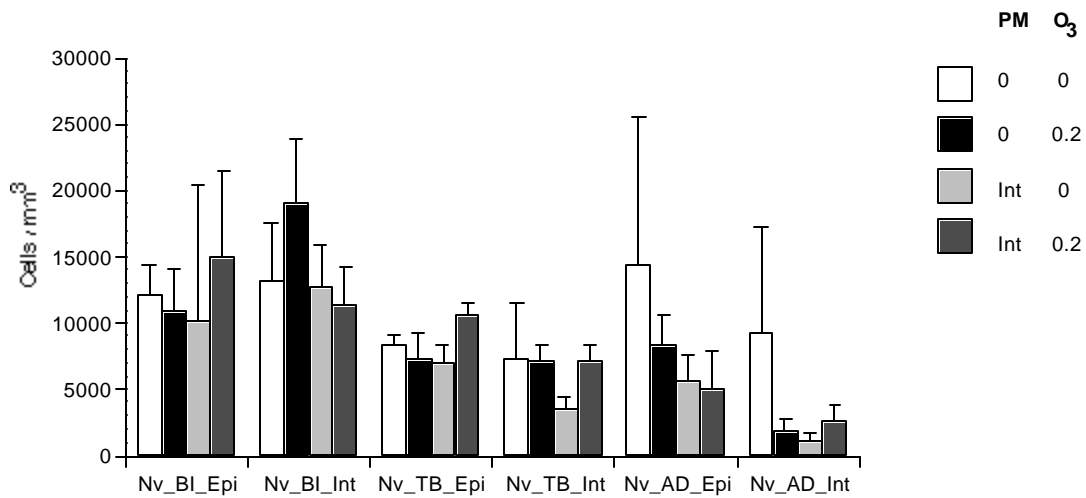


Figure 25 Bar graph of BrdU labeling index for cells of the proximal alveolar region in adult male SD rats. This region is defined as all parenchymal tissue within 400 μm of the bronchiole-alveolar duct junction. Cell counting is for all cell types found within the region until a total of 1,000 cells is counted per animal. The number of animals per exposure group was 6. All values are the mean \pm SEM.

Repeated 3 day exposure regimen to particles in senescent male F344 rats.

To compare the effect of age on repeated exposure of 6 h per day for 3 days with PM alone or in combination with ozone, senescent F344 rats were used. The intermediate target concentration of PM (150 $\mu\text{g}/\text{m}^3$ NH_4NO_3 and 100 $\mu\text{g}/\text{m}^3$ carbon) was selected. Senescent male F344 rats are shown in Figure 26. Although all PM- and ozone-exposed rats showed increased labeling as compared with filtered air control rats, at the intermediate dose of PM, there were no significant increases in labeled cells in any sampled airway or compartment for PM, PM + ozone or ozone exposure groups.

Figure 26. Intermediate Concentration ($154 \mu\text{g}/\text{m}^3 \text{NH}_4\text{NO}_3$, $116 \mu\text{g}/\text{m}^3 \text{C}$) F344 Senescent Rats Exposed 6 Hours/Day for 3 Days



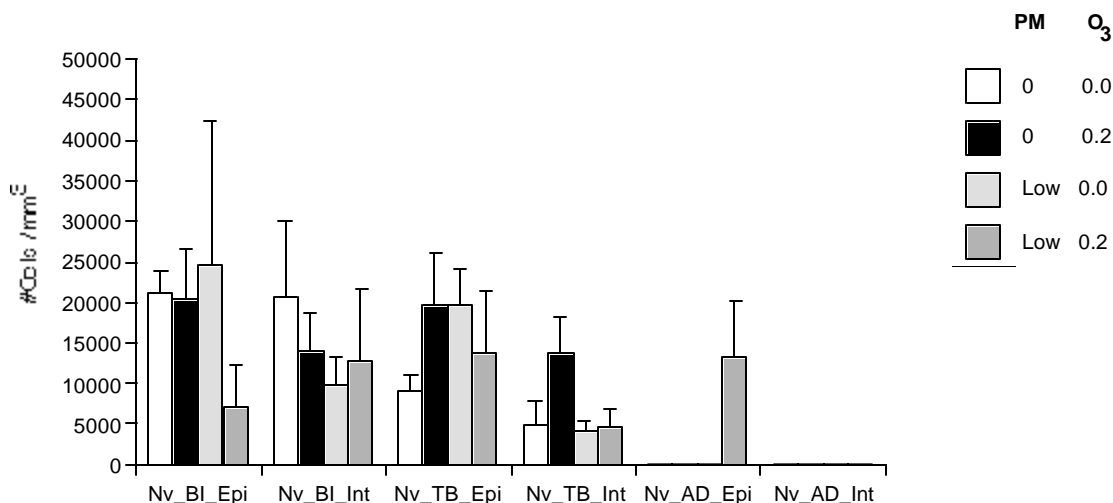
The number of animals per exposure group was 6. All values are the mean \pm SEM. No significant differences were noted between groups.

Abbreviations are $N_V \mathbf{BI}_{EPI}$ = number of BrdU-labeled epithelial cells at bronchial bifurcations per mm^3 of epithelium, $N_V \mathbf{BI}_{INT}$ = the number of BrdU-labeled interstitial cells at bronchial bifurcations per mm^3 of interstitium, $N_V \mathbf{TB}_{EPI}$ = number of BrdU-labeled terminal bronchiolar epithelial cells per mm^3 of epithelium, $N_V \mathbf{TB}_{INT}$ = the number of BrdU-labeled terminal bronchiolar interstitial cells per mm^3 of interstitium, $N_V \mathbf{AD}_{EPI}$ = number of BrdU-labeled alveolar duct epithelial cells per mm^3 of epithelium and $N_V \mathbf{AD}_{INT}$ = number of BrdU-labeled interstitial cells in alveolar ducts per mm^3 of interstitium.

Repeated 3 day exposure regimen to particles in neonatal male and female F344 rats.

Exposure of neonatal rats at low, intermediate, and high concentrations of NH_4NO_3 and carbon were done as daily exposures for 6 hours over 3 consecutive days. The outcome of exposure to low (Figure 27, intermediate (Figure 28) and high (Figure 29) concentrations of PM are shown below. Exposure to low and intermediate concentrations of PM in neonatal rats showed no significant increases in labeled cells in any sampled airway or compartment for PM, PM + ozone or ozone exposure groups (Figures 27-28). However, exposure to a high concentration of PM in neonatal rats showed significantly more labeled cells in the epithelial compartment of terminal bronchioles for PM, PM + ozone and ozone exposure groups as compared with filtered air control groups (Figure 29).

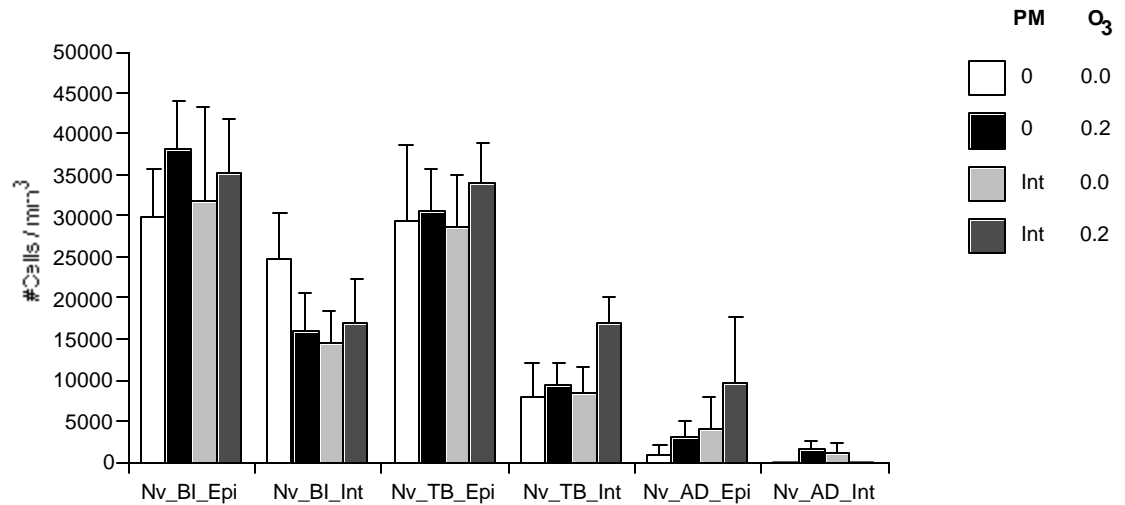
Figure 27. Low Concentration ($76 \mu\text{g}/\text{m}^3 \text{NH}_4\text{NO}_3$, $56 \mu\text{g}/\text{m}^3 \text{C}$) F344 Rat Neonates Exposed 6 Hours/Day for 3 Days First & Third Weeks of Life



The number of animals per exposure group was 6. All values are the mean \pm SEM. No significant differences were noted between groups.

Abbreviations are **N_vBI_{EPI}** = number of BrdU-labeled epithelial cells at bronchial bifurcations per mm^3 of epithelium, **N_vBI_{INT}** = the number of BrdU-labeled interstitial cells at bronchial bifurcations per mm^3 of interstitium, **N_vTB_{EPI}** = number of BrdU-labeled terminal bronchiolar epithelial cells per mm^3 of epithelium, **N_vTB_{INT}** = the number of BrdU-labeled terminal bronchiolar interstitial cells per mm^3 of interstitium, **N_vAD_{EPI}** = number of BrdU-labeled alveolar duct epithelial cells per mm^3 of epithelium and **N_vAD_{INT}** = number of BrdU-labeled interstitial cells in alveolar ducts per mm^3 of interstitium.

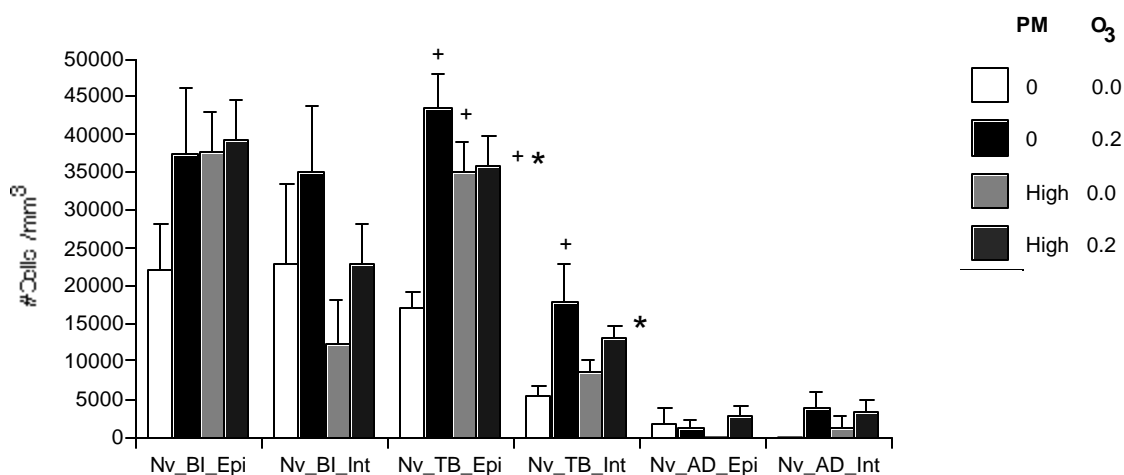
Figure 28. Intermediate Concentration ($143 \mu\text{g}/\text{m}^3 \text{NH}_4\text{NO}_3$, $119 \mu\text{g}/\text{m}^3 \text{C}$) F344 Rat Neonates Exposed 6 Hours/Day for 3 Days First & Third Weeks of Life



The number of animals per exposure group was 6. All values are the mean \pm SEM. No significant differences were noted between groups.

Abbreviations are $N_V \mathbf{BI}_{EPI}$ = number of BrdU-labeled epithelial cells at bronchial bifurcations per mm^3 of epithelium, $N_V \mathbf{BI}_{INT}$ = the number of BrdU-labeled interstitial cells at bronchial bifurcations per mm^3 of interstitium, $N_V \mathbf{TB}_{EPI}$ = number of BrdU-labeled terminal bronchiolar epithelial cells per mm^3 of epithelium, $N_V \mathbf{TB}_{INT}$ = the number of BrdU-labeled terminal bronchiolar interstitial cells per mm^3 of interstitium, $N_V \mathbf{AD}_{EPI}$ = number of BrdU-labeled alveolar duct epithelial cells per mm^3 of epithelium and $N_V \mathbf{AD}_{INT}$ = number of BrdU-labeled interstitial cells in alveolar ducts per mm^3 of interstitium.

Figure 29. High Concentration (288 $\mu\text{g}/\text{m}^3$ NH_4NO_3 , 243 $\mu\text{g}/\text{m}^3$ C) F344 Rat Neonates Exposed 6 Hours/Day for 3 Days First & Third Weeks of Life



*Significant difference ($P < 0.05$) between groups by ANOVA

+Significantly different ($P < 0.05$) from 0 PM concentration, 0 Ozone ppm (filtered air control animals) by the Bonferroni multiple comparison test.

The number of animals per exposure group was 6. All values are the mean \pm SEM.

Abbreviations are $\text{N}_V \text{BI}_{\text{EPI}}$ = number of BrdU-labeled epithelial cells at bronchial bifurcations per mm^3 of epithelium, $\text{N}_V \text{BI}_{\text{INT}}$ = the number of BrdU-labeled interstitial cells at bronchial bifurcations per mm^3 of interstitium, $\text{N}_V \text{TB}_{\text{EPI}}$ = number of BrdU-labeled terminal bronchiolar epithelial cells per mm^3 of epithelium, $\text{N}_V \text{TB}_{\text{INT}}$ = the number of BrdU-labeled terminal bronchiolar interstitial cells per mm^3 of interstitium, $\text{N}_V \text{AD}_{\text{EPI}}$ = number of BrdU-labeled alveolar duct epithelial cells per mm^3 of epithelium and $\text{N}_V \text{AD}_{\text{INT}}$ = number of BrdU-labeled interstitial cells in alveolar ducts per mm^3 of interstitium.

E. Measure 4: Particle Deposition/Fate

The overall goal of these studies was to determine patterns of particle deposition and fate based on (a) prior PM exposure, (b) particle size, (c) rat strain, and (d) age. Since NH_4NO_3 and carbon are both particles that are virtually impossible to visualize in the lungs, fluorescent microspheres afforded the opportunity to observe the deposition, translocation and clearance of these particles in the lungs. This section is a summary of those experiments done in adult, senescent and young animals.

Deposition and fate of 0.5 μm microspheres in the lungs of adult F344 rats following prior PM (NH_4NO_3 and carbon) and ozone exposure.

Exposure to aerosolized fluorescent microspheres 0.5 μm for a period of 2 hours was done following a single 6 hour exposure to NH_4NO_3 and carbon using 20 healthy adult male Fischer 344 rats. The concentrations of NH_4NO_3 (155 $\mu\text{g}/\text{m}^3$), carbon (260 $\mu\text{g}/\text{m}^3$) were used. In addition, animals were exposed to ozone (0.20 ppm). A group of sham controls were exposed

simultaneously to filtered air. These animals were examined following the end of a two-hour nose only exposure to aerosolized 0.5 μm diameter fluorescent yellow green microspheres. Animals were also examined 2 and 7 days later. The distribution of particles as observed within the conducting airways of these animals immediately following exposure is illustrated in Figures 30, 31, 32, 33. Clear visualization of fluorescent microspheres facilitated the identification of intrapulmonary patterns of deposition as well as subsequent redistribution of particles within the respiratory tract with progressive post-exposure time. These microspheres depositing on the airways were clearly visible and found along the entire bronchial tree. Preferential distribution of microspheres was noted at bifurcation points along the bronchial tree (Figures 32 and 33). This pattern of microsphere distribution was noted in both filtered air control animals as well as in animals previously exposed to NH_4NO_3 and carbon. No significant differences were noted between each group of animals.



Figure 30 Microdissected airway of the right infracardiac lobe.



Figure 31 0.5µm yellow-green fluorescent microspheres litter the airway surface.



Figure 32 High magnification view of the airway bifurcation shown in figure 31.



Figure 33 0.5 μ m yellow-green microspheres litter the bifurcation point of the airway.

To better understand patterns of particle deposition and clearance from specific regions of the lung airways, the main axial pathway entering into the caudal lobe was microdissected along its longitudinal axis as well as the daughter airway paths branching from the main axial path (Figure 34). Microdissection allowed us to examine both complementary halves of the airways generated by the technique so that the total distribution of microspheres in the airways could be validated and analyzed. The airway branch points along the axial pathway designated as bifurcation points: A, B, C, and D beginning with the most proximal intrapulmonary bifurcation of the axial pathway (Figure 34). In some instances, microdissections going beyond the fourth bifurcation of the airway contained a fifth branch point designated bifurcation E.

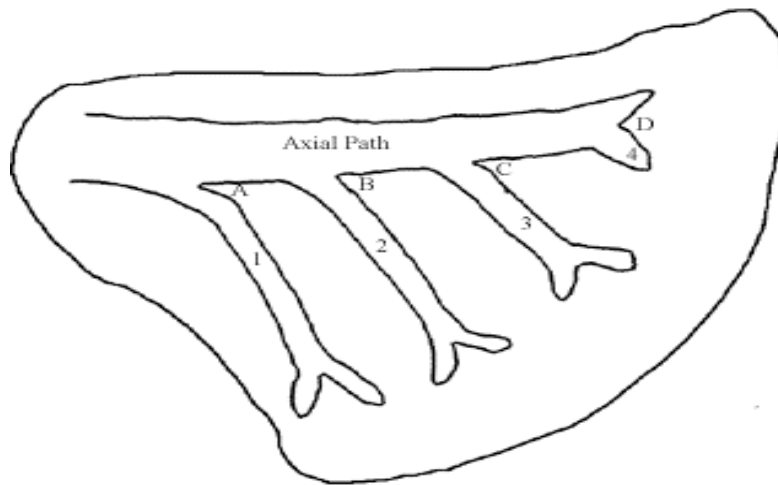


Figure 34 Diagram of airway locations within the right caudal lung lobe for examination of microsphere distribution.

Vascular perfusion was used to fix the lungs to preserve the airway lining fluids and the actual distribution of microspheres in airways. Intravascular perfusion minimizes the displacement of microspheres in contrast to intratracheal instillation. The distribution of microspheres along each of these airway paths was also examined for the axial path and each of the major daughter airway paths. A semiquantitative approach was applied to analyze the frequency (density) of microspheres present in airway. A numeric designation based on the relative numbers of particles at each site was used with 1 designating the complete absence of particles through 10 designating the heaviest concentration of particles observed in the lungs. These measurements were calibrated using NIH Image program which allowed us to validate the numeric scoring (range 1 to 10) of the relative abundance of microspheres by areal measurement of the spheres within the airways. The numbers obtained were subsequently analyzed by analysis of variance to determine the significance of microsphere abundance within the airways and at airway bifurcations over time.

The highest concentration of microspheres along airway paths and on bifurcation ridges was found immediately following exposure. With greater time postexposure, a typical pattern of particle clearance was observed (Figures 35 and 36). Microspheres were most heavily concentrated on bifurcation ridges (Figure 37), but were also found to litter the surfaces of all airways. The number and distribution of microspheres along the airways and bifurcations at the "0" hr time point were compared to identical airways in the lungs of animals 7 days following exposure. Although animal-to-animal variability was present, a statistically significant reduction in microspheres was found in animals previously exposed to filtered air. A significant decrease in microspheres was found along the axial airway path as well as all four daughter branches arising from the axial pathway. In contrast, in the lungs of animals previously exposed to

NH_4NO_3 , carbon black and ozone, clearance of microspheres had occurred, but not to a statistically significant degree (Figures 38 and 39).

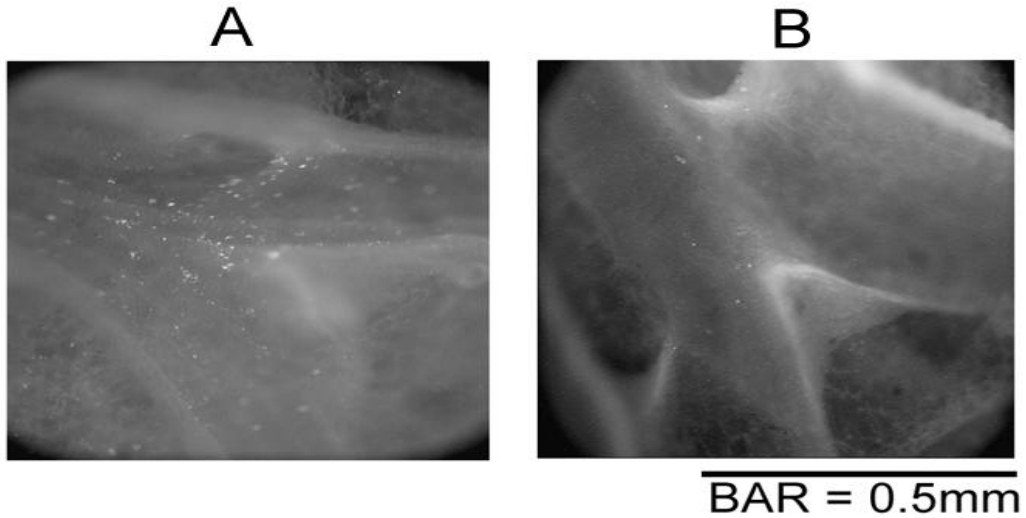


Figure 35 Images of the microdissected airway from two animals exposed to filtered air only followed by exposure to fluorescent. (A) shows the distribution pattern on bifurcation D immediately after exposure and (B) shows the same bifurcation 7 days after exposure.

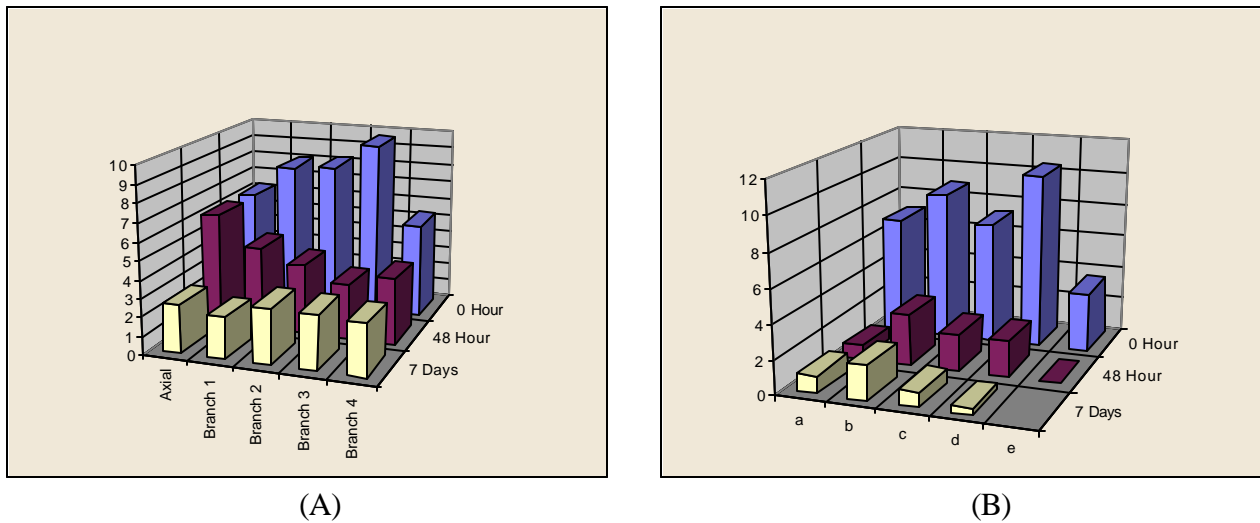


Figure 36 Microsphere distribution in the lungs of filtered air control animals. (A) Distribution of microspheres along the airways with increasing post exposure time. (B) Distribution of microspheres on bifurcations in the caudal lobe with increasing post exposure time. The overall reduction of microsphere abundance on airway bifurcations was significantly reduced with increasing post exposure time in the lungs of filtered air control animals.

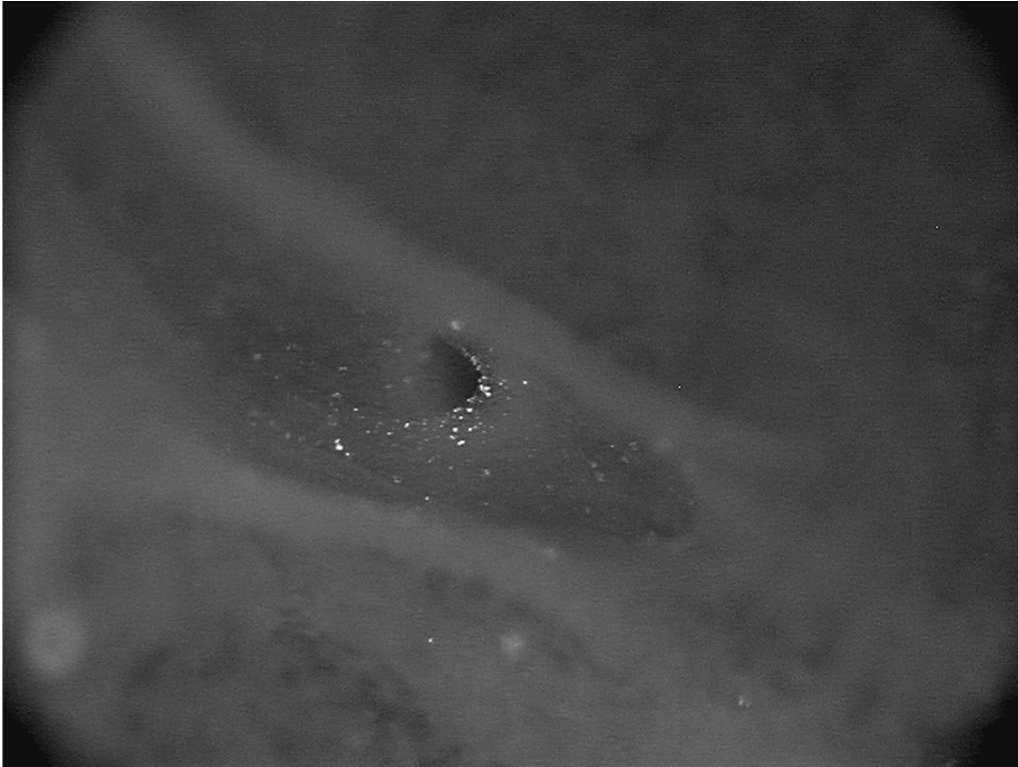
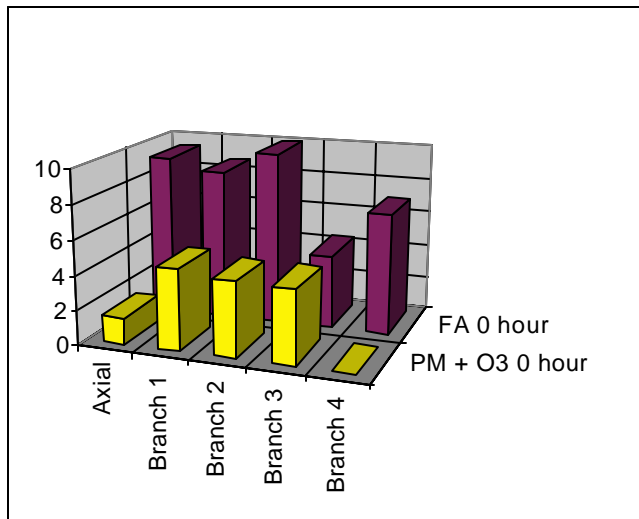
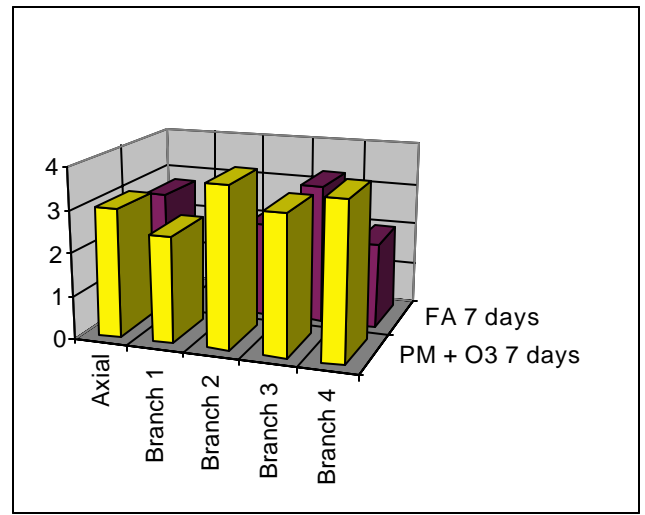


Figure 37 Fluorescent microspheres are preferentially located on airway bifurcations ridges as shown in this microdissected airway image.

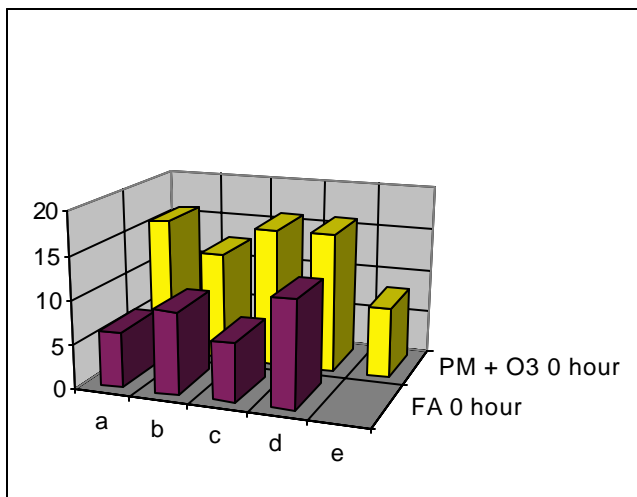


(A)

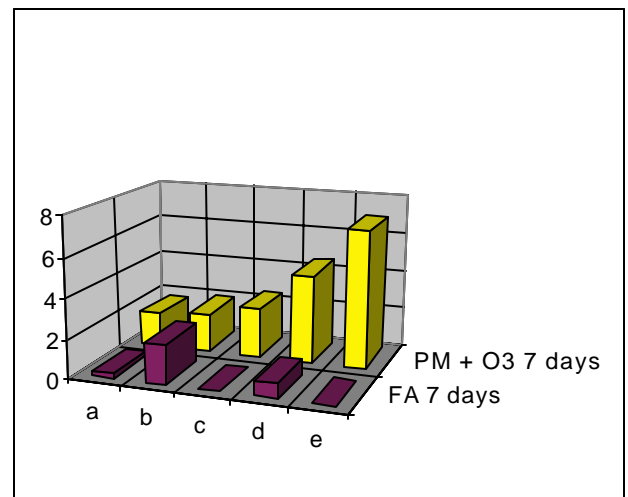


(B)

Figure 38 (A) Frequency of microspheres on major and minor daughter airway paths. (B) Frequency of microspheres on major and minor daughter airway paths.



(A)



(B)

Figure 39 (A) Frequency of microspheres on axial airway path bifurcations. (B) Frequency of microspheres on axial airway path bifurcations. Microsphere abundance at airway bifurcations over time was significantly reduced in filtered air (FA) control animals, but not in animals previously exposed to PM and ozone.

Since this study had involved prior exposure of the animals to NH_4NO_3 , carbon, and ozone, we wished to determine if the initial numbers of microspheres depositing in the lungs or their retention in the lungs over time could have been affected. Therefore, the right cranial lobe of each rat was digested in potassium hydroxide to determine the number of microspheres present. An aliquot of the suspension obtained for each lobe was analyzed by counting the number of microspheres using a hemocytometer. The number of microspheres present in the right

cranial lobe was determined immediately following exposure as well as two and seven days later (Table 11). Similar numbers of microspheres were present in the right cranial lobe of animals exposed to filtered air compared with animals exposed previously to particulates and ozone. Minimal clearance of microspheres occurred during the two days following exposure. By 7 days, approximately 10 percent of the microspheres had been cleared from the right cranial lobe.

Table 11. Number of 0.5 µm fluorescent microspheres in the right cranial lobe (millions) of adult male F344 rats following exposure to NH₄NO₃ (155 µg/m³), carbon (260 µg/m³) and ozone (0.2 ppm)

<u>Treatment</u>	<u>Post-exposure time</u>		
	0 Hour	2 Days	7 Days
Filtered Air	6.2 ± 0.5	7.1 ± 0.7	5.7 ± 0.4
Carbon Black Ammonium, nitrate, and ozone	6.8 ± 0.1	6.1 ± 0.1	5.8 ± 0.9

*Values represent mean ± standard error.

These findings demonstrate that previous exposure to NH₄NO₃, carbon and ozone did not significantly affect either overall microsphere deposition or retention over time in the lungs of healthy adult rats.

Deposition and fate of different size particles in the lungs of adult male SD rats

We wished to determine the influence of particle size on the number and distribution of inhaled particles in the lungs. Adult male S-D rats previously exposed to only filtered air were chosen for these studies. We had already conducted PM studies in this strain of rat for comparison to F344 rats, but only wished to determine the importance of particle size on patterns of deposition and retention in the lungs in this series of studies. A number of studies suggest that fine-mode particles (PM_{2.5}) may significantly contribute to the adverse health effects associated with exposure to particulate matter. We elected to use fluorescent microspheres as a simple way to define particle clearance from the lungs. The influence of particle size on lung deposition, clearance, retention and translocation could be studied using microspheres of different sizes. Adult male S-D rats were exposed to aerosolized 0.5, 1.0, 3.0 µm microspheres three hr/day for three consecutive days, each day to a different sized particle. Animals were examined following the end of each exposure period as well as 24 and 48 hr following the last day of aerosolization. The sequence in which the microspheres were aerosolized allowed for the calculation of clearance rates for each particle size within the same animals. Right cranial lobe digestion revealed statistically significant differences in total microsphere number recovered for all particle sizes (0.5 > 1.0 > 3.0 µm). The mass concentrations of aerosolized 0.5, 1.0, and 3.0 µm diameter microspheres were 0.3, 1.7, and 2.1 mg/m³, respectively. Total particle burden in the lung for 0.5 µm microspheres was 2x and 240x greater compared to that for 1.0 and 3.0 µm microspheres, respectively. Significant clearance of 3.0 µm microspheres was noted (50% after 48 hr), whereas little clearance was found for 0.5 and 1.0 µm particles. These findings allowed

us to: (1) determine the relative numbers of particles depositing in the lungs for 0.5, 1.0, and 3.0 μm diameter particles, and (2) observe the degree of particle clearance (based on particle retention) from the lungs for each sized particle.

Particle deposition and clearance in senescent rats

To further understand the effects of exposure to filtered air (FA) or NH_4NO_3 and carbon (PM) on particle deposition and clearance in the lungs of older animals, senescent F344 rats previously exposed to an intermediate concentration of NH_4NO_3 ($150 \mu\text{g}/\text{m}^3$) and carbon ($100 \mu\text{g}/\text{m}^3$) were exposed for two hours to polychromatic (PC) red fluorescent microspheres with a diameter of $0.952 \pm 0.016 \mu\text{m}$. Exposure to PC red microspheres took place seventeen hours prior to FA or PM exposure. These identical rats were also exposed to yellow-green (YG) microspheres ($0.973 \pm 0.028 \mu\text{m}$ diameter) 19 hours after FA or PM exposure. Exposure of these rats to albumin-coated microspheres was done in a nose-only exposure system. Each rat was held in a cylinder with a small opening at the head end through which the aerosol passed so that the nasal area was continuously exposed to a fresh supply of particles and air. The mass concentration of PC red microspheres was $2.02 \text{ mg}/\text{m}^3$ and for the YG microspheres was $2.75 \text{ mg}/\text{m}^3$. These gravimetric measurements were done using Pallflex™ filters to collect a mass of aerosol from a known volume of air. Exposure to this concentration resulted in an abundance of single particles deposited in the lungs during two hours to allow for detailed morphological analysis of particle deposition and subsequent clearance.

Following the second period of fluorescent microsphere exposure, animals were examined immediately after or 7 days later. The cranial and accessory lung lobes were taken from each animal and the lobe volume measured. Each lobe was placed in 20% potassium hydroxide solution to allow for complete digestion of the tissues. The volume of solution was measured and the concentration of the PC and YG microspheres was determined by using a hemocytometer. The total number of PC red and YG microspheres in each lobe is given in the following Tables 12.

Table 12. Microsphere (1.0 μm diameter) Deposition/Retention/Clearance in F344 Senescent Male Rats following exposure to an intermediate level of NH_4NO_3 and carbon.

(a) Number of Microspheres in millions from the Right Cranial Lobe

<u>Exposure</u>	MS Type	<u>Post Exposure Time</u>	
		0 Day	7 Day
<u>FA</u>	PC Red	1.01 ± 0.10	1.30 ± 0.08
	YG	1.49 ± 0.13	1.61 ± 0.18
<u>PM</u>	PC Red	0.99 ± 0.08	1.01 ± 0.24
	YG	2.15 ± 0.16	1.65 ± 0.14

(b) Number of Microspheres in millions from the Right Accessory Lobe

<u>Exposure</u>	MS Type	<u>Post Exposure Time</u>	
		0 Day	7 Day
<u>FA</u>	PC Red	0.70 ± 0.06	0.76 ± 0.16
	YG	1.13 ± 0.13	1.33 ± 0.10
<u>PM</u>	PC Red	0.69 ± 0.15	0.71 ± 0.12
	YG	1.62 ± 0.08	1.34 ± 0.10

(c) Number of Microspheres in millions per ml tissue from the Right Cranial Lobe

<u>Exposure</u>	MS Type	<u>Post Exposure Time</u>	
		0 Day	7 Day
<u>FA</u>	PC Red	1.01 ± 0.14	1.15 ± 0.11
	YG	1.49 ± 0.37	1.40 ± 0.07
<u>PM</u>	PC Red	0.99 ± 0.15	1.04 ± 0.20
	YG	2.15 ± 0.35	1.73 ± 0.15

(d) Number of Microspheres in millions per ml tissue from the Right Accessory Lobe

<u>Exposure</u>	MS Type	<u>Post Exposure Time</u>	
		0 Day	7 Day
<u>FA</u>	PC Red	0.75 ± 0.17	0.77 ± 0.19
	YG	1.26 ± 0.36	1.39 ± 0.26
<u>PM</u>	PC Red	0.61 ± 0.01	0.70 ± 0.10
	YG	1.58 ± 0.33	1.37 ± 0.28

A number of conclusions arise from observations made in this study using senescent male F344 rats. The first observation is that particle deposition/retention is consistently higher in the cranial lobe compared with the accessory lobe, although both lobes are of identical size, suggesting the importance of a short airway path (cranial lobe) versus long airway path (accessory lobe) to enhance particle deposition/retention in each lung lobe. Second, particle deposition/retention is not affected by prior exposure to NH_4NO_3 and carbon. Third, clearance of particles from the lungs is not affected by subsequent exposure to NH_4NO_3 and carbon. Finally, particles with a diameter of $1\mu\text{m}$ demonstrate little overall clearance over a period of one week following deposition. These findings suggest particles of this size result in deep lung deposition rather than simply airway deposition.

Particle clearance in young (neonatal) male and female F344 rats

To better understand the effects of particle exposure on the neonatal lungs, F344 male and female rats were exposed to yellow green (YG) fluorescent microspheres in the first week of postnatal life and again to polychromatic (PC) red fluorescent microspheres during the third week of life. Fluorescent microspheres served as a surrogate for particles to facilitate quantification of particle deposition and retention in the lungs. All microspheres were delivered to the animals by inhalation in whole body chambers. YG microspheres were inhaled at 5 days of age, while PC red microspheres were inhaled at 20 days of age. The mean diameter of the YG microspheres was $0.485 \pm 0.010 \mu\text{m}$, while the mean diameter of the PC red microspheres was $0.526 \pm 0.011 \mu\text{m}$. Each microsphere was prepared as a suspension to a dilution of 1:400 to optimize for the aerosolization of single particles. The total suspension volume of YG and PC red microspheres was 300 and 550 mL, respectively. The chamber mass concentration was $351\mu\text{g}/\text{m}^3$ for YG microspheres and $381\mu\text{g}/\text{m}^3$ for PC red microspheres. Gravimetric measurements of the chamber concentration of microspheres during exposure were done using Pallflex™ filters to collect a mass of aerosol from a known volume of air.

Neonatal rats were examined immediately following each exposure to fluorescent microspheres. Animals exposed to microspheres during the third week of life were also exposed to microspheres during the first week of life. The total number of microspheres present in selected lung lobes was determined as well as the number of microspheres per mL of fixed lung tissue. The cranial and accessory lobes were taken from each animal and the lobe volume measured. Each lobe was placed in 20% potassium hydroxide solution to allow for complete digestion of the tissues. The volume of solution was measured and the concentration of the PC and YG microspheres was determined by using a hemocytometer. The total number of PC red and YG microspheres in each lobe is given in the following Table 13:

Table 13. Total Number of Microspheres in thousands from neonatal F344 rats

Lung lobe	MS Type	Postnatal Age	
		5 Days	20 Days
Cranial	YG	23.3 ± 0.8	20.8 ± 0.7
	PC Red	-	90.0 ± 3.8
Accessory	YG	25.4 ± 1.4	19.7 ± 0.6
	PC Red	-	86.8 ± 1.5

Table 13 shows the total number of microspheres present within the cranial and accessory lobes of the lungs. Table 14 shows the number of microspheres per mL of fixed lung for both the cranial and accessory lobes.

Table 14. Number of Microspheres in thousands per ml fixed tissue volume from neonatal F344 rats

Lung lobe	MS Type	Postnatal Age	
		5 Days	20 Days
Cranial	YG	231.2 ± 20.8	87.2 ± 3.3
	PC Red	-	377.4 ± 18.8
Accessory	YG	231.2 ± 8.4	84.2 ± 1.1
	PC Red	-	372.4 ± 5.9

These findings demonstrate that particles are effectively deposited in the lungs in the first week of life (5 days postnatal age) and are virtually uncleared two weeks later (20 days postnatal age). Further exposure to particles later in life is associated with even greater numbers of particles that deposit in the neonatal lungs. This finding may explain in part the adverse effects of high target concentrations of NH₄NO₃ and C noted in neonatal male and female F344 rats following the first and third weeks of life.

E. Measure 5: Bronchoalveolar lavage

To examine the potential effects of PM exposure on the inflammatory response in the lungs bronchoalveolar lavage was used to measure total cell number, viability, and cell differentials in F344 and SD rats. The initial studies to use this method were in adult male SD rats exposed to an intermediate concentration of NH₄NO₃ and carbon over a period of 3 days. Subsequent studies were completed in adult and senescent male F344 rats also at the intermediate concentration of PM. Male and female neonatal F344 rats were studied using low, intermediate and high concentrations of NH₄NO₃ and carbon.

The analysis of bronchoalveolar lavage for adult male SD rats following exposure to an intermediate concentration of NH₄NO₃ and carbon (actual concentration NH₄NO₃, 142 µg/m³; carbon, 190 µg/m³) for 6 hours per day for 3 day exposure is presented in Table 15. A statistically significant elevation in total cells recovered from the lungs of rats exposed to PM or

PM plus ozone was noted compared with filtered air controls. Cell viability, cell differentials, and protein lavage values are also given in Table 15. A total of 9-10 animals were analyzed for each group.

Table 15. Bronchoalveolar lavage characteristics of recovered cells and fluids in male adult male Sprague Dawley Rats

Percent (%)							
	Cell No. (10 ⁶)	Viability	Macrophages	Lymphocytes	Neutrophils ⁺	Epithelial cells	Lavage Protein ^δ (μg/ml)
FA	1.45±0.45	93.48±5.15	94.85±0.39	1.74±0.25	<0.1	3.38±0.35	195±5
O ₃	1.83±0.65	96.18±3.05	93.29±0.52	1.73±0.16	<0.1	4.84±0.42*	202±5
PM	2.62±0.81 *	94.74±3.37	94.75±0.39	1.94±0.16	<0.1	3.81±0.28	207±8
PM+O ₃	2.19±0.69 *	95.44±3.73	92.95±0.44 **	1.87±0.21	<0.1	4.70±0.33*	203±9

Note: Bronchoalveolar lavage cytospin preparations from Sprague-Dawley rats.

Values are means ± SEM, n is nine to ten animals for each group.

*P < 0.05 or ** P< 0.01, significantly different from FA by Student's *t*-test

⁺Only rare neutrophils were found in the BAL of all groups.

^δProtein concentration was measured only in the first aliquot (8ml) of lavage fluid recovered from the lungs of each animal.

In subsequent experiments, male adult and senescent (18 month-old) F344 rats were also exposed to an intermediate concentration of NH₄NO₃ and carbon (actual NH₄NO₃ concentration, 166 μg/m³; carbon concentration, 116 μg/m³) for 6 hours/day for 3 days. Bronchoalveolar lavage was performed immediately following the end of the third day of exposure. Tables 16 and 17 present these results. Exposure of adult and senescent F344 rats were done simultaneously to permit direct comparison of the response of healthy adult rats to aged senescent rats following particle exposure.

Table 16. Comparisons of Lung Lavage Cell Numbers, Viabilities, Differentials and Protein ("Intermediate" PM exposure, F344 Adult male Rats)

Percent (%)							
	Cell No. (10 ⁶)	Viability	Mac .	Lymph .	Neut.	Epithelial Cells	Protein (μg/μl)
FA	5.75 ± 0.21	86.2 ± 2.7	97.6 ± 0.3	1.41 ± 0.07	0.62 ± 0.20	0.35 ± 0.08	52.8±3.6
PM	5.29 ± 0.33	83.5 ± 2.5	96.8 ± 0.6	1.75 ± 0.30	0.62 ± 0.08	0.83 ± 0.26	51.4 ± 1.5

Note: Values are means ± SEM , n equals 5 animals per group.

Mac. = macrophage; Lymph. = lymphocyte; Neut. = neutrophil

No significant differences in total cells recovered from the lungs were noted between groups following PM exposure in adult male F344 rats. In was in contrast to what was observed in SD rats (Table 15). No significant changes in cell differentials or protein content were noted in the lavage fluid of these adult male F344 rats.

Table 17. Comparisons of Lung Lavage Cell Numbers, Viabilities, Differentials and Protein (“Intermediate” PM exposure, F344 Senescent male Rats)

	Percent (%)						Protein ($\mu\text{g}/\mu\text{l}$)
	Cell No. (10^6)	Viability	Mac .	Lymph .	Neut.	Epithelial Cells	
FA	2.44 \pm 0.30	92.7 \pm 1.5	86.5 \pm 5.7	9.64 \pm 5.9	0.82 \pm 0.36	3.01 \pm 0.67	67.9 \pm 9.0
PM	3.56 \pm 0.34*	95.1 \pm 1.5	94.2 \pm 1.1	2.50 \pm 0.6	0.57 \pm 0.35	2.72 \pm 0.79	50.0 \pm 2.4

Note: Values are means \pm SEM, n equals 4 animals per group.

*P < 0.05, significantly different from FA by Student’s *t*-test

Particle exposure in senescent male F344 rats was associated with a statistically significant increase in the number of cells recovered from the lungs by lavage in contrast to adult male F344 rats (Table 16). However, particle exposure for 3 days in adult male SD rats did demonstrate a significant increase in total cell number (Table 15). No changes in cell differentials or protein content were noted in the lavage fluid of these senescent rats or in adult male SD rats (Table 15).

Bronchoalveolar lavage in neonatal rats

Bronchoalveolar lavage was actively used as a measure of short-term particle exposure effects in neonatal animals. Neonatal F344 rats were exposed to NH_4NO_3 and carbon for 6 hours/day for 3 days during the first week of life and again during the third week of life. All three concentrations of particles were used. Bronchoalveolar lavage was performed immediately following the end of the third day of exposure in the third week of life. Tables 18, 19 and 20 list the findings for low (NH_4NO_3 , 75 $\mu\text{g}/\text{m}^3$; C, 50 $\mu\text{g}/\text{m}^3$), intermediate (NH_4NO_3 , 150 $\mu\text{g}/\text{m}^3$; C, 100 $\mu\text{g}/\text{m}^3$), and high (NH_4NO_3 , 300 $\mu\text{g}/\text{m}^3$; C, 150 $\mu\text{g}/\text{m}^3$) of PM, respectively.

Table 18. Bronchoalveolar Lavage: Male and Female F344 Rats Neonates Exposed 6 Hours/Day for 3 Days during the First & Third Weeks of Life to a Low PM Concentration (76 $\mu\text{g}/\text{m}^3$ NH_4NO_3 , 56 $\mu\text{g}/\text{m}^3$ C)

	Body Weight (g)	Total Cell Number (10^5)	Cell Viability (%)
FA (16)	32.4 \pm 2.50	9.71 \pm 3.02	92.9 \pm 2.12
PM (15)	32.8 \pm 3.17	8.63 \pm 3.10	91.1 \pm 7.16
O₃ (5)	33.5 \pm 2.93	5.90 \pm 2.48*	86.6 \pm 7.65*
PM/O₃ (6)	35.0 \pm 1.71	5.83 \pm 1.42*	89.6 \pm 5.62

Note: Values are means \pm SD.

Numbers in parenthesis are the number of animals in each group.

* $P < 0.05$ significantly different from FA by *ANOVA test*.

Table 19. Bronchoalveolar Lavage: Male and Female F344 Rats Neonates Exposed 6 Hours/Day for 3 Days during the First & Third Weeks of Life to an Intermediate PM Concentration (143 $\mu\text{g}/\text{m}^3$ NH_4NO_3 , 119 $\mu\text{g}/\text{m}^3$ C)

	Body Weight (g)	Total Cell Number (10^5)	Cell Viability (%)
FA (16)	32.0 \pm 10.78	8.6 \pm 3.32	93.2 \pm 4.64
PM (15)	29.4 \pm 10.12	6.7 \pm 2.37	90.8 \pm 6.22
O₃ (13)	33.9 \pm 7.55	7.0 \pm 3.35	94.3 \pm 2.86
PM/O₃ (14)	30.9 \pm 10.69	6.7 \pm 3.86	93.0 \pm 4.27

Note: Values are means \pm SD.

Numbers in parenthesis are the number of animals in each group.

Table 20. Bronchoalveolar Lavage: Male and Female F344 Rats Neonates Exposed 6 Hours/Day for 3 Days during the First & Third Weeks of Life to a High PM Concentration (288 $\mu\text{g}/\text{m}^3$ NH_4NO_3 , 243 $\mu\text{g}/\text{m}^3$ C)

	Body Weight (g)	Total Cell Number (10^5)	Cell Viability (%)
FA (22)	34.5 \pm 5.90	8.94 \pm 2.92	92.9 \pm 4.55
PM (20)	32.5 \pm 4.45	8.75 \pm 1.84	91.3 \pm 4.16
O₃ (9)	28.2 \pm 2.78*	7.31 \pm 2.60	88.7 \pm 4.93
PM/O₃ (18)	35.4 \pm 4.70	9.19 \pm 2.41	93.0 \pm 4.57

Note: Values are means \pm SD.

Numbers in parenthesis are the number of animals in each group.

* $P < 0.05$ significantly different from FA by *ANOVA test*.

In general, total cell numbers or cell viability was not significantly affected by particle and/or ozone exposure in male and female neonatal F344 rats. It is interesting to note in the series of experiments done at the lowest concentration of PM, a significant reduction in the total number of cells recovered from the lungs was observed in animals exposed to ozone or to PM plus ozone compared with filtered air control animals (Table 18). However, the significance of this finding is doubtful since subsequent experiments at intermediate and high PM concentrations failed to demonstrate a similar effect in neonatal animals receiving exposure to ozone alone or in combination with PM (Tables 19 and 20).

Discussion

There is considerable scientific evidence from community-based studies that suggests a link between particulate matter (PM) air pollution exposure and a variety of health effects. These effects range from aggravation of existing respiratory disease to decreased life expectancy in people, especially the elderly, who have pre-existing heart or lung disease. Scientists do not yet know how PM causes these serious health effects or do they know which characteristic(s) of PM, i.e. particle size, particle number or chemical composition, are most important. There is little or no information on the biologic mechanism(s) responsible for these health effects and the scientific community has recognized the need to advance our knowledge in this area.

Under the direction of the California Air Resources Board, investigators at the University of California, Davis and the University of California, Irvine initiated three-year collaborative projects to examine the mechanisms of particulate matter toxicity on the respiratory tract of animals exposed to PM. The goal of investigators at UC Davis was to examine the effects of particle composition and particle concentration on the respiratory tract of young, adult and old rats. The goal of investigators at UC Irvine was to examine the effects of particle size on the respiratory tract of similarly aged animals.

The major challenge facing investigators at both institutions was to examine the mechanisms of respiratory tract toxicity with short-term exposure to PM composed of NH_4NO_3 and carbon, two primary constituents found in California PM. For studies completed at UC Davis, specific indicators of response including cell injury and/or proliferation, influx of inflammatory cells, as well as other indicators of lung toxicity were examined following single or repeated exposure to NH_4NO_3 and carbon at different concentrations. For the purposes of simplicity, these concentration ranges were designated as low, intermediate and high. To better understand the potential for particle-gas interactions, four specific exposure conditions were created for direct comparison of effects: (1) PM (NH_4NO_3 and carbon), (2) PM plus ozone (0.20 ppm), (3) ozone (0.20 ppm), and (4) filtered air (FA). Initial studies were done using a single 6-hour exposure period in adult male F344 rats. Subsequent studies used a repeated 3-day exposure regimen using the intermediate target range of PM in adult male SD and F344 rats. Simultaneous studies were conducted using senescent male F344 rats to compare PM-induced effects in the lungs. The final exposures of this study were done in male and female neonatal F344 rats using the repeated 3-day exposure regimen after the first week of life and again after the third week of life. All three PM target concentration ranges were examined for neonatal animals.

To better understand the behavior of inhaled particles in the rodent respiratory tract in terms of deposition, clearance and short-term retention patterns, fluorescent polycarbonate microspheres were used. Since NH_4NO_3 and carbon were difficult to visualize in the lungs following deposition, fluorescent microspheres served as a surrogate to elucidate how particles would be handled in the lungs of young, adult and old rats.

Short-term exposure using a single 6-hour period was designed at the beginning of the project to serve as a study in particle concentration range-finding to determine potential particle effects on the respiratory system. Adult male F344 rats were used for exposure to NH_4NO_3 and

carbon by inhalation. The three target concentrations were low (NH_4NO_3 , $75 \mu\text{g}/\text{m}^3$; C, $50 \mu\text{g}/\text{m}^3$), intermediate (NH_4NO_3 , $150 \mu\text{g}/\text{m}^3$; C, $100 \mu\text{g}/\text{m}^3$), and high (NH_4NO_3 , $300 \mu\text{g}/\text{m}^3$; C, $150 \mu\text{g}/\text{m}^3$) respectively. These ranges were selected to include in part a range of particle concentrations that could possibly be present during excursions of the PM_{10} air quality standard for the state of California. The proportion of NH_4NO_3 and carbon used in these experiments was designed to approximate their actual ratios in the ambient environment of California. Although it is impossible to exactly mimic such pollution conditions, the use of experimental systems to generate different concentrations of these two major constituents of California PM_{10} afforded the opportunity to identify novel endpoints that could serve as biomarkers of exposure and effect to these constituents. Such studies could help us to begin to explore if effects are noted, the potential mechanisms of particle toxicity in the respiratory tract.

NH_4NO_3 and carbon were used to expose young, adult and old rats to examine the influence of varying particle concentration on potential adverse effects to the respiratory tract. Differences in age were used to explore whether young, adult and old rats respond in a different manner to inhaled particles. Fischer 344 rats were selected to study the issues of age based on the availability of senescent F344 rats through the National Institutes of Aging program supplied by Harlen Inc. (Indianapolis, IN). For a limited number of studies in adult animals, male Sprague Dawley rats were used for pilot studies and to compare potential inter-strain differences in response to inhaled particles. In all instances, only healthy animals were used rather than attempting to create a condition of compromise for either the respiratory or cardiovascular systems in these animals.

The effects of PM on the respiratory tract were compared to the effects of ozone on the respiratory tract. Health effects associated with exposure to ambient air pollutants may be the result of the combined mixture of particles and gases. Therefore, we wished to examine the effects of PM and ozone alone on the respiratory tract as well as the effects of combined exposure to both pollutants. Experimental conditions to carefully control the inhalation of PM of defined composition in the presence or absence ozone would allow us to directly examine the relative toxicity of PM to a specific concentration of ozone as well as potential interactive effects of PM with ozone, the major oxidant air pollutant.

Single and repeated 3-day exposure to NH_4NO_3 and carbon were found to lead to alterations in the normal homeostasis of the lungs in neonatal, adult and senescent rats. These changes could occur either in the presence or absence of simultaneous exposure to ozone. PM-induced changes appeared to be age- and dose-dependent, although the lack of an effect was noted at a higher overall PM concentration ($310 \mu\text{g}/\text{m}^3$ NH_4NO_3 and $236 \mu\text{g}/\text{m}^3$ carbon), compared with pulmonary effects measured at an overall lower PM concentration ($154 \mu\text{g}/\text{m}^3$ NH_4NO_3 and $267 \mu\text{g}/\text{m}^3$ carbon) following a single 6-hour period of exposure. In general, alterations in the normal homeostasis of the lungs following exposure to airborne NH_4NO_3 /carbon particles appeared to be triggered in the healthy rat when the concentration of NH_4NO_3 reached or exceeded $150 \mu\text{g}/\text{m}^3$ and the carbon concentration reached or exceeded $195 \mu\text{g}/\text{m}^3$. These studies confirm that Fischer 344 and Sprague Dawley rats can serve as reasonable animal models to investigate the effects of PM on the respiratory tract. Mixtures of NH_4NO_3 and carbon, common components of California PM, evoke cellular injury in the lungs under conditions that could occur under high ambient concentrations in the state of California.

Studies to examine particle deposition and clearance from the lungs of Fisher 344 and Sprague Dawley rats using fluorescent microspheres provide a number of insights. First, particles with an mean diameter of 1.0 μm can be deposited in the lungs and are found throughout the airways and alveoli. Second, particles of this size appear to be distributed throughout the airways with preferential placement (via deposition and/or translocation) on airway bifurcations. Third, particles appear to be rapidly cleared from the airways (by visual and semiquantitative analysis of whole mount airway preparations). Four, inhaled particles of a mean diameter of 1 μm are slowly cleared from the alveolar regions of the lungs (based on lobe digestion studies). Microsphere deposition (acting as a surrogate for particles) in the lungs of animals previously exposed to NH_4NO_3 , carbon and ozone, may be associated with a deeper penetration of microspheres (i.e., particles) subsequently inhaled into the lungs with less deposition in bronchial airway tree (Figure 38A). In a similar manner, clearance of microspheres (acting again as a surrogate for particles) from the lungs via the airways may be slowed in animals exposed to particulate matter in contrast to those exposed to filtered air (Figure 38B), suggesting a direct effect on cells and/or fluids responsible for particle trapping and clearance via the mucociliary blanket lining the bronchial tree.

Additional studies using fluorescent microspheres in neonatal and old rats focused more on microsphere deposition and fate in the lungs. Of particulate interest was the long-term retention of microspheres in the lungs of neonatal rats. These studies also demonstrated that particles are clearly deposited in rapidly developing lungs of neonatal animals. Although these studies cannot provide a direct measure of the deposition and eventual fate of NH_4NO_3 and carbon particles in the lungs of rats, microsphere studies do demonstrate that this size of particle can be effectively inhaled and deposited in the lungs of young, adult and senescent rats.

Numerous epidemiological studies present mounting evidence of adverse health effects associated with exposure to ambient airborne particles. These health effects center on the respiratory and cardiovascular systems (USEPA, 1996). Those individuals with pre-existing respiratory or cardiovascular disease appear to be especially sensitive to the effects of airborne particles (Dockery et al., 1993; Pope et al., 1995). In this study we examined the potential mechanisms by which airborne particles in the lungs might elicit effects on the respiratory tract following short-term inhalation in healthy adult animals.

Exposure of F344 or SD rats to NH_4NO_3 and carbon at varying concentrations was associated with a variable alteration in the permeability of epithelial cells lining the respiratory tract as measured by the uptake of ethidium homodimer. However, these changes in permeability failed to demonstrate significance. In contrast, both F344 and SD rats were found to have an increase in cellular proliferation (measured as the number of cells incorporating BrdU) located in anatomically distinct regions of the respiratory tract. These sites of cellular proliferation in adult male SD rats were found at bifurcations along the bronchial tree as well as within the proximal alveolar regions of the lungs. For adult male F344 rats sites of cellular proliferation were found within the interstitium of the airways following a single 6 hour exposure, but not after 3 days of particle exposure. Senescent male F344 rats also failed to demonstrate any significant changes in cell proliferation following particle exposure. In neonatal male and female F344 rats, only the highest concentration of NH_4NO_3 and carbon in the presence

of ozone demonstrated a significant increase in cellular proliferation of the epithelial and interstitial cells of the terminal bronchioles. When adverse effects of inhaled particles were noted in the lungs of F344 and SD rats, these changes were typically not limited to the epithelial lining of the airways and alveoli, but were also found in the underlying interstitium. However, not all concentrations of NH_4NO_3 and carbon or all ages (studied only in F344 rats) were associated with significant cellular changes following particle exposure.

Measures using bronchoalveolar lavage demonstrated a significant increase in the total number of alveolar macrophages recovered from the lungs following exposure to PM or to PM plus ozone only in adult male SD rats and senescent male F344 rats following 3 days of exposure to the intermediate concentration of NH_4NO_3 and carbon. Changes brought about by particle exposure in adult male SD rats were highly reproducible, with similar results observed in repeated studies using identical exposure conditions. However, for other ages of F344 rats studied using different concentrations of NH_4NO_3 and carbon, no significant effects were noted in bronchoalveolar lavage parameters. The relevance of these findings based on age may suggest that adult and senescent animals may be more responsive to the effects of inhaled particles with recruitment of macrophages to the air spaces of the lungs. Such observations may suggest that older animals are more prone to eliciting an inflammatory response following environmental insult to inhaled particles. Perhaps in the neonatal lung, the immune defense system is not sufficiently developed to mount the appropriate response to particles entering the respiratory tract. We know from our studies with fluorescent microspheres that particles are able to enter the respiratory tract of neonatal rats and can be retained for considerable periods of time.

The current study demonstrates that NH_4NO_3 and carbon in the presence or absence of 0.2 ppm ozone can elicit cellular effects, even in healthy adult animals. A number of studies using instillation have examined the effects of ambient PM in the lungs (Vincent et al., 1997; Samet et al., 1997; Kodavanti et al. 1999). These studies have used both instillation and inhalation approaches to measure effects in the lungs. Various cellular markers of response have been used following instillation or inhalation of ambient PM. These include increases in the number and types of cells recovered, as well as protein levels measured by bronchoalveolar lavage. Reduction in pulmonary glutathione levels has also been measured following PM instillation (Li et al., 1997). A number of investigations have centered on particle characteristics in understanding health effects. Questions regarding size, composition, the presence of trace metals, or relative acidity of particles may be important in the health effects observed. The interaction of particles with other air pollutants may also be critical in toxicity. A number of investigators have used materials obtained from filters or bagging procedures from diverse locations to study effects. In general, these materials represent a complex mixture of particulates. We chose to use only two materials, NH_4NO_3 and carbon black.

Previous studies to measure the effects of NH_4NO_3 exposure on the lungs have been largely negative. In the current set of animal studies reported here, BrdU uptake into cells of the respiratory tract was the only measure to consistently demonstrate a moderate, but significant effect in a limited number of studies involving F344 and SD rats. Exposure to NH_4NO_3 /carbon particles in the presence or absence of ozone was associated with an increase in the number or proportion of BrdU positive cells in the airways (typically involving epithelium, but occasionally the interstitium) for neonatal F344 rats at the highest concentration and adult male F344 and SD

rats at the intermediate concentration. These findings could be due to differences in the relative amounts of particles deposited and/or translocated to key anatomical sites in the lungs. The most striking effects of exposure to NH_4NO_3 /carbon particles was limited to adult male SD rats exposed to an intermediate concentration of NH_4NO_3 /carbon particles. These effects were confined to highly specific anatomical locations within the lungs and defined as a significant increase in BrdU labeling of cells. The anatomical sites in which these moderate, but significant effects were noted included airway bifurcations and the proximal alveolar regions of the lungs. In contrast, studies in F344 rats demonstrated less effects of exposure to NH_4NO_3 and carbon particles. Significant elevation in the number of BrdU positive cells was found only following a single 6 hour exposure in adult male F344 rats at the intermediate concentration of particles and at the highest concentration of particles with repeated exposure in male and female neonatal rats.

Potential differences in the relative sensitivity of animals based on age (neonatal, adult, and senescent) and particle concentration under our experimental setting could be due to varying concentrations of carbon and/or NH_4NO_3 . To complete each exposure condition, multiple exposures per group had to be generated. Therefore, further variability in the target particle concentration could have occurred. However, particle size was consistently maintained with a MMAD of 1.0-1.1 μm for most experiments. In addition, the target concentrations of NH_4NO_3 and ozone were typically achieved through out these studies. However, achieving the desired carbon concentration was more problematic due to carbon content and analysis. During a number of exposures during the early stages of the study target levels of carbon were greatly exceeded. An improved carbon analysis by Dr. Kochy Fung (1990) was used in the later stages of our study to allow for the proper adjustments to come closer to the target concentrations intended. Therefore, we cannot completely exclude differences in carbon concentration in combination with NH_4NO_3 as also influencing the outcome of earlier projects completed in adult F344 and SD rats.

Site-specific effects of particle exposure within the lungs offer some insights as to the potential mechanisms of particle toxicity. Sparing of the epithelium and underlying interstitium along the airways following particle inhalation, while eliciting significant changes at airway bifurcations and central acinar regions in adult male SD rats, reflects the importance of particle deposition within specific target sites of the lungs. This distinct pattern of injury has been classically associated with inhalation of particles and fibers (Lippmann et al., 1980; Fang et al., 1993). However, these same sites correlate to some degree with sites of injury in the lungs following exposure to ozone. Ozone also has its own unique pattern of injury as observed in terminal bronchioles where particles had no observed effect. Yet, immediately distal to the terminal bronchiole, inhaled particles had a marked effect within the centriacinar regions of the lungs as did ozone. This pattern was not seen as consistently in F344 rats, but should not be ruled out as being of importance in this strain of rat. Differences could be due to sampling techniques (more limited sampling used for F344 rats), strain differences in breathing patterns, and/or differences in the relative sensitive of different strains of animals to inhaled particles.

Exposure to particles alone and in combination with 0.2 ppm of ozone provided a unique opportunity to examine potential interactions between particles and an oxidant gas. Tissue sampling of the lungs at precise locations permitted detection of cellular responses to these ambient air pollutants along the entire respiratory tract beginning at the lobar bronchus.

Continuous exposure to 0.2 ppm of ozone for prolonged periods has been demonstrated to elicit mild changes within the centriacinar regions of the lungs (Last and Pinkerton, 1997). No effects were measured in other regions of the respiratory tract. Vincent and colleagues found exposure to high levels of inhaled PM in senescent rats was not associated with lung injury. However, simultaneous exposure to PM and 0.8 ppm of ozone was associated with significant cellular changes (Vincent et al., 1997). Since the primary target of ozone in the lungs is the epithelium, injury to this compartment by ozone may have facilitated the movement of particles into the epithelial lining as well as the underlying interstitium to produce even greater injury. Our findings suggest that PM effects in healthy adult rats involve both the epithelium and underlying interstitium.

The mechanism of particle/cell interaction at each level of the respiratory tract is not well understood. Inhaled particles could not be visualized in this study to elucidate patterns of deposition or subsequent translocation from initial sites of deposition in the lungs. However, inhalation studies completed using fluorescent microspheres demonstrated that particles with a MMAD of 0.5 to 1.0 μm are able to deposit in the airways and alveoli of both F344 and SD rats, independent of age. The effects of intrapulmonary particles could be observed indirectly on epithelial surfaces as well as in the underlying interstitium. These effects were identified by possible changes in cell permeability and increased frequency of BrdU incorporation in cells. Although a significant change in cell permeability was not observed, a significant increase in BrdU incorporation into cells was confirmed. Significant changes were present following 3 days of exposure to particles in neonatal F344 rats at the highest concentration, as well as in adult F344 (single day exposure) and SD rats (3-day exposure) at the intermediate concentration. This effect was present following exposure to particles in most instances, and always following exposure to particles plus ozone. Therefore, an important finding of this study is that particles can elicit a biological effect in the respiratory tract that is independent of the effects of ozone.

From this study it has been shown particles at certain concentrations can affect the lungs, even in healthy animals. Bronchoalveolar lavage demonstrated that the number of recovered cells from the lungs was significantly increased following particle exposure in adult SD rats and senescent F344 rats. However, exposure to particles and/or ozone under the conditions used did not change protein levels within the lavage supernatant, suggesting that the increase in the number of cells within the air spaces of the lung may occur in the absence of marked injury to epithelial cells. In no instance in any study with F344 rats of all ages or with adult SD rats was the epithelium of the airways or alveoli found to be lifting off from the basal lamina.

We hypothesized that the epithelium of the respiratory tract could serve as a sensitive marker of injury following particle inhalation. Markers of cell permeability, measures of GSH levels along the airways and parenchyma, BrdU uptake to identify those cells undergoing DNA synthesis and/or repair would all serve as sensitive indicators of change. Markers of cell permeability using ethidium homodimer failed to demonstrate a significant change due to particle exposure. GSH levels along the airways were highly variable and were not significantly altered by exposure to particles and/or ozone. BrdU uptake was consistently the most sensitive marker to identify those areas of the respiratory tract susceptible to the effects of exposure to different concentrations of inhaled particles and/or ozone. A number of investigators have demonstrated that airway bifurcations represent important sites for particle deposition

(Schlesinger, 1995). A statistically significant increase was noted in the cell labeling index for both epithelial and interstitial compartments following particle exposure. Animals exposed only to ozone also demonstrated a similar pattern, however, these changes did not reach a level of statistical significance. The absence of injury along the airways confirmed the importance of airflow within the airways and greater deposition/interception of gases and particles at airway branch points. Only terminal bronchioles demonstrated a greater sensitivity to ozone than to PM.

These observations of epithelial effects on the surfaces of airways and bifurcations are also associated with the involvement of the interstitial compartment at these same levels of the conducting airways. Involvement of tissues of the central acinar regions of the lungs immediately beyond the terminal bronchioles is also a distinct likelihood. Such findings suggest that the interaction of particles with cells at sites of deposition may be key in triggering local release of mediators and cytokines, that potentially could be distributed systemically via the blood flow that supplies these same areas of the respiratory tract. In conclusion, we have found (1) NH_4NO_3 and carbon cause injury to the lungs, (2) these effects can be independent of ozone and (3) airway bifurcations and centriacinar regions are important sites of injury to inhaled particulate matter. These findings confirm that measures of biological effect can be used to determine short-term responses to PM exposure. These findings further support the need for additional studies in toxicology to better define the mechanisms of PM-related health effects. This study also emphasizes the importance of age- and dose-related effects to airborne particles as well as the relevance of studying the long-term implications of chronic exposure to PM.

With regard to public health relevance, these studies emphasize the importance of NH_4NO_3 and carbon, the two most prevalent constituents present in airborne particles found in California, to produce subtle, but significant effects in the respiratory system. Although these two constituents are typically thought to have little health implications, we found in rats of all ages (young, adult and old), clear measures of respiratory response following short-term inhalation of these particles. Consequences of particle exposure by age were difficult to clearly assess in terms of severity, but it was obvious in these studies that all ages can be affected by exposure to airborne particles common to the state of California.

Summary and Conclusions

Neonatal, adult and senescent F344 rats were exposed to NH_4NO_3 and carbon, two major components of California PM in the presence or absence of 0.20 ppm ozone. Exposures were done at three different concentrations defined as low (NH_4NO_3 , $75 \mu\text{g}/\text{m}^3$; C, $50 \mu\text{g}/\text{m}^3$), intermediate (NH_4NO_3 , $150 \mu\text{g}/\text{m}^3$; C, $100 \mu\text{g}/\text{m}^3$), and high (NH_4NO_3 , $300 \mu\text{g}/\text{m}^3$; C, $150 \mu\text{g}/\text{m}^3$). Exposures were for 6 hours/day for one or 3 days. A limited number of studies were done using adult male SD rats. Five measures of biological effects were done to determine the relative effects of PM exposure on the respiratory tract. The findings are summarized as follows:

- (1) Cell injury reflected by an increased number or proportion of cells taking up BrdU was noted following PM exposure in both F344 and SD rats. Adult male SD rats demonstrated these changes with positive BrdU cells seen along airway bifurcations and within the proximal alveolar regions of the lungs following 3 days of exposure to the intermediate PM concentration. Increased numbers of BrdU positive cells were also seen in neonatal male and female F344 rats at the high PM concentration, and in adult male F344 rats at the intermediate PM concentration following a single day of exposure. BrdU positive cells typically included epithelial and interstitial cells of the airways.
- (2) Significant labeling of interstitial cells within the same regions of significant epithelial cell labeling suggests the possibility of particle translocation and/or mediators from the airways to the interstitium.
- (3) Intermediate and high concentrations of PM produce limited, but significant effects in neonatal, adult and senescent animals. However, a clearly defined dose response effect of PM exposure was not observed.
- (4) The effects of PM are independent of the effects of ozone (seen in neonatal rats at the highest PM concentration and in adult male F344 and SD rats following a single or 3-day exposure to the intermediate PM concentration, respectively).
- (5) The effects of PM can be seen in healthy animals (neonatal F344 rats at the highest concentration of PM, adult male F344 rats and SD rats following a single or 3-day exposure to an intermediate concentration of PM, and senescent male F344 rats at the intermediate concentration of PM).
- (6) These studies confirm that Fischer 344 and Sprague Dawley rats can serve as models to investigate the effects of PM in the respiratory tract.
- (7) These studies validate the utility of using biological endpoints to determine potential mechanisms of particle-induced lung toxicity within site-specific regions of the lungs.
- (8) These studies support the need to continue studies in animal toxicology. In a similar manner, further studies are needed to elucidate the mechanisms of PM-related health effects.

- (9) For certain parameters, rodent studies may be more sensitive to define particle effects on the respiratory tract than those that can be used in epidemiological studies. Direct effects on cell and tissue compartments of the lungs can be precisely measured following exposure to well-characterized conditions of particulates.
- (10) Since an effect from short-term exposure to PM was observed, these findings raise questions about the long-term implications of chronic exposure to PM.

Unique aspects of this study

Inhalation studies conducted under this contract to the California Air Resources Board provide the following unique contributions to our understanding of health effects to airborne particles:

- (1) The examination of particulate matter generated in carefully controlled conditions and composed of NH_4NO_3 and elemental carbon. Exposures to these particles were done in the presence and absence of ozone.
- (2) The range of particle concentrations used in this study, although high, may approach environmentally relevant conditions that could occur during acute pollution episodes in the state of California.
- (3) NH_4NO_3 and carbon are major constituents of California PM.
- (4) A uniform particle size range was used for all NH_4NO_3 and carbon particle concentrations studied.
- (5) PM effects are independent of ozone.
- (6) Age-specific effects were noted.
- (7) Novel endpoints used in these inhalation studies are proving useful in identifying adverse responses of the respiratory tract to exposure to PM.

Recommendations

The presence of airborne particulate matter in our environment and the health effects associated with exposure to these particles drives in large measure the relevance of why the California Air Resources Board should support endeavors to study the potential causes for PM toxicity. PM is a major component of California air pollution. PM consists of a complex mixture associated with numerous health effects with adverse consequences in particular to the cardiovascular and respiratory systems. The precise biological mechanisms for PM toxicity are unknown. Different mechanisms may exist for different types of PM. We clearly know sensitive populations of individuals exist to the effects of PM, including children, elderly and those with pre-existing cardiovascular and respiratory disease. Of critical importance is the need to identify which characteristics or components of PM are most harmful to minimize public health risk.

We know that PM air pollution causes health effects based on numerous epidemiological studies in which mortality and morbidity track PM levels. There also appears to be a high degree of consistency and coherence among these studies. Health effects measured due to PM exposure are seen worldwide. However, there are many things that we do not know regarding how PM air pollution causes health effects. Which characteristics of PM are most important? Is it particle size, particle composition, particle number or possibly other confounding factors such as other co-pollutants? We do not know what the specific mechanisms are that cause adverse effects. They may be allergic responses, or the result of inflammation, or simply a function of cellular injury and damage. Complex immune responses may also be an important factor in the health effects observed.

The mechanisms involved probably depend on what health effects you are investigating. Different particulate matter “species” are likely to act by different mechanisms. Some may be involved in the worsening of asthma conditions, while others may play a larger role in decreased life expectancy. We also do not yet understand what are the short-term versus long-term effects of PM exposure.

To answer these questions, controlled laboratory exposure studies are needed that can systematically investigate mechanisms associated with particulate toxicity. Studies should be conducted to involve both human clinical research as well as animal exposure efforts. Studies to address similar issues of particle size, particle composition and particle number in a coordinated and controlled manner would begin to provide critical answers. Collaborative efforts based on scientifically sound and well-coordinated plans through the Research Division of CARB could also be highly cost effective.

Specific areas of investigation need to target issues of particle size and particle composition. Such information is critical to design effective health protective programs for the state of California. Sensitive populations such as children or people with pre-existing cardiovascular or respiratory diseases and animal models of such conditions would be ideal for study. Controlled human clinical studies coordinated with animal toxicity studies could begin to address critical issues regarding both effects as well as mechanisms. An important issue is the effect of PM on those with asthma. Asthma affects individuals of all ages. Studies directed to better understand the effects of PM on children or young adults with asthma are particularly

relevant. The Children's Environmental Health Protection Act (California State Senate Bill 25) is a prime example of our need to better understand the health effects of PM in children. Such information is essential to assess whether the current California air quality standard for PM is sufficient to provide adequate protection for the health of our children.

References

- Bolender, R.P., D.M. Hyde, and R.T. Dehoff. (1993). Lung morphometry: A new generation of tools and experiments for organ, tissue, cell, and molecular biology. *Am.J.Physiol.Lung Cell Mol.Physiol.* 265:L521-L548.
- Brody, A.R. and Roe, M.W. (1983). Deposition pattern of inorganic particles at the alveolar level in the lungs of rats and mice. *Am. Rev. Respir. Dis.* 128:724-729.
- California Air Resources Board Monitoring and Laboratory Division. (1992). Standard operating procedure for analyzing anions from ambient air particulate samples from the California acidic dry deposition monitoring network. S. O. P. No. MLD 044, November 12, 1992.
- California Air Resources Board Monitoring and Laboratory Division. (Undated) Standard operating procedure for analysis of dry deposition samples: Field preparation, mass analysis and extraction procedures. S. O. P. No. MLD 041.
- Cambrey, J. (1997). (Personal communication). Cabot Corporation, Billerica, MA, August 27, 1997.
- Chow, J.C., J.G. Watson, D.H. Lowenthal, P.A. Solomon, K.L. Magliano, S.D. Ziman, and L.W. Richards. (1993). PM10 and PM2.5 compositions in California's San Joaquin Valley. *Aerosol Science and Technology* 18:105-128.
- Chow, J.C., et. al. (1992). PM 10 source apportionment in California's San Joaquin Valley. *Atmospheric Environment* 26A: 3335-3354.
- Clegg, S.L., P. Brimblecombe and A.S. Wexler. (1998). A thermodynamic model of the system $H^+ - NH_4^+ - Na^+ - SO_4^{2-} - NO_3^- - Cl^- - H_2O$ at 298.15K. *J. Phys. Chem A* 102:2155-2171.
- Clegg, S.L., P. Brimblecombe and A.S. Wexler. (2001). The aerosol inorganics model project. <<http://www.hpcl.uea.ac.uk/~e770/aim/aim.html>> (May 15, 2001)
- Dockery, D.W., C.A. Pope III, X. Xu, J.D. Spengler, J.H. Ware, M.E. Fay, B.G. Ferris, Jr., and F.E. Speizer. (1993). An association between air pollution and mortality in six U.S. cities. *N. Engl. J. Med.* 329:1753-1759.
- Duan, X., Plopper, C., Brennan, P., and Buckpitt, A. (1996). Rates of glutathione synthesis in lung subcompartments of mice and monkeys: Possible role in species and site selective injury. *J Pharmacol Exp Ther*, 277: 1402-1409.
- Fang, C., J.E. Wilson, D.M. Spektor, and M.Lippmann. (1993). Effect of lung airway branching pattern and gas composition on particle deposition in bronchial airways: III. Experimental studies with radioactively tagged aerosol in human and canine lungs. *Exp Lung Res* 19: 377-396.
- Fung, K. (1990). Particulate carbon speciation by MnO_2 oxidation. *Aerosol Sci. and Technol* 12:122-127.

- Griffith, O. and Meister, A. (1979). Potent and specific inhibition of glutathione synthesis by buthionine sulfoximine (S-n-butyl homocysteine sulfoximine). *J Biol Chem*, 254, 7558-7560.
- Harris, G.W., Carter, W.P.L., Winer, A.M., Graham, R.A. and Pitts, J.N., Jr. (1982). Studies of trace non-ozone species produced in a corona discharge ozonizer. *J. Air Poll. Control Assoc.* 32, 274-276.
- Hinners, R.G., J.K. Burkhart and C.L. Punte. (1968). Animal inhalation exposure chambers. *Arch. Environ. Health* 16:194-206.
- Hobbs, P.C.D., Gross, V.P. and Murray, K.D. (1990). Suppression of particle generation in a modified clean room corona air ionizer. *J. Aerosol Sci.* 21, 463-465.
- Hsu, S.M., L. Raine, and H. Fanger. (1981). The use of avidin-biotin peroxidase complex (ABC) in Immunoperoxidase techniques: A comparison between ABC and unlabeled (PAP) procedures. *J Histochem Cytochem.* 26:577-580.
- Hyat, M.A. (1989) Chemical fixation. In: *Principles and Techniques of Electron Microscopy*. M.A. Hyat, ed. CRC Press, Boca Raton, pp. f1-78.
- Institute of Laboratory Animal Resources National Research Council. (1996). *Guide for the Care and Use of Laboratory Animals*, 127 p. National Academy Press, Washington, DC.
- Kennedy G.L. (1989) Inhalation Toxicology. In: *Principles and Methods of Toxicology*, 2nd ed. A.W. Hayes, ed. Raven Press, New York, pp. 361-382.
- Kleinman, M.T., C. Bufalino, R. Rasmussen, D. Hyde, D.K. Bhalla, and W.J. Mautz. (2000). Toxicity of chemical components of ambient fine particulate matter (PM 2.5) inhaled by aged rats. *J. Appl. Toxicol* 20:357-364.
- Kleinman, M.T. (2001). (Personal communication). University of California at Irvine, May 2, 2001.
- Kodavanti, U.P., Hauser, R., Christiani, D.C., Meng, Z.H., McGee, J., Ledbetter, A., Richards, J., and Costa, D.L. (1998). Pulmonary responses to oil fly ash particles in the rat differ by virtue of their specific soluble metals. *Tox Sci* 43:202-212.
- Lakritz, J., C.G. Plopper, and A.R. Buckpitt. (1997). Validated high-performance liquid chromatography-electrochemical method for determination of glutathione and glutathione disulfide in small tissue samples. *Anal. Biochem.* 247:63-68.
- Last, J. and K.E. Pinkerton. (1997). Chronic exposure of rats to ozone and sulfuric acid aerosol; biochemical and structural responses. *Toxicology* 116: 133-146.
- Li, X.Y., P.S. Gilmour, K. Donaldson, and W. MacNee. (1997). In vivo and in vitro proinflammatory effects of particulate air pollution (PM 10). *Environ Health Perspect* 105: 1279-1283.
- Lippmann, M., D. Yeates, and R. Albert. 1980. Deposition, retention, and clearance of inhaled particles. *Br J Ind Med* 37(4): 337-362.

- Lippmann M. 1992. Introduction and background. In: Environmental Toxicants: Human Exposures and their Health Effects. M. Lippmann, ed. Van Nostrand Reinhold, New York, pp 1-29.
- MacFarland, H.N. (1983). Designs and operational characteristics of inhalation exposure equipment - a review. *Fundam. Appl. Toxicol.* 3:603-613.
- Meister, A. (1994). Glutathione, ascorbate, and cellular protection. *Cancer Res.* 54:1969s-1975s.
- Mercer, T.T., M.I. Tillary and G.J. Newton. (1970). A multi-stage low flow rate cascade impactor. *Aerosol Sci.* 1:9-15.
- Miller, F.J., S. Anjilvel, M.G. Menache, B. Asgharian, and T.R. Gerrity. 1995. Dosimetric issues relating to particulate toxicity. *Inhalation Toxicol.* 7: 615-632.
- Oberdorster, G., R.M. Gelein, J. Ferin, and B. Weiss. (1995). Association of particulate air pollution and acute mortality: Involvement of ultrafine particles? *Inhalation Toxicol.* 7:111-124.
- Pinkerton, K.E., Gallen J.T., Mercer, R.R., Wong, V.C., Plopper C.G. and Tarkington B.K. (1993) Aerosolized fluorescent microspheres detected in the lung using confocal scanning laser microscopy. *Microscopy Research and Technique* 26:437-443.
- Pope, A., D.W. Dockery, J.D. Spengler, and M.E. Raizenne. 1991. Respiratory Health and PM10 Pollution. *Am Rev Respir Dis* 144: 668-674.
- Pope, C.A. III, M.J. Thun, M.M. Namboodiri, D.W. Dockery, J.S. Evans, F.E. Speizer, and C.W. Heath. (1995). Particulate air pollution as a predictor of mortality in a prospective study of U. S. adults. *Am. J Respir. Crit. Care.* 151:669-674.
- Postlethwait, R.M., J.P. Joad, D.M. Hyde, E.S. Schelegle, J.M. Bric, A.J. Weir, L.F. Putney, V.J. Wong, L.W. Velsor, and C.G. Plopper. (2000). Three-dimensional mapping of ozone-induced acute cytotoxicity in tracheobronchial airways of isolated perfused rat lung. *Am. J. Respir. Cell Mol. Biol.* 22:191-199.
- Raabe, O.G. (1968). The dilution of monodisperse suspensions for aerosolization. *Am. Ind. Hyg. Assoc. J.* 29:439-443.
- Rahman, Q., P. Abidi, F. Afaq, D. Schiffmann, B.T. Mossman, D.W. Kamp, and M. Athar. (1999). Glutathione redox system in oxidative lung injury. *Crit.Rev.Toxicol.* 29:543-568.
- Rajini, P., T.R. Gelzleichter, J.A. Last, and H. Witschi. (1993). Airway epithelial labeling index as an indicator of ozone induced lung injury. *Toxicology* 83:159-168.
- Saldiva, P.H.N., C.A.I. Pope, J. Schwartz, D.W. Dockery, A.J. Lichtenfels, J.M. Salge, I. Barone, and G.M. Bohm. (1995). Air Pollution and Mortality in Elderly People: A Time-Series Study in Sao Paulo, Brazil. *Arch Environ Health* 50: 159-163.

- Samet, J.M., S. L. Zeger, and K. Birhane. (1995). The association of mortality and particulate air pollution. In: *Particulate Air Pollution and Daily Phase I Report of the Particle Epidemiology Evaluation Project*. Health Effects Institute, Cambridge, MA.
- Samet, J.M., Stonehuerner, J., Reed, W., Devlin, R.B., Dailey, L.A., Kennedy, T.P., Bromberg, P.A., Ghio, A.J. (1997). Disruption of protein tyrosine phosphate homeostasis in bronchial epithelial cells exposed to oil fly ash. *Am J Physiol Lung Cell Mol Physiol* 272:L427-432.
- Schlesinger, R.B. (1995). Toxicological evidence for health effects from inhaled particulate pollution: Does it support the human experience? *Inhalation Toxicol.* 7:99-109.
- Schwarz, J. and Morris, R. (1995). Air pollution and hospital admissions for cardiovascular disease in Detroit, Michigan. *Am. J. Epidemiol.* 142: 23-35.
- Schwartz, J. (1996). Air pollution and hospital admissions for respiratory disease. *Epidemiology* 7: 20-28.
- Schwartz, J. (1995). Short-term fluctuations in air pollution and hospital admissions of the elderly for respiratory disease. *Thorax* 50:531-538.
- Schwartz, J. (1994). What are people dying of on high pollution days? *Environ. Res.* 64:26-35.
- Teague, S.V., Yeh, H.C., and Newton, G.J. (1978). Fabrication and use of krypton-85 aerosol discharge devices. *Health Phys.* 35:392-395.
- United States Code of Federal Regulations. (1988). Measurement principle and calibration procedure for the measurement of ozone in the atmosphere, Protection of the Environment, Title 40, Environmental Protection Agency, pp. 667-683, Office of the Federal Register, Washington, DC.
- Valberg, P.A. (1985). Determination of retained lung dose. In: *Toxicology of Inhaled Materials, Handbook of Experimental Pharmacology*, Vol. 75 H.P. Witschi, J.D. Brain, eds. Springer-Verlag, New York.
- Van Winkle, L.S., Z.A. Johnson, S.J. Nishio, C.D. Brown, and C.G. Plopper. (1999). Early events in naphthalene-induced acute Clara cell toxicity: Comparison of membrane permeability and ultrastructure. *Am. J. Respir. Cell Mol. Biol.* 21:44-53.
- Vincent, R., S. Bjarnason, I. Adamsom, C. Hedgecock, P. Kumarathanan, J. Guenette, M. Potvin, P. Goegan, and L. Bouthiller. (1997). Acute pulmonary toxicity of urban particulate matter and ozone. *Am J Pathol* 151: 1563-1570.
- Warheit, D.B., Chang, L.Y., Hill, L.H., Hook, G.E.R., Crapo, J.D. and Brody, A.R. (1984). Pulmonary macrophage accumulation and asbestos-induced lesions at sites of fiber deposition. *Am. Rev. Respir. Dis.* 129:301-310.

Glossary of Terms, Abbreviations, and Symbols

EtD-1	Ethidium homodimer – 1
PM	Particulate matter
F344	Fischer 344 rat
$\mu\text{g}/\text{m}^3$	Microgram per cubic meter
S-D	Sprague-Dawley
SD	Standard deviation
BSO	Buthionine sulfoximine
n	Sample number
hr	Hour
O ₃	Ozone
PM+O ₃	Particulate matter plus ozone
μm	Micrometer
BrdU	Bromodeoxyuridime
FA	Filtered air control
NH ₄ NO ₃	Ammonium nitrate
C	Carbon
DNA	Deoxyribonucleic acid
CARB	California Air Resources Board
UC	University of California
m ³	Cubic meter
m ³ /min	Cubic meter per minute
⁸⁵ Kr	Krypton 85
MMAD	Mass median aerodynamic diameter
cm	Centimeter
σ_g	Sigma g
YoPRO-1	A fluorescent dye with a high binding affinity to DNA
F-12	Media used to keep cells viable
$\mu\text{L}/\text{h}$	Microliter per hour
°C	Degrees centigrade (Celsius)
HCl	Hydrogen chloride (hydrochloric acid)
PBS	Physiologic buffered saline
Z-fix	Formalin-based fixative containing zinc ions
H&E	Hematoxylin and eosin
N _v	Numerical volume density
Epi	Epithelial
A	Area
H	Height
YG	Yellow green fluorescent microspheres
PC-red	Polychromatic red fluorescent microspheres
P	Probability
ANOVA	Analysis of variance
ppm	Parts per million
HPLC	High pressure liquid chromatography

nmoles	Nanomoles
mg	Milligram
TB _{EPI}	Epithelial cells of the terminal bronchiole
TB _{INT}	interstitial cells of the terminal bronchiole
AD _{EPI}	Epithelial cells of the alveolar duct
AD _{INT}	Interstitial cells of the alveolar duct
BI _{EPI}	Epithelial cells at bronchial bifurcation
BI _{INT}	Interstitial cells at bronchial bifurcation
ml	Milliliter
Mac	Macrophage
Lymph	Lymphocyte
Neut	neutrophil

APPENDIX A

<u>PM Exposure</u>	<u>Rat Species</u>	<u>PM Concentration</u>	<u>Exposure Time</u>
PM-1 to PM-6	F344 – Healthy Adult	High	6 hours for 1 day
PM-7 to PM-12	F344 – Healthy Adult	Intermediate	6 hours for 1 day
PM-13, PM-14	Hsd:Sd – Healthy Adult	Intermediate	6 hours per day for 3 days
PM-15, PM-16	F344 – Healthy Adult	Low	6 hours for 1 day
PM-17, PM-18	Hsd:Sd – Healthy Adult	Intermediate	6 hours per day for 3 days
PM-19	F344 – Healthy Adult	Intermediate	6 hours per day for 3 days
PM-20	F344 – Senescent	Intermediate	6 hours per day for 3 days
PM-21	F344 – Healthy Adult	Intermediate	6 hours per day for 3 days
PM-22	F344 – Senescent	Intermediate	6 hours per day for 3 days
PM-23, PM-24	F344 – Senescent	Intermediate	6 hours per day for 3 days
PM-25, PM-26	F344 – Neonatal	Intermediate	6 hours per day for 3 days
PM-28, PM-29	F344 – Neonatal	Intermediate	6 hours per day for 3 days
PM-30 to PM-33	F344 – Neonatal	High	6 hours per day for 3 days
Pm-34 to PM-37	F344 – Neonatal	Low	6 hours per day for 3 days
PM-38, PM-39	F344 – Neonatal	Intermediate	6 hours per day for 3 days

Protocol for measurement of GSH in dissected airways

Preparation of solutions

A: (200 mM methane sulfonic acid/5 mM DTPA): 1316 μ l methane sulfonic acid + 196.6 mg DTPA (diethylenepentaacetic acid)

GSH Standard A: Make up a 1 mg/ml solution in water with 10% solution A

GSSG Standard A: Make up a 1 mg/ml solution in water with 10% solution A
(These can be stored in small aliquots at -80°C).

Stock Solution B (GSH): 20 μ l Standard GSH A and 20 μ l GSSG A and dilute to 200 μ l.

Stock Solution C (GSH): 20 μ l Stock solution B and dilute to 200 μ l.

Stock Solution D (GSH): 20 μ l Stock solution C and dilute to 200 μ l.

Mobile Phase: weigh 6.9 g NaH_2PO_4 into 800 ml polished water. Filter through a 0.22 μ membrane. Add 11 mg octane sulfonic acid and adjust the pH to 2.7 with H_3PO_4 . Add 20 ml acetonitrile. Adjust acetonitrile as necessary to obtain adequate separation of GSH from the "front."

Column: ODS 2 Phase sep 25 cm

Detector Settings: Guard cell +950 mv

E1 +400 mv

E2 +875 mv

Steps:

1. Samples should be either rapidly frozen on dry ice or placed directly in a small quantity of solution A. If dissected airways are being used, samples should be homogenized thoroughly in 100 μ l solution A. The sample is transferred to a microcentrifuge tube, with rinsing, and the protein is pelleted by centrifugation. An aliquot of the supernatant is diluted with mobile phase in an autosampler vial. The amount of dilution is dependent upon the sample size but a 1:1 dilution usually works well. For example 10^5 Clara cells should be resuspended in 25 μ l solution A. 50 μ l mobile phase should be added and 25 μ l of the sample injected.
2. Pellets will be dissolved in 1 M NaOH and an aliquot will be taken for protein determination. Data will be calculated as nmoles GSH per mg protein.

Standard curve: 1 mg/ml, 0.1 mg/ml, 0.01 mg/ml, 0.001 mg/ml

Standard #	µl GSH A	Stock Soln. B	Stock Soln. C	Stock Soln. D	µl mobile phase	ul injected	ng injected
1	10				190	20	1000
2	---				190	20	1000
3	5				190	20	500
4		25			175	20	250
5		20			180	20	200
6		15			185	20	150
7		10			190	20	100
8		7.5			192.5	20	75.0
9		5.0			195	20	50.0
10			25		175	20	25.0
11			20		180	20	20.0
12			15		185	20	15.0
13			10		190	20	10.0
14			5.0		195	20	5.0
15			2.5		197.5	20	2.5
16				10.0	190	20	1.0
17				5.0	195	20	0.5
18				2.5	197.5	20	0.25

PM Exposure Series

	Target	PM-1		PM-2		PM-3	
		EX6-1	EX6-2	EX6-1	EX6-2	EX6-1	EX6-2
NH ₄ NO ₃ , μg/m ³ ± SD	300	211 ± 9	238 ± 14	255 ± 30	287 ± 106	305 ± 32	356 ± 29
Carbon, μg/m ³ ± SD	200	~10	~10	87	111 ± 32	97 ± 47	133 ± 159
Mass Monitor, μg/m ³ ± SD		NA	NA	NA	NA	NA	NA
Total Mass Concentration, μg/m ³		NA	NA	380	415	437	NA
Carbon by Difference ^a , μg/m ³		NA	NA	125	128	132	NA
Slurry							
NH ₄ NO ₃ , g/liter			7.07		7.07		7.07
Carbon, g/liter			7.07		7.07		14.1
Ratio, NH ₄ NO ₃ :Carbon			1:1		1:1		1:1.99
Aerosol Mass Concentrations							
Ratio, NH ₄ NO ₃ :Carbon		1:~0.05	1:~0.04	1:0.34	1:0.39	1:0.32	1:0.37
Aerosol Size							
MMAD ^b , μm		0.97	1.20	1.05	0.88	0.59	0.70
σ _g ^c		2.22	2.63	2.24	2.67	2.15	2.21
O ₃ , ppm ± SD	0.20	0.20 ± 0.01		0.20 ± 0.01		0.20 ± 0.01	

^aCarbon by Difference, μg/m³ = Total Mass Concentration, μg/m³ - NH₄NO₃, μg/m³

^bMass median aerodynamic diameter

^cGeometric standard deviation

PM Exposure Series

	Target	PM-4		PM-5		PM-6	
		EX6-1	EX6-2	EX6-1	EX6-2	EX6-1	EX6-2
NH ₄ NO ₃ , μg/m ³ ± SD	300	329 ± 8	293 ± 142	408 ± 25	283 ± 99	409 ± 67	346 ± 48
Carbon, μg/m ³ ± SD	200	?	?	467 ± 157	246 ± 180	391 ± 168	354 ± 125
Mass Monitor, μg/m ³ ± SD		NA	NA	NA	NA	640 ± 140 ^d	570 ± 110 ^d
Total Mass Concentration, μg/m ³		560	547	764	386	625	560
Carbon by Difference ^a , μg/m ³		231	254	356	103	216	221
Slurry							
NH ₄ NO ₃ , g/liter			7.07		7.07		7.07
Carbon, g/liter			14.1		14.1		14.1
Ratio, NH ₄ NO ₃ :Carbon			1:1.99		1:1.99		1:1.99
Aerosol Mass Concentrations							
Ratio, NH ₄ NO ₃ :Carbon		?	?	1:1.14	1:0.87	1:0.96	1:1.02
Aerosol Size							
MMAD ^b , μm		0.77	1.00	0.94	0.86	0.93	0.85
σ _g ^c		2.14	1.95	2.02	1.92	1.83	1.91
O ₃ , ppm ± SD	0.20	0.20 ± 0.01		0.21 ± 0.01		0.20 ± 0.01	

^aCarbon by Difference, μg/m³ = Total Mass Concentration, μg/m³ - NH₄NO₃, μg/m³

^bMass median aerodynamic diameter

^cGeometric standard deviation

^dITEH monitor serial no. 178

PM Exposure Series

	Target	PM-7		PM-8		PM-9	
		EX6-1	EX6-2	EX6-1	EX6-2	EX6-1	EX6-2
NH ₄ NO ₃ , μg/m ³ ± SD	150	233 ± 24	203 ± 26	122 ± 44	126 ± 33	149 ± 27	145 ± 10
Carbon, μg/m ³ ± SD	100	325 ± 164	314 ± 150	218 ± 28	224 ± 43	?	?
Mass Monitor, μg/m ³ ± SD		NA	NA	340 ± 130 ^d	340 ± 140 ^d	340 ± 40 ^d	340 ± 120 ^d
Total Mass Concentration, μg/m ³		497	387	314	287	295	290
Carbon by Difference ^a , μg/m ³		264	184	181	124	146	145
Slurry							
NH ₄ NO ₃ , g/liter			4.86		4.86		4.86
Carbon, g/liter			7.1		7.1		7.1
Ratio, NH ₄ NO ₃ :Carbon			1:1.46		1:1.46		1:1.46
Aerosol Mass Concentrations							
Ratio, NH ₄ NO ₃ :Carbon		1:1.39	1:1.55	1:1.64	1:1.78	?	?
Aerosol Size							
MMAD ^b , μm		0.98	0.91	0.97	0.98	0.98	0.91
σ _g ^c		2.14	2.14	2.06	2.14	1.95	2.03
O ₃ , ppm ± SD	0.20	0.20 ± 0.01		0.20 ± 0.01		0.20 ± 0.01	

^aCarbon by Difference, μg/m³ = Total Mass Concentration, μg/m³ - NH₄NO₃, μg/m³

^bMass median aerodynamic diameter

^cGeometric standard deviation

^dITEH monitor serial no. 166 corrected, y = 1.2734x + 0.0173

PM Exposure Series

	Target	PM-10		PM-11		PM-12	
		EX6-1	EX6-2	EX6-1	EX6-2	EX6-1	EX6-2
NH ₄ NO ₃ , μg/m ³ ± SD	150	138 ± 22	122 ± 27	154 ± 11	163 ± 16	138 ± 4	161 ± 13
Carbon, μg/m ³ ± SD	100	273 ± 47	243 ± 70	235 ± 16	309 ± 68	249 ± 16	282 ± 42
Mass Monitor, μg/m ³ ± SD		340 ± 70 ^d	290 ± 100 ^d	340 ± 40 ^d	360 ± 110 ^d	330 ± 50 ^d	360 ± 50 ^d
Total Mass Concentration, μg/m ³		336	277	334	396	312	389
Carbon by Difference ^a , μg/m ³		198	155	180	233	174	228
Slurry							
NH ₄ NO ₃ , g/liter			4.86		4.86		4.86
Carbon, g/liter			7.1		7.1		7.1
Ratio, NH ₄ NO ₃ :Carbon			1:1.46		1:1.46		1:1.46
Aerosol Mass Concentrations							
Ratio, NH ₄ NO ₃ :Carbon		1:1.98	1:1.99	1:1.53	1:1.90	1:1.80	1:75
Aerosol Size							
MMAD ^b , μm		1.01	0.96	0.97	0.90	1.00	0.97
σ _g ^c		2.07	1.97	1.96	2.02	2.10	1.96
O ₃ , ppm ± SD	0.20	0.20 ± 0.01		0.21 ± 0.01		0.20 ± 0.01	

^aCarbon by Difference, μg/m³ = Total Mass Concentration, μg/m³ - NH₄NO₃, μg/m³

^bMass median aerodynamic diameter

^cGeometric standard deviation

^dITEH monitor serial no. 166 corrected, y = 1.2734x + 0.0173

PM Exposure Series

	Target	PM-13 (3 Days)		PM-14 (3 Days)	
		EX6-1	EX6-2	EX6-1	EX6-2
NH ₄ NO ₃ , μg/m ³ ± SD	150	151 ± 13	148 ± 10	132 ± 28	150 ± 25
Carbon, μg/m ³ ± SD	100	252 ± 81 ^e	238 ± 78 ^e	166 ± 41 ^e	219 ± 65 ^e
Mass Monitor, μg/m ³ ± SD		380 ± 100 ^d	390 ± 110 ^d	310 ± 50 ^d	310 ± 80 ^d
Total Mass Concentration, μg/m ³		455 ± 84	423 ± 81	381 ± 69	400 ± 24
Carbon by Difference ^a , μg/m ³		304	275	249	250
Slurry					
NH ₄ NO ₃ , g/liter			4.86		4.86
Carbon, g/liter			7.1		7.1
Ratio, NH ₄ NO ₃ :Carbon			1:1.46		1:1.46
Aerosol Mass Concentrations					
Ratio, NH ₄ NO ₃ :Carbon		1:1.67	1:1.61	1:1.26	1:1.46
Aerosol Size					
MMAD ^b , μm		1.09	0.99	1.05	0.99
σ _g ^c		1.93	1.94	2.19	2.32
O ₃ , ppm ± SD	0.20	0.20 ± 0.01		0.20 ± 0.01	

^aCarbon by Difference, μg/m³ = Total Mass Concentration, μg/m³ - NH₄NO₃, μg/m³

^bMass median aerodynamic diameter

^cGeometric standard deviation

^dFor PM-13 ITEH monitor serial no. 166 corrected, $y = 1.2734x + 0.0173$; for PM-14 Exp. Fac. monitor serial no. 557899

^eAnalyzed by Dr. Kochy Fung of Atmospheric Assessment Associates, Inc.

PM Exposure Series

	Target	Pre PM-15 (Test)		PM-15		PM-16	
		EX6-1	EX6-2	EX6-1	EX6-2	EX6-1	EX6-2
NH ₄ NO ₃ , μg/m ³ ± SD	75	83 ± 12	---	80 ± 3	81 ± 9	77 ± 11	72 ± 10
Carbon, μg/m ³ ± SD	50	6 ± 3	---	61 ± 16 ^e	70 ± 8 ^e	60 ± 12 ^e	57 ± 20 ^e
Mass Monitor, μg/m ³ ± SD		120 ± 40 ^d	---	180 ± 20 ^d	170 ± 20 ^d	160 ± 20 ^d	140 ± 30 ^d
Total Mass Concentration, μg/m ³		151	---	173	172	163	130
Carbon by Difference ^a , μg/m ³		68	---	93	91	86	58
Slurry							
NH ₄ NO ₃ , g/liter			2.43		2.43		2.43
Carbon, g/liter			2.43		2.43		2.43
Ratio, NH ₄ NO ₃ :Carbon			1:1		1:1		1:1
Aerosol Mass Concentrations							
Ratio, NH ₄ NO ₃ :Carbon		1:0.07	---	1:0.76	1:0.86	1:0.78	1:0.79
Aerosol Size							
MMAD ^b , μm		---	---	1.00	0.97	0.95	1.20
σ _g ^c		---	---	2.15	1.96	1.95	1.83
O ₃ , ppm ± SD	0.20	---		0.20 ± 0.01		0.20 ± 0.01	

^aCarbon by Difference, μg/m³ = Total Mass Concentration, μg/m³ - NH₄NO₃, μg/m³

^bMass median aerodynamic diameter

^cGeometric standard deviation

^dExp. Fac. monitor serial no. 557899

^eAnalyzed by Dr. Kochy Fung of Atmospheric Assessment Associates, Inc.

PM Exposure Series

	Target	PM-17 (3 Days)		PM-18 (3 Days)	
		EX6-1	EX6-2	EX6-1	EX6-2
NH ₄ NO ₃ , μg/m ³ ± SD	150	136 ± 25	156 ± 13	124 ± 20	135 ± 17
Carbon, μg/m ³ ± SD	100	140 ± 29 ^e	173 ± 31 ^e	170 ± 44 ^e	193 ± 32 ^e
Mass Monitor, μg/m ³ ± SD		290 ± 70 ^d	340 ± 60 ^d	230 ± 70 ^d	250 ± 70 ^d
Total Mass Concentration, μg/m ³		351 ± 26	378 ± 49	328 ± 36	328 ± 10
Carbon by Difference ^a , μg/m ³		215	222	204	193
Slurry					
NH ₄ NO ₃ , g/liter			4.86		4.86
Carbon, g/liter			7.1		7.1
Ratio, NH ₄ NO ₃ :Carbon			1:1.46		1:1.46
Aerosol Mass Concentrations					
Ratio, NH ₄ NO ₃ :Carbon		1:1.03	1:1.11	1:1.37	1:1.43
Aerosol Size					
MMAD ^b , μm		1.00	1.02	1.18	1.10
σ _g ^c		2.01	2.06	1.86	1.95
O ₃ , ppm ± SD	0.20	0.20 ± 0.01		0.20 ± 0.01	

^aCarbon by Difference, μg/m³ = Total Mass Concentration, μg/m³ - NH₄NO₃, μg/m³

^bMass median aerodynamic diameter

^cGeometric standard deviation

^dExp. Fac. monitor serial no. 557899

^eAnalyzed by Dr. Kochy Fung of Atmospheric Assessment Associates, Inc.

PM Exposure Series

	Target	PM-19 (3 Days)		PM-20 (3 Days)	
		EX6-1	EX6-2	EX6-1	EX6-2
NH ₄ NO ₃ , μg/m ³ ± SD	150	152 ± 4	160 ± 11	148 ± 13	152 ± 13
Carbon, μg/m ³ ± SD	100	104 ± 11 ^e	105 ± 11 ^e	99 ± 11 ^e	107 ± 11 ^e
Mass Monitor, μg/m ³ ± SD		210 ± 20 ^d	210 ± 22 ^d	210 ± 20 ^d	200 ± 22 ^d
Total Mass Concentration, μg/m ³		285 ± 45	285 ± 36	247 ± 23	255 ± 19
Carbon by Difference ^a , μg/m ³		133	125	99	103
Slurry					
NH ₄ NO ₃ , g/liter			5.10		5.10
Carbon, g/liter			4.08		4.08
Ratio, NH ₄ NO ₃ :Carbon			1:0.8		1:0.8
Aerosol Mass Concentrations					
Ratio, NH ₄ NO ₃ :Carbon		1:0.68	1:0.67	1:0.67	1:0.70
Aerosol Size					
MMAD ^b , μm ± SD		0.88 ± 0.08	0.87 ± 0.09	0.88 ± 0.08	0.87 ± 0.09
σ _g ^c ± SD		2.48 ± 0.20	2.43 ± 0.37	2.48 ± 0.20	2.43 ± 0.37
O ₃ , ppm ± SD	0.20	0.20 ± 0.01		0.20 ± 0.01	

^aCarbon by Difference, μg/m³ = Total Mass Concentration, μg/m³ - NH₄NO₃, μg/m³

^bMass median aerodynamic diameter

^cGeometric standard deviation

^dExp. Fac. monitor serial no. 557899

^eAnalyzed by Dr. Kochy Fung of Atmospheric Assessment Associates, Inc.

PM Exposure Series

	Target	PM-21 (3 Days)		PM-22 (3 Days)	
		EX6-1	EX6-2	EX6-1	EX6-2
NH ₄ NO ₃ , μg/m ³ ± SD	150	174 ± 16	179 ± 18	173 ± 15	177 ± 11
Carbon, μg/m ³ ± SD	100	130 ± 13 ^e	128 ± 24 ^e	135 ± 15 ^e	129 ± 12 ^e
Mass Monitor, μg/m ³ ± SD		270 ± 60 ^d	280 ± 60 ^d	240 ± 30 ^d	270 ± 20 ^d
Total Mass Concentration, μg/m ³		282 ± 11	304 ± 18	283 ± 12	292 ± 1
Carbon by Difference ^a , μg/m ³		108	125	110	115
Slurry					
NH ₄ NO ₃ , g/liter			5.10		5.10
Carbon, g/liter			4.08		4.08
Ratio, NH ₄ NO ₃ :Carbon			1:0.8		1:0.8
Aerosol Mass Concentrations					
Ratio, NH ₄ NO ₃ :Carbon		1:0.75	1:0.72	1:0.78	1:0.73
Aerosol Size					
MMAD ^b , μm		1.03	0.84	1.03	0.84
σ _g ^c		2.38	2.32	2.38	2.32
O ₃ , ppm ± SD	0.20	0.19 ± 0.02		0.18 ± 0.01	

^aCarbon by Difference, μg/m³ = Total Mass Concentration, μg/m³ - NH₄NO₃, μg/m³

^bMass median aerodynamic diameter

^cGeometric standard deviation

^dExp. Fac. monitor serial no. 557899

^eAnalyzed by Dr. Kochy Fung of Atmospheric Assessment Associates, Inc.

PM Exposure Series

	Target	PM-23 (3 Days)		PM-24 (3 Days)	
		EX6-1	EX6-2	EX6-1	EX6-2
NH ₄ NO ₃ , μg/m ³ ± SD	150	139 ± 20	150 ± 20	145 ± 19	152 ± 22
Carbon, μg/m ³ ± SD	100	110 ± 23 ^e	118 ± 3 ^e	110 ± 23 ^e	119 ± 11 ^e
Mass Monitor, μg/m ³ ± SD		210 ± 60 ^d	230 ± 60 ^d	210 ± 50 ^d	220 ± 50 ^d
Total Mass Concentration, μg/m ³		259 ± 63	258 ± 10	272 ± 54	257 ± 13
Carbon by Difference ^a , μg/m ³		120	108	127	105
Slurry					
NH ₄ NO ₃ , g/liter			5.10		5.10
Carbon, g/liter			4.08		4.08
Ratio, NH ₄ NO ₃ :Carbon			1:0.8		1:0.8
Aerosol Mass Concentrations					
Ratio, NH ₄ NO ₃ :Carbon		1:0.79	1:0.79	1:0.76	1:0.78
Aerosol Size					
MMAD ^b , μm		1.10	1.10	1.10	1.10
σ _g ^c		2.32	2.45	2.32	2.45
O ₃ , ppm ± SD	0.20	0.19 ± 0.01		0.19 ± 0.01	

^aCarbon by Difference, μg/m³ = Total Mass Concentration, μg/m³ - NH₄NO₃, μg/m³

^bMass median aerodynamic diameter

^cGeometric standard deviation

^dExp. Fac. monitor serial no. 557899

^eAnalyzed by Dr. Kochy Fung of Atmospheric Assessment Associates, Inc.

PM Exposure Series

	Target	PM-25 (3 + 3 Days)		PM-26 (3 + 3 Days)	
		EX6-1	EX6-2	EX6-1	EX6-2
NH ₄ NO ₃ , μg/m ³ ± SD	150	143 ± 17	149 ± 14	143 ± 16	147 ± 17
Carbon, μg/m ³ ± SD	100	107 ± 20 ^e	107 ± 22 ^e	106 ± 22 ^e	103 ± 28 ^e
Mass Monitor, μg/m ³ ± SD		240 ± 50 ^d	250 ± 60 ^d	240 ± 50 ^d	240 ± 60 ^d
Total Mass Concentration, μg/m ³		258 ± 29	280 ± 22	248 ± 21	275 ± 32
Carbon by Difference ^a , μg/m ³		115	131	105	128
Slurry					
NH ₄ NO ₃ , g/liter			5.10		5.10
Carbon, g/liter			4.08		4.08
Ratio, NH ₄ NO ₃ :Carbon			1:0.8		1:0.8
Aerosol Mass Concentrations					
Ratio, NH ₄ NO ₃ :Carbon		1:0.75	1:0.72	1:0.74	1:0.70
Aerosol Size					
MMAD ^b , μm ± SD		1.18 ± 0.11	1.33 ± 0.39	1.18 ± 0.11	1.33 ± 0.39
σ _g ^c ± SD		2.59 ± 0.26	2.50 ± 0.43	2.59 ± 0.26	2.50 ± 0.43
O ₃ , ppm ± SD	0.20	0.20 ± 0.01		0.20 ± 0.01	

^aCarbon by Difference, μg/m³ = Total Mass Concentration, μg/m³ - NH₄NO₃, μg/m³

^bMass median aerodynamic diameter

^cGeometric standard deviation

^dExp. Fac. monitor serial no. 557899

^eAnalyzed by Dr. Kochy Fung of Atmospheric Assessment Associates, Inc.

PM Exposure Series

	Target	PM-27 (3 Days)		
		EX6-1	EX6-2	EX6-0
NH ₄ NO ₃ , μg/m ³ ± SD	150	134 ± 12	126 ± 9	
Carbon, μg/m ³ ± SD	100	98 ± 13 ^e	90 ± 7 ^e	
Mass Monitor, μg/m ³ ± SD		270 ± 46 ^d	300 ± 42 ^d	
Total Mass Concentration, μg/m ³		280 ± 49	286 ± 29	
Carbon by Difference ^a , μg/m ³		146	160	
Slurry				
NH ₄ NO ₃ , g/liter			5.10	
Carbon, g/liter			4.08	
Ratio, NH ₄ NO ₃ :Carbon			1:0.8	
Aerosol Mass Concentrations				
Ratio, NH ₄ NO ₃ :Carbon		1:0.73	1:0.71	
Aerosol Size				
MMAD ^b , μm		1.28	1.30	
σ _g ^c		2.07	2.15	
O ₃ , ppm ± SD	0.20		0.19 ± 0.02	0.20 ± 0.01

^aCarbon by Difference, μg/m³ = Total Mass Concentration, μg/m³ - NH₄NO₃, μg/m³

^bMass median aerodynamic diameter

^cGeometric standard deviation

^dITEH monitor serial no. 178

^eAnalyzed by Dr. Kochy Fung of Atmospheric Assessment Associates, Inc.

PM Exposure Series

	Target	PM-28 (3 + 3 Days)		PM-29 (3 + 3 Days)	
		EX6-1	EX6-2	EX6-1	EX6-2
NH ₄ NO ₃ , μg/m ³ ± SD	150	156 ± 23	149 ± 21	158 ± 20	151 ± 21
Carbon, μg/m ³ ± SD	100	138 ± 45 ^e	128 ± 35 ^e	140 ± 44 ^e	129 ± 34 ^e
Mass Monitor, μg/m ³ ± SD		310 ± 60 ^d	300 ± 60 ^d	310 ± 60 ^d	300 ± 50 ^d
Total Mass Concentration, μg/m ³		300 ± 39	288 ± 38	304 ± 34	298 ± 32
Carbon by Difference ^a , μg/m ³		144	139	146	147
Slurry					
NH ₄ NO ₃ , g/liter			5.10		5.10
Carbon, g/liter			4.08		4.08
Ratio, NH ₄ NO ₃ :Carbon			1:0.8		1:0.8
Aerosol Mass Concentrations					
Ratio, NH ₄ NO ₃ :Carbon		1:0.88	1:0.86	1:0.89	1:0.85
Aerosol Size					
MMAD ^b , μm ± SD		1.30 ± 0.00	1.23 ± 0.11	1.30 ± 0.00	1.23 ± 0.11
σ _g ^c ± SD		2.19 ± 0.27	2.22 ± 0.30	2.19 ± 0.27	2.22 ± 0.30
O ₃ , ppm ± SD	0.20	0.19 ± 0.01		0.20 ± 0.01	

^aCarbon by Difference, μg/m³ = Total Mass Concentration, μg/m³ - NH₄NO₃, μg/m³

^bMass median aerodynamic diameter

^cGeometric standard deviation

^dExp. Fac. monitor serial no. 557899 used for first 3 day exposure and ITEH monitor serial no. 178 used for second 3 day exposure

^eAnalyzed by Dr. Kochy Fung of Atmospheric Assessment Associates, Inc.

PM Exposure Series

	Target	PM-30 (3 + 3 Days)		PM-31 (3 + 3 Days)	
		EX6-1	EX6-2	EX6-1	EX6-2
NH ₄ NO ₃ , μg/m ³ ± SD	300	305 ± 15	290 ± 19	295 ± 26	296 ± 21
Carbon, μg/m ³ ± SD	200	247 ± 23 ^e	251 ± 39 ^e	244 ± 28 ^e	252 ± 40 ^e
Mass Monitor, μg/m ³ ± SD		480 ± 40 ^d	470 ± 40 ^d	480 ± 40 ^d	480 ± 50 ^d
Total Mass Concentration, μg/m ³		546 ± 39	546 ± 17	536 ± 43	552 ± 14
Carbon by Difference ^a , μg/m ³		241	256	241	256
Slurry					
NH ₄ NO ₃ , g/liter			10.20		10.20
Carbon, g/liter			8.16		8.16
Ratio, NH ₄ NO ₃ :Carbon			1:0.8		1:0.8
Aerosol Mass Concentrations					
Ratio, NH ₄ NO ₃ :Carbon		1:0.81	1:0.87	1:0.83	1:0.85
Aerosol Size					
MMAD ^b , μm ± SD		1.10 ± 0.00	1.13 ± 0.18	1.10 ± 0.00	1.13 ± 0.18
σ _g ^c ± SD		2.56 ± 0.37	2.84 ± 0.06	2.56 ± 0.37	2.84 ± 0.06
O ₃ , ppm ± SD	0.20	0.19 ± 0.02		0.19 ± 0.02	

^aCarbon by Difference, μg/m³ = Total Mass Concentration, μg/m³ - NH₄NO₃, μg/m³

^bMass median aerodynamic diameter

^cGeometric standard deviation

^dExp. Fac. monitor serial no. 557899

^eAnalyzed by Dr. Kochy Fung of Atmospheric Assessment Associates, Inc.

PM Exposure Series

	Target	PM-32 (3 + 3 Days)		PM-33 (3 + 3 Days)	
		EX6-1	EX6-2	EX6-1	EX6-2
NH ₄ NO ₃ , μg/m ³ ± SD	300	280 ± 27	273 ± 23	287 ± 24	281 ± 27
Carbon, μg/m ³ ± SD	200	237 ± 30 ^e	240 ± 18 ^e	241 ± 24 ^e	236 ± 19 ^e
Mass Monitor, μg/m ³ ± SD		470 ± 50 ^d	470 ± 50 ^d	480 ± 50 ^d	470 ± 40 ^d
Total Mass Concentration, μg/m ³		531 ± 30	535 ± 15	537 ± 29	537 ± 15
Carbon by Difference ^a , μg/m ³		251	262	250	256
Slurry					
NH ₄ NO ₃ , g/liter			10.20		10.20
Carbon, g/liter			8.16		8.16
Ratio, NH ₄ NO ₃ :Carbon			1:0.8		1:0.8
Aerosol Mass Concentrations					
Ratio, NH ₄ NO ₃ :Carbon		1:0.85	1:0.88	1:0.84	1:0.84
Aerosol Size					
MMAD ^b , μm ± SD		1.10 ± 0.00	1.22 ± 0.05	1.10 ± 0.00	1.22 ± 0.05
σ _g ^c ± SD		2.41 ± 0.58	2.46 ± 0.60	2.41 ± 0.58	2.46 ± 0.60
O ₃ , ppm ± SD	0.20	0.19 ± 0.01		0.19 ± 0.01	

^aCarbon by Difference, μg/m³ = Total Mass Concentration, μg/m³ - NH₄NO₃, μg/m³

^bMass median aerodynamic diameter

^cGeometric standard deviation

^dExp. Fac. monitor serial no. 557899

^eAnalyzed by Dr. Kochy Fung of Atmospheric Assessment Associates, Inc.

PM Exposure Series

	Target	PM-34 (3 + 3 Days)		PM-35 (3 + 3 Days)	
		EX6-1	EX6-2	EX6-1	EX6-2
NH ₄ NO ₃ , μg/m ³ ± SD	75	73 ± 12	76 ± 11	76 ± 10	76 ± 12
Carbon, μg/m ³ ± SD	50	53 ± 10 ^e	55 ± 9 ^e	53 ± 10 ^e	55 ± 9 ^e
Mass Monitor, μg/m ³ ± SD		120 ± 20 ^d	130 ± 10 ^d	130 ± 20 ^d	130 ± 20 ^d
Total Mass Concentration, μg/m ³		127 ± 26	134 ± 21	133 ± 25	132 ± 23
Carbon by Difference ^a , μg/m ³		54	58	57	56
Slurry					
NH ₄ NO ₃ , g/liter			2.55		2.55
Carbon, g/liter			2.04		2.04
Ratio, NH ₄ NO ₃ :Carbon			1:0.8		1:0.8
Aerosol Mass Concentrations					
Ratio, NH ₄ NO ₃ :Carbon		1:0.73	1:0.72	1:0.70	1:0.72
Aerosol Size					
MMAD ^b , μm ± SD		0.94 ± 0.07	0.95 ± 0.07	0.94 ± 0.07	0.95 ± 0.07
σ _g ^c ± SD		2.06 ± 0.19	2.10 ± 0.01	2.06 ± 0.19	2.10 ± 0.01
O ₃ , ppm ± SD	0.20	0.20 ± 0.01		0.19 ± 0.02	

^aCarbon by Difference, μg/m³ = Total Mass Concentration, μg/m³ - NH₄NO₃, μg/m³

^bMass median aerodynamic diameter

^cGeometric standard deviation

^dExp. Fac. monitor serial no. 557899

^eAnalyzed by Dr. Kochy Fung of Atmospheric Assessment Associates, Inc.

PM Exposure Series

	Target	PM-36 (3 + 3 Days)		PM-37 (3 + 3 Days)	
		EX6-1	EX6-2	EX6-1	EX6-2
NH ₄ NO ₃ , μg/m ³ ± SD	75	78 ± 10	79 ± 12	78 ± 10	79 ± 12
Carbon, μg/m ³ ± SD	50	60 ± 7 ^e	56 ± 9 ^e	59 ± 7 ^e	57 ± 9 ^e
Mass Monitor, μg/m ³ ± SD		140 ± 20 ^d	130 ± 30 ^d	130 ± 20 ^d	130 ± 30 ^d
Total Mass Concentration, μg/m ³		144 ± 18	138 ± 28	140 ± 19	135 ± 29
Carbon by Difference ^a , μg/m ³		66	59	62	56
Slurry					
NH ₄ NO ₃ , g/liter			2.55		2.55
Carbon, g/liter			2.04		2.04
Ratio, NH ₄ NO ₃ :Carbon			1:0.8		1:0.8
Aerosol Mass Concentrations					
Ratio, NH ₄ NO ₃ :Carbon		1:0.77	1:0.71	1:0.76	1:0.72
Aerosol Size					
MMAD ^b , μm ± SD		1.01 ± 0.06	0.99 ± 0.01	1.01 ± 0.06	0.99 ± 0.01
σ _g ^c ± SD		2.04 ± 0.09	1.90 ± 0.01	2.04 ± 0.09	1.90 ± 0.01
O ₃ , ppm ± SD	0.20	0.20 ± 0.03		0.20 ± 0.02	

^aCarbon by Difference, μg/m³ = Total Mass Concentration, μg/m³ - NH₄NO₃, μg/m³

^bMass median aerodynamic diameter

^cGeometric standard deviation

^dExp. Fac. monitor serial no. 557899

^eAnalyzed by Dr. Kochy Fung of Atmospheric Assessment Associates, Inc.

PM Exposure Series

	Target	PM-38 (3 + 3 Days)		PM-39 (3 + 3 Days)	
		EX6-1	EX6-2	EX6-1	EX6-2
NH ₄ NO ₃ , μg/m ³ ± SD	150	137 ± 20	136 ± 21	141 ± 21	137 ± 22
Carbon, μg/m ³ ± SD	100	127 ± 21 ^e	132 ± 38 ^e	132 ± 24 ^e	139 ± 44 ^e
Mass Monitor, μg/m ³ ± SD		240 ± 40 ^d	250 ± 50 ^d	240 ± 40 ^d	250 ± 50 ^d
Total Mass Concentration, μg/m ³		271 ± 17	275 ± 52	276 ± 18	280 ± 56
Carbon by Difference ^a , μg/m ³		134	139	135	143
Slurry					
NH ₄ NO ₃ , g/liter			5.10		5.10
Carbon, g/liter			4.08		4.08
Ratio, NH ₄ NO ₃ :Carbon			1:0.8		1:0.8
Aerosol Mass Concentrations					
Ratio, NH ₄ NO ₃ :Carbon		1:0.93	1:0.97	1:0.94	1:1.02
Aerosol Size					
MMAD ^b , μm ± SD		1.03 ± 0.04	1.10 ± 0.07	1.03 ± 0.04	1.10 ± 0.07
σ _g ^c ± SD		2.34 ± 0.20	2.36 ± 0.10	2.34 ± 0.20	2.36 ± 0.10
O ₃ , ppm ± SD	0.20	0.20 ± 0.01		0.20 ± 0.01	

^aCarbon by Difference, μg/m³ = Total Mass Concentration, μg/m³ - NH₄NO₃, μg/m³

^bMass median aerodynamic diameter

^cGeometric standard deviation

^dExp. Fac. monitor serial no. 557899

^eAnalyzed by Dr. Kochy Fung of Atmospheric Assessment Associates, Inc.

APPENDIX B

**Compounds contained in carbon black provided by
the UC Davis container**

Sample Weight = 1.0054g

Sheet1

Data File Name: CEC047.D
Data File Path: D:\CE-CERT\
Date Acquired: 07/18/97
Method File: CE-CERT1

Sample Name: carbon, CONT. 8
Misc Info:
Vial Number: 14

UCD
CONTAINER
8

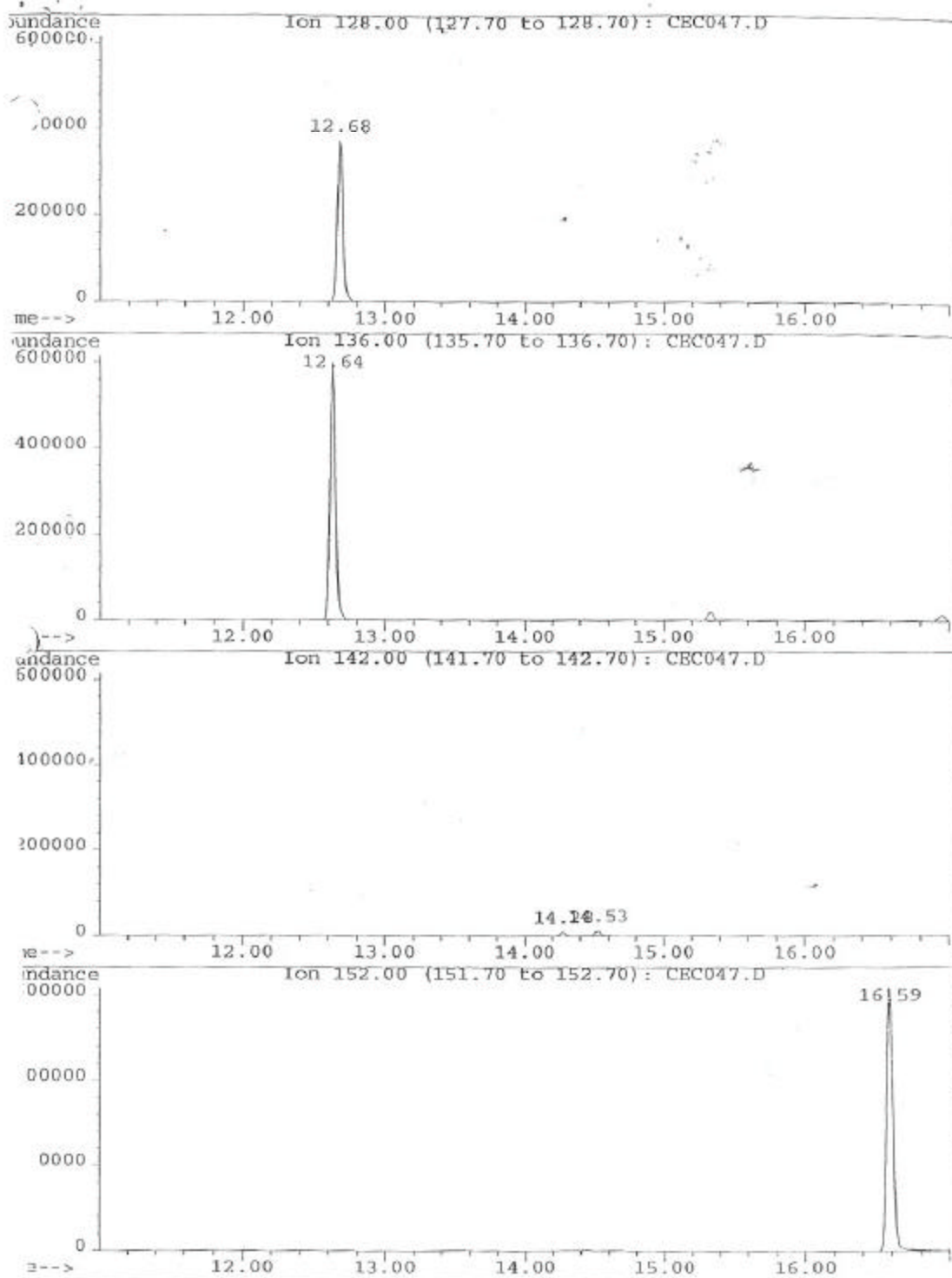
ug/1.0054g

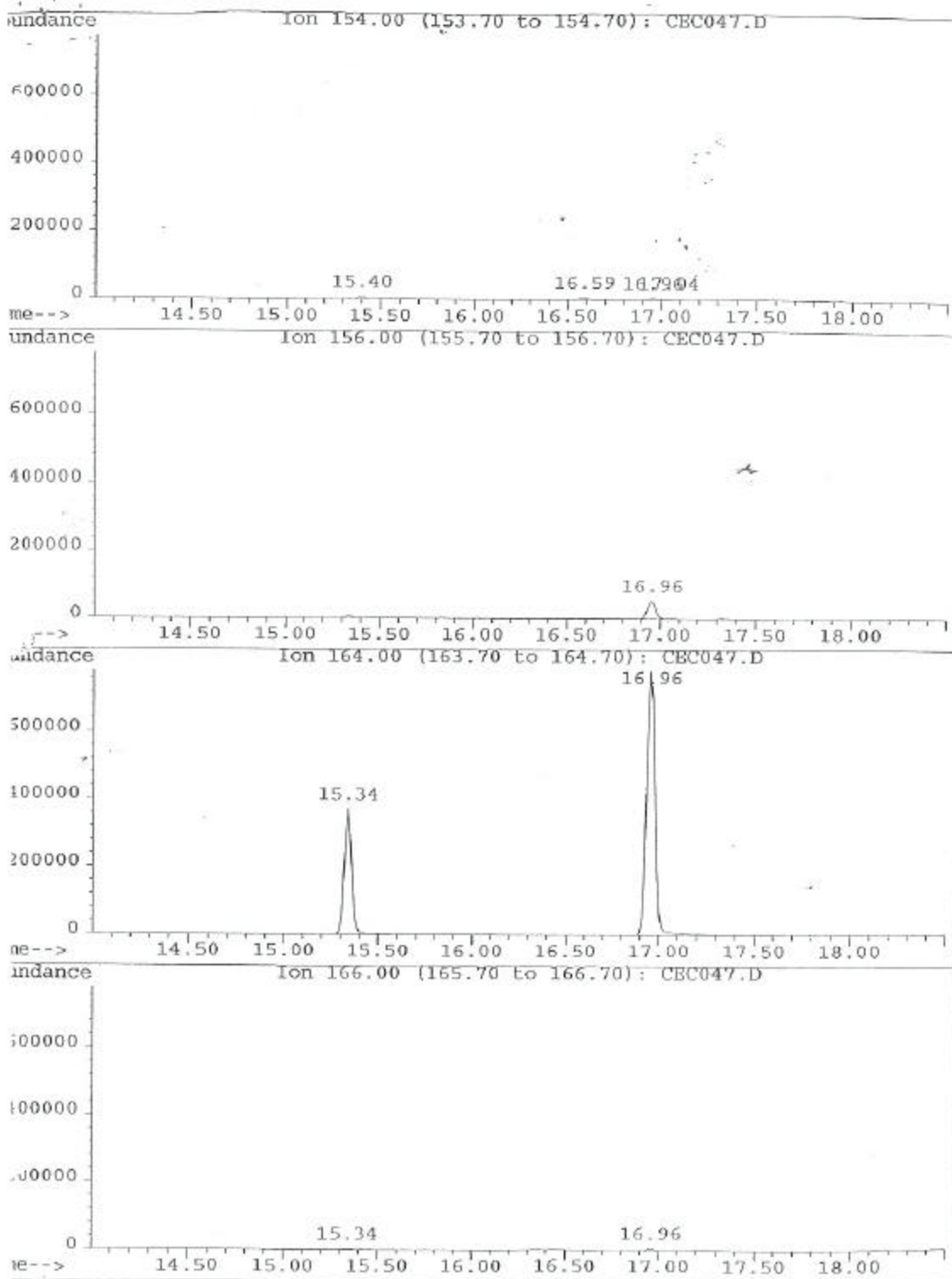
#	Compound	m/z	Ret. Time	Area	Amount	Peak Type
1	Naphthalene-d8	136	12.63	16201183	9.30	*ISTD
2	Naphthalene	128	12.68	10169572	4.96	
3	2-menaphthalene	142	14.28	219790	0.15	
4	1-menaphthalene	142	14.53	313967	0.25	
5	Biphenyl-d10	164	15.35	10436945	6.85	*ISTD
6	2,6+2,7-dimenaphthalene	156	15.83	31972	0.03	
7	1,7+1,3+1,6-dimenaphthalene	156	16.02	48933	0.04	
8	2,3+1,4+1,5-dimenaphthalene	156	16.34	16061	0.01	
9	1,2-dimenaphthalene	156	16.56	43262	0.04	
10	1,8-dimenaphthalene	156	16.90	12435	0.01	
11	Biphenyl	154	15.40	172634	0.09	
12	A-Methylbiphenyl	168	0.00	0	0.00	
13	2-Methylbiphenyl	168	15.59	3574	0.00	
14	B-Methylbiphenyl	168	15.60	3791	0.02	
15	3-Methylbiphenyl	168	16.85	25974	0.02	
16	4-Methylbiphenyl	168	17.01	20934	0.02	
17	C-Methylbiphenyl	168	17.01	20748	0.07	
18	A-Trimethylnaphthalene	170	17.19	8397	0.01	
19	1-Ethyl-2-methylnaphthalene	170	17.29	13536	0.02	
20	B-Trimethylnaphthalene	170	17.45	11304	0.01	
21	C-Trimethylnaphthalene	170	17.57	12943	0.02	
22	2-Ethyl-1-methylnaphthalene	170	17.67	459	0.00	
23	E-Trimethylnaphthalene	170	17.78	9595	0.01	
24	F-Trimethylnaphthalene	170	17.86	9865	0.01	
25	G-Trimethylnaphthalene	170	18.03	8570	0.01	
26	H-Trimethylnaphthalene	170	18.29	782	0.00	
27	1,2,8-Trimethylnaphthalene	170	18.79	559	0.00	
28	Acenaphthene-d10	164	16.96	24121541	11.29	*ISTD
29	Acenaphthylene	152	16.59	18572584	4.57	
30	Acenaphthene	154	17.04	69517	0.03	
31	Fluorene	166	18.48	42429	0.02	
32	Phenanthrene-d10	188	21.20	32817731	5.00	*ISTD
33	Phenanthrene	178	21.27	121062103	13.52	
34	A-Methylfluorene	180	19.95	21145	0.00	
35	1-Methylfluorene	180	20.09	17105	0.00	
36	B-Methylfluorene	180	20.26	4074	0.00	
37	C-Methylfluorene	180	20.61	4788218	0.90	
38	A-Methylphenanthrene	192	22.72	183653	0.02	
39	2-Methylphenanthrene	192	22.81	202668	0.02	
40	B-Methylphenanthrene	192	22.96	21135	0.00	
41	C-Methylphenanthrene	192	23.06	465261	0.05	
42	1-Methylphenanthrene	192	23.14	394662	0.05	
43	3,6-Dimethylphenanthrene	206	24.09	14033	0.00	

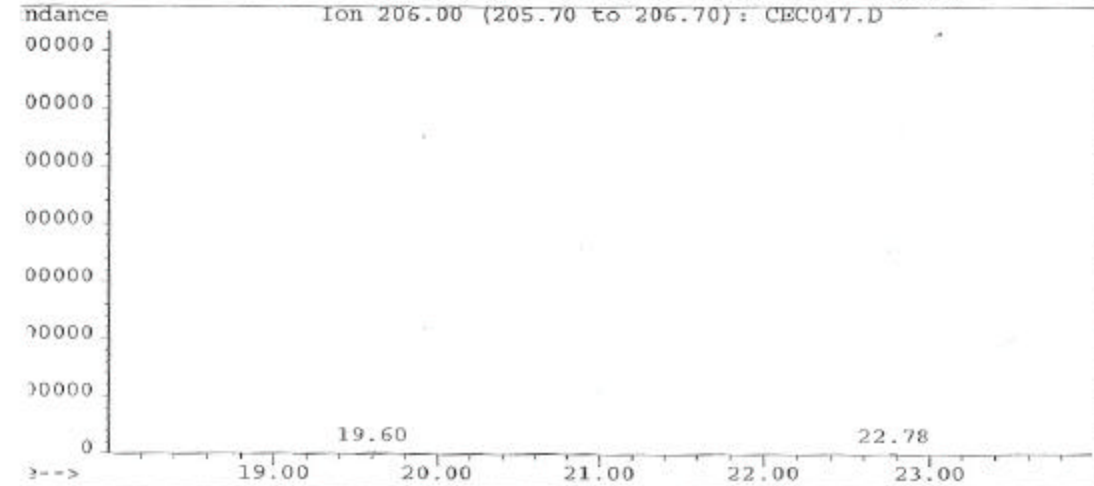
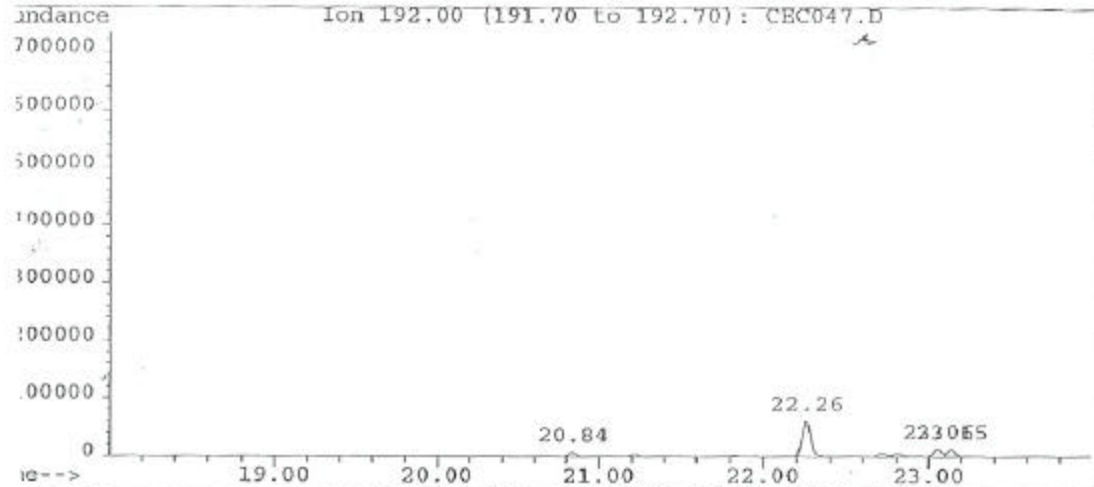
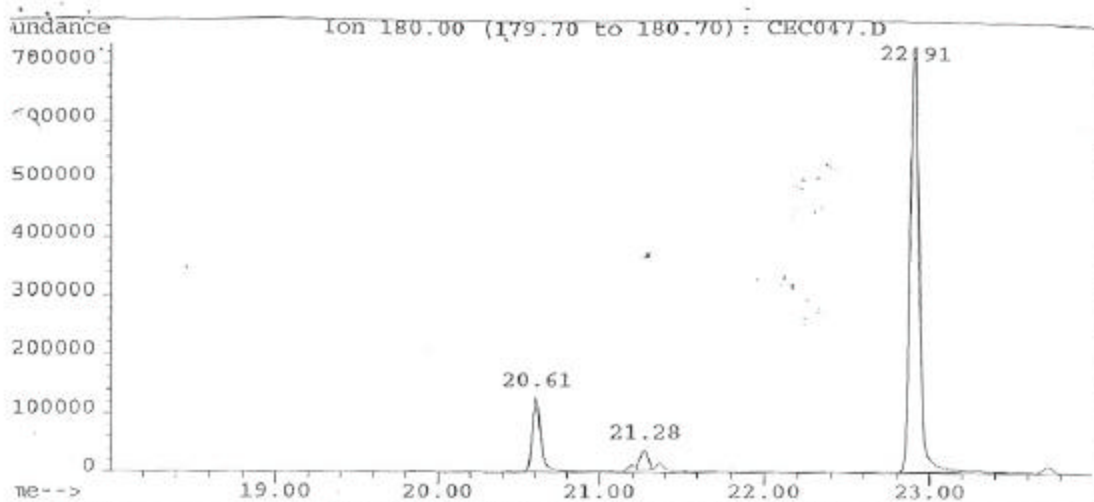


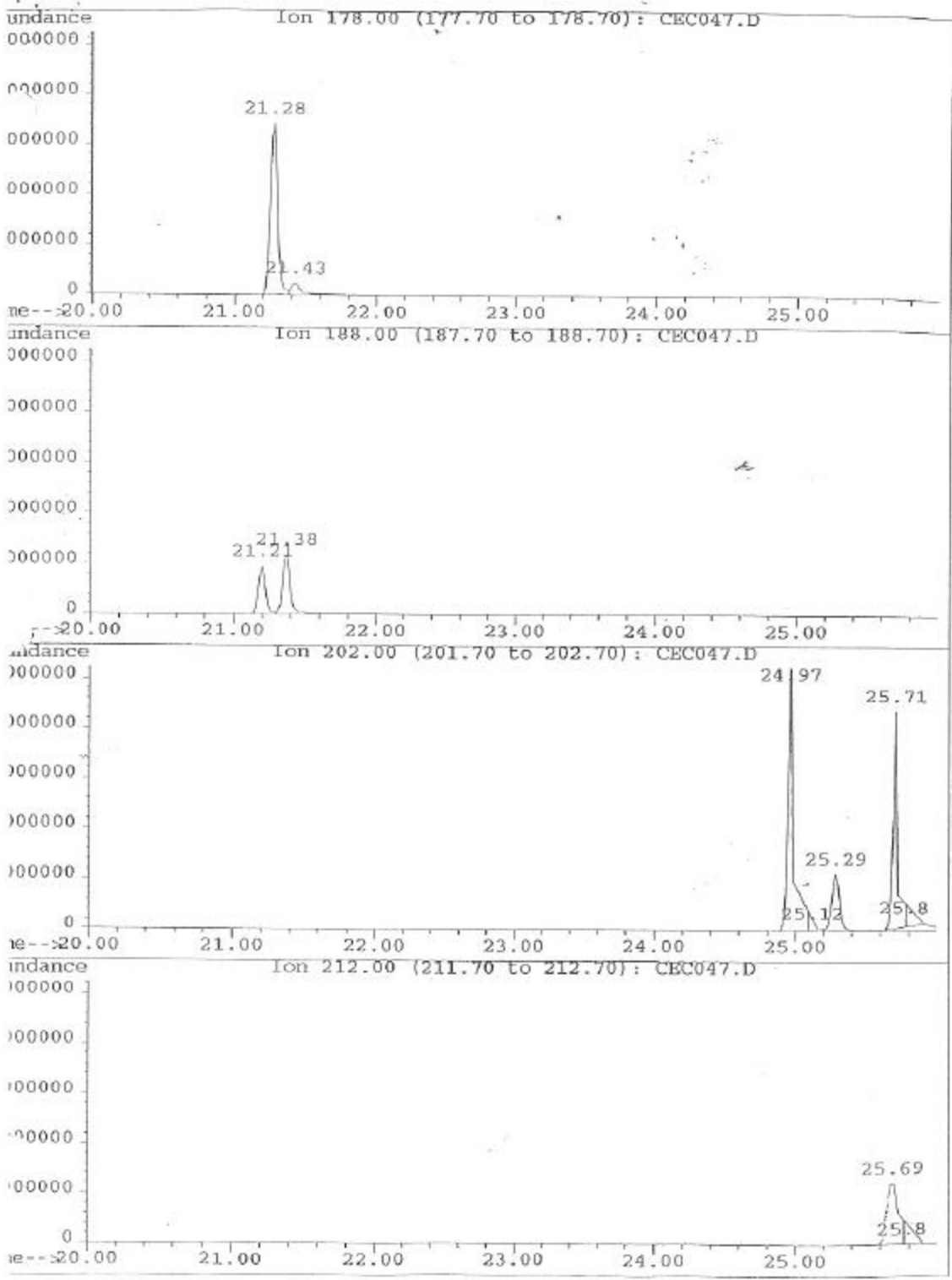
Sheet1

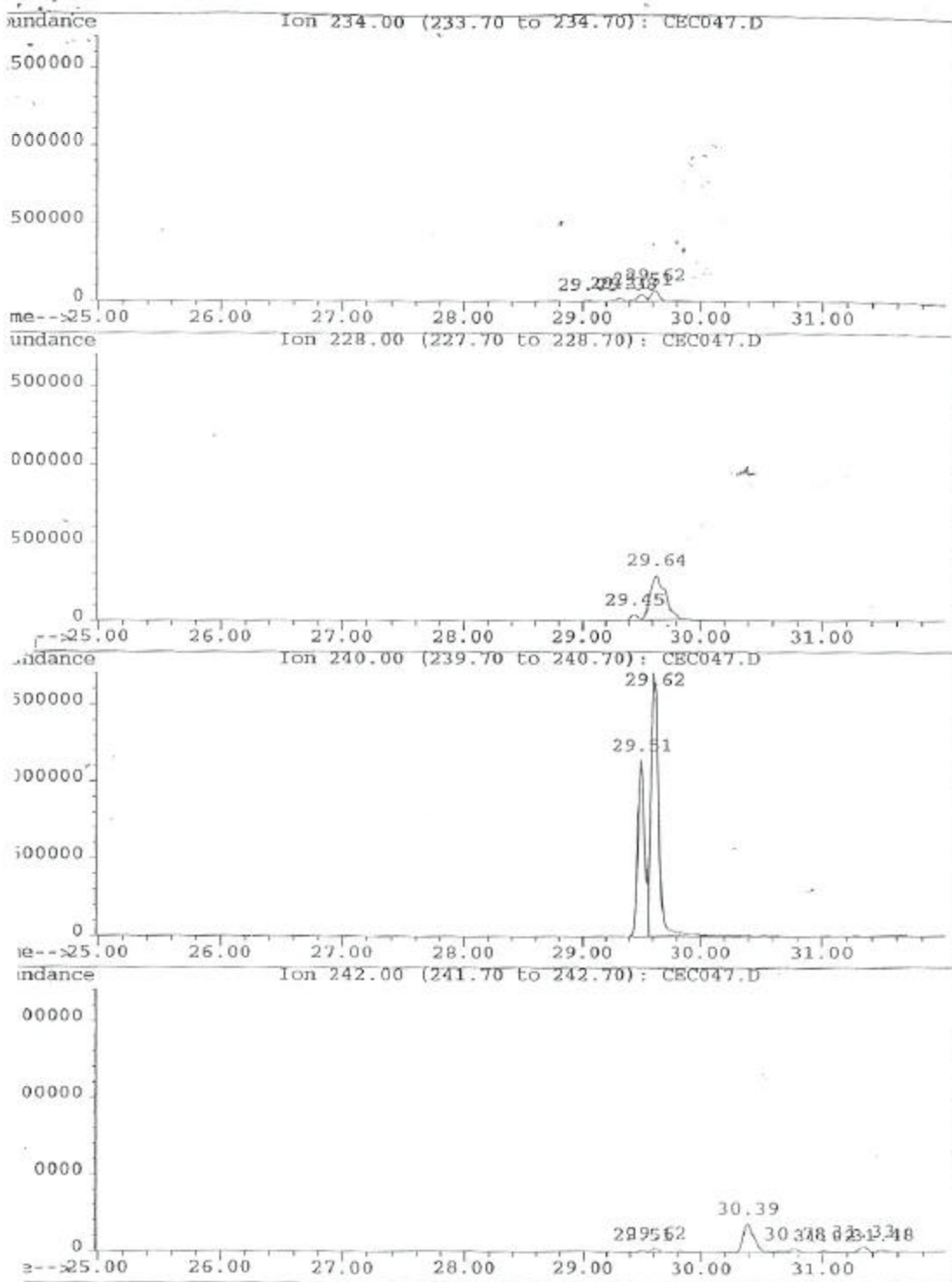
44 A-Dimethylphenanthrene	206	24.19	14402	0.00
45 B-Dimethylphenanthrene	206	24.27	4718	0.00
46 C-Dimethylphenanthrene	206	24.43	13183	0.00
47 1,7-Dimethylphenanthrene	206	24.54	2848	0.00
48 D-Dimethylphenanthrene	206	24.62	6574	0.00
49 E-Dimethylphenanthrene	206	24.75	350310	0.04
50 Anthracene-d10	188	21.38	43316705	6.25 *ISTD
51 Anthracene	178	21.43	11765506	1.23
52 9-Methylanthracene	192	23.60	7367	0.00
53 Pyrene-d12	212	25.68	84233015	5.62 *ISTD
54 Fluoranthene	202	24.96	146186248	8.46 29.88
55 Pyrene	202	25.71	116841761	6.68 108.92
56 Retene	234	26.55	47946	0.00
57 Benzonaphthothiophene	234	28.78	257781	0.01
58 A-Methylpyrene	216	25.45	1190631	0.08
59 B-Methylpyrene	216	26.40	301903	0.02
60 C-Methylpyrene	216	26.69	838909	0.06
61 D-Methylpyrene	216	26.87	9451	0.00
62 E-Methylpyrene	216	27.09	1733212	0.11
63 4-Methylpyrene	216	27.39	4919816	0.32
64 F-Methylpyrene	216	27.49	2221952	0.15
65 Benz(a)anthracene-112	240	29.50	44105255	1.96 *ISTD
66 Benz(a)anthracene	228	29.63	18328826	0.48
67 7-Methylbenz(a)anthracene	242	31.75	3332	0.00
68 Chrysene-d12	240	29.62	69983270	3.93 *ISTD
69 Chrysene	228	29.75	1974237	0.06
70 Benzo(k)fluoranthene-d12	264	33.53	46243000	2.01 *ISTD
71 Benzo(b+j+k)FL	252	33.51	22150838	1.07
72 Cholestane	217	33.98	178927	0.07
73 7-Methylbenzo(a)pyrene	266	37.23	65590	0.00
74 BeP-d12	264	34.56	114810745	4.60 *ISTD
75 BeP	252	34.67	76818255	2.70
76 BaP-d12	264	34.80	139109044	6.95 *ISTD
77 BaP	252	34.91	41681830	1.19
78 Benzo(ghi)Perylene-d12	288	42.00	78869899	1.10 *ISTD
79 Indeno[123-cd]Pyrene	276	40.54	40729076	0.54
80 Benzo(ghi)Perylene	276	42.19	312499148	5.07
81 Dibenz(ah+ac)anthracene	278	40.53	1435726	0.02
82 Benzo(b)chrysene	278	41.18	4095	0.00
83 Coronene-d12	312	54.56	45933393	0.62 *ISTD
84 Coronene	300	54.87	64126741	1.19

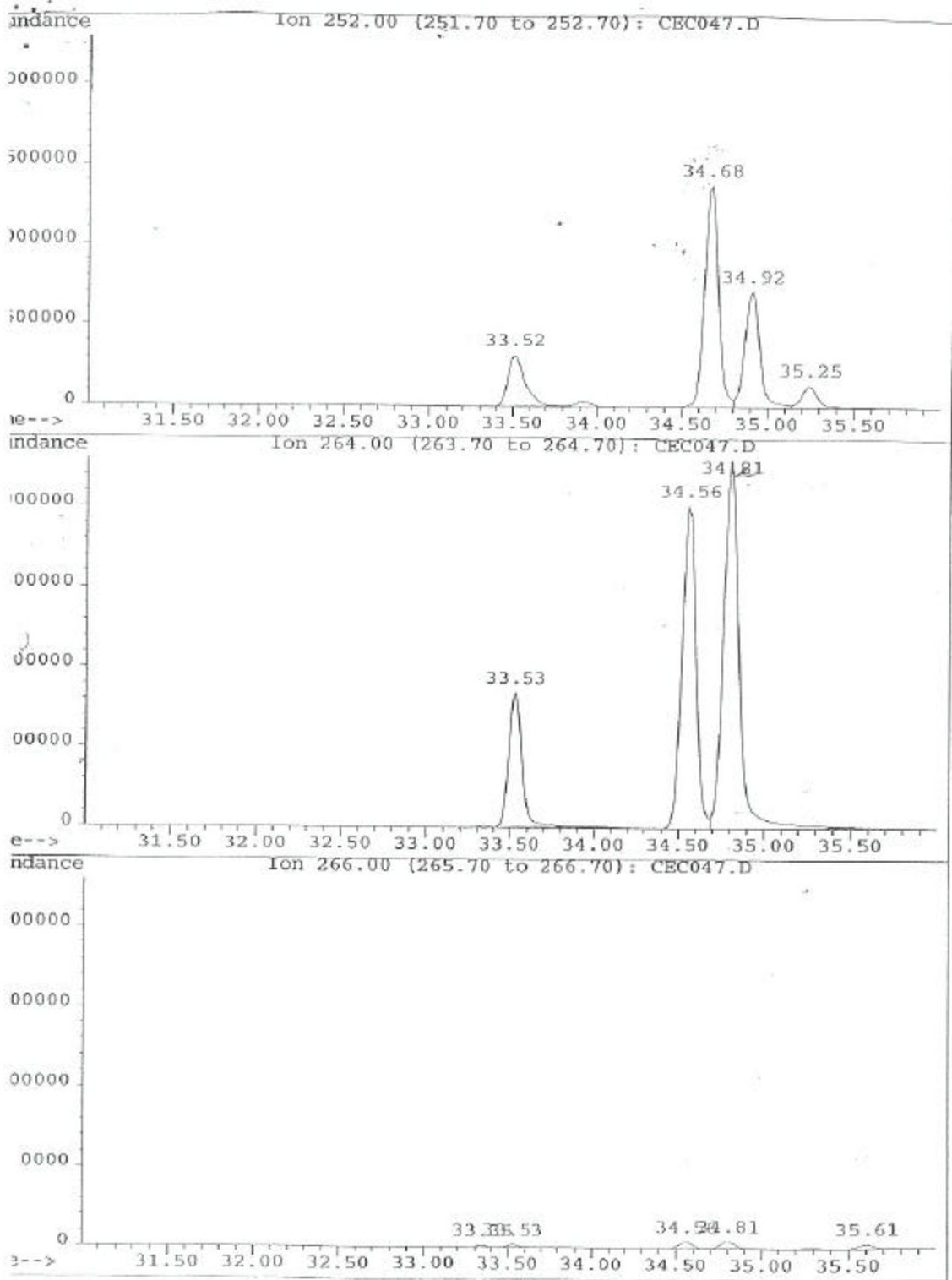


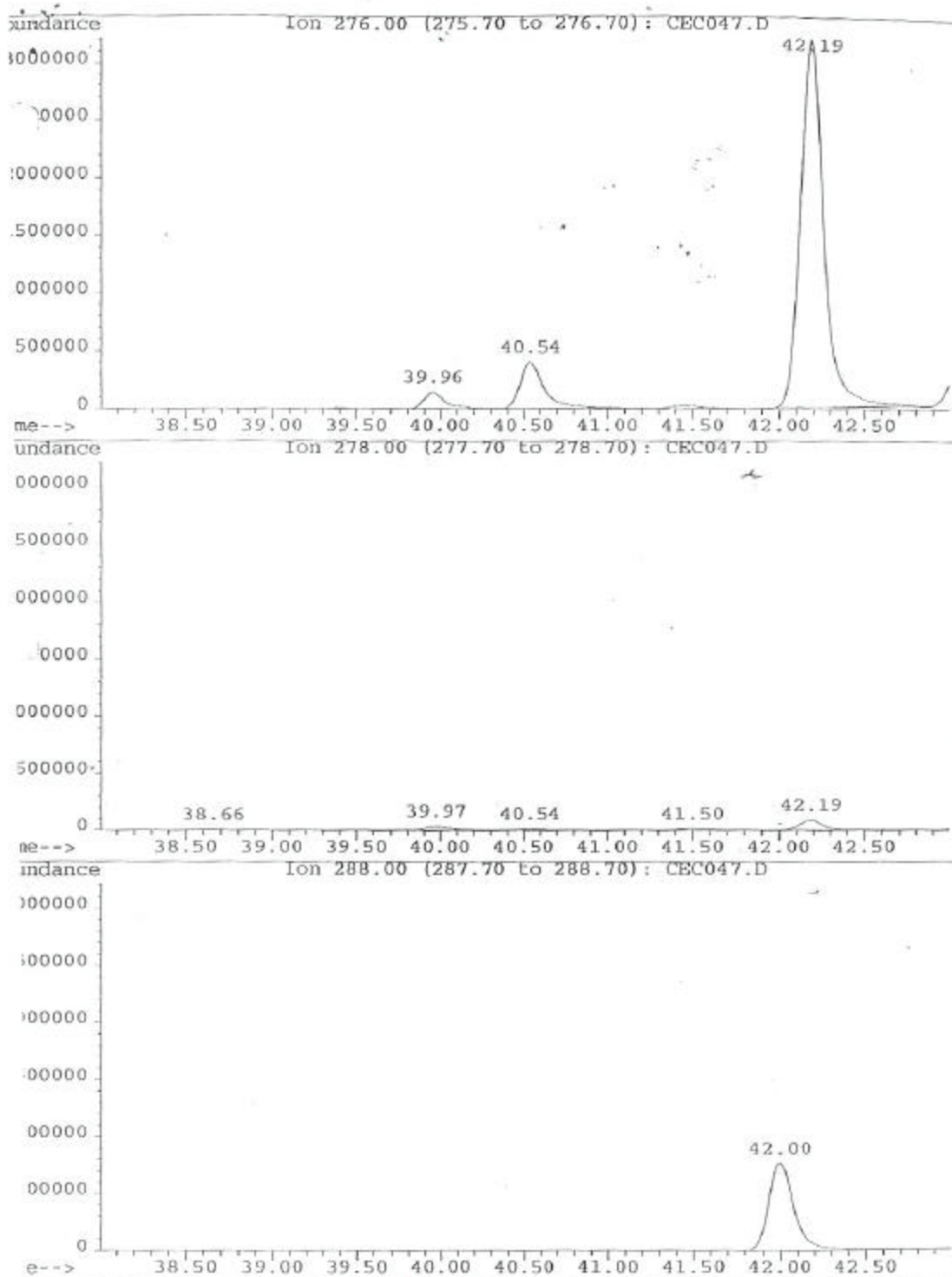


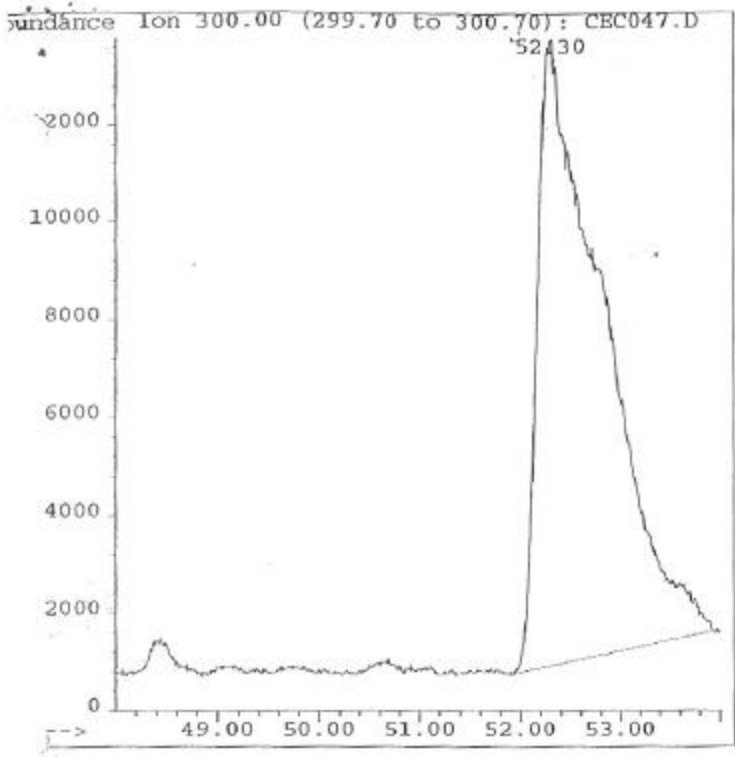












Compounds contained in carbon black provided by
the UC Irvine container

Sample weight = 1.0265g

Sheet1

Data File Name: CEC046.D
Data File Path: D:\CE-CERT
Date Acquired: 07/18/97
Method File: CE-CERT1

Sample Name: carbon, CONT. 6
Misc Info:
Vial Number: 13

UCI
CONTAINER
6

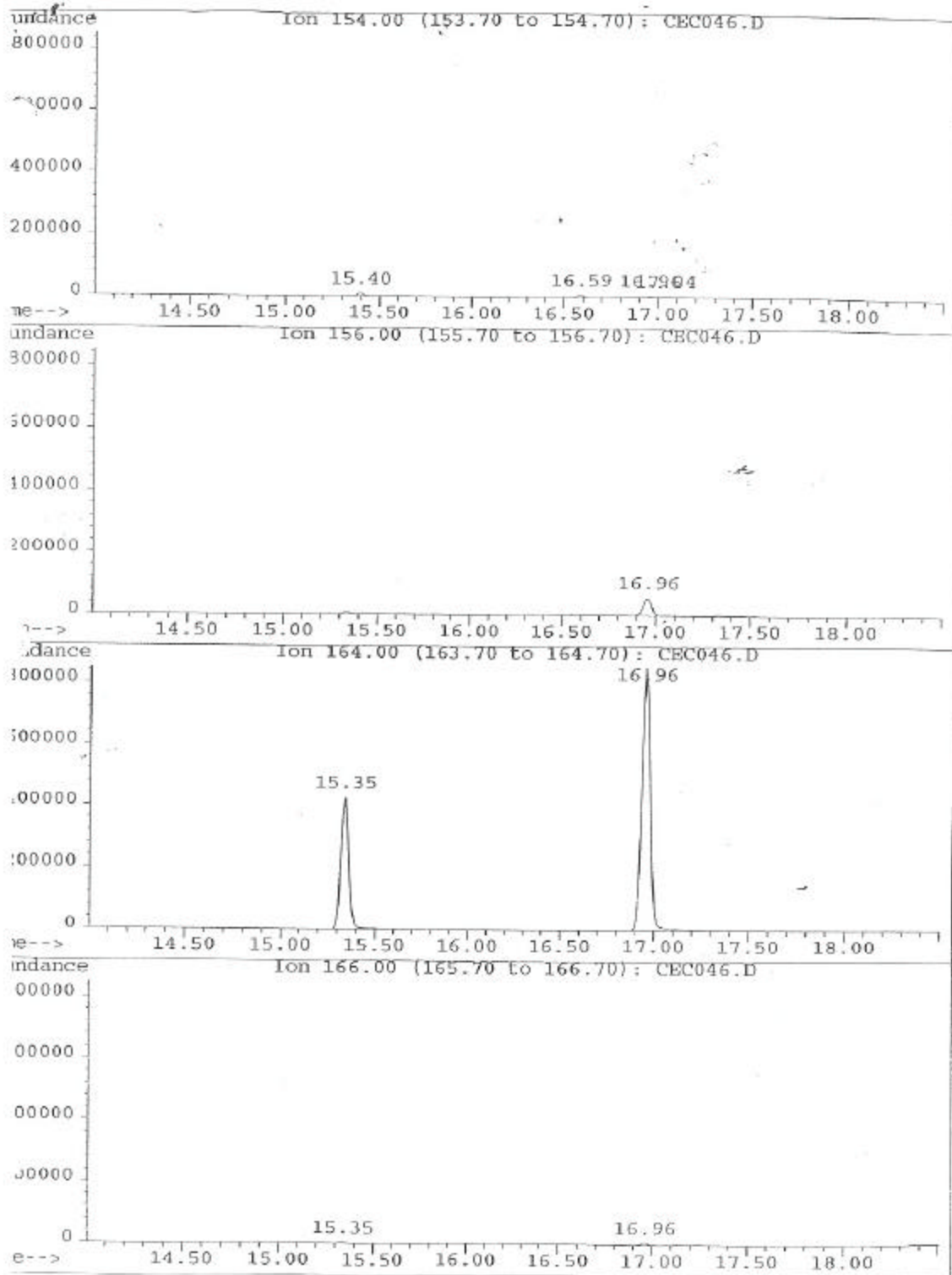
ug/1.0265g

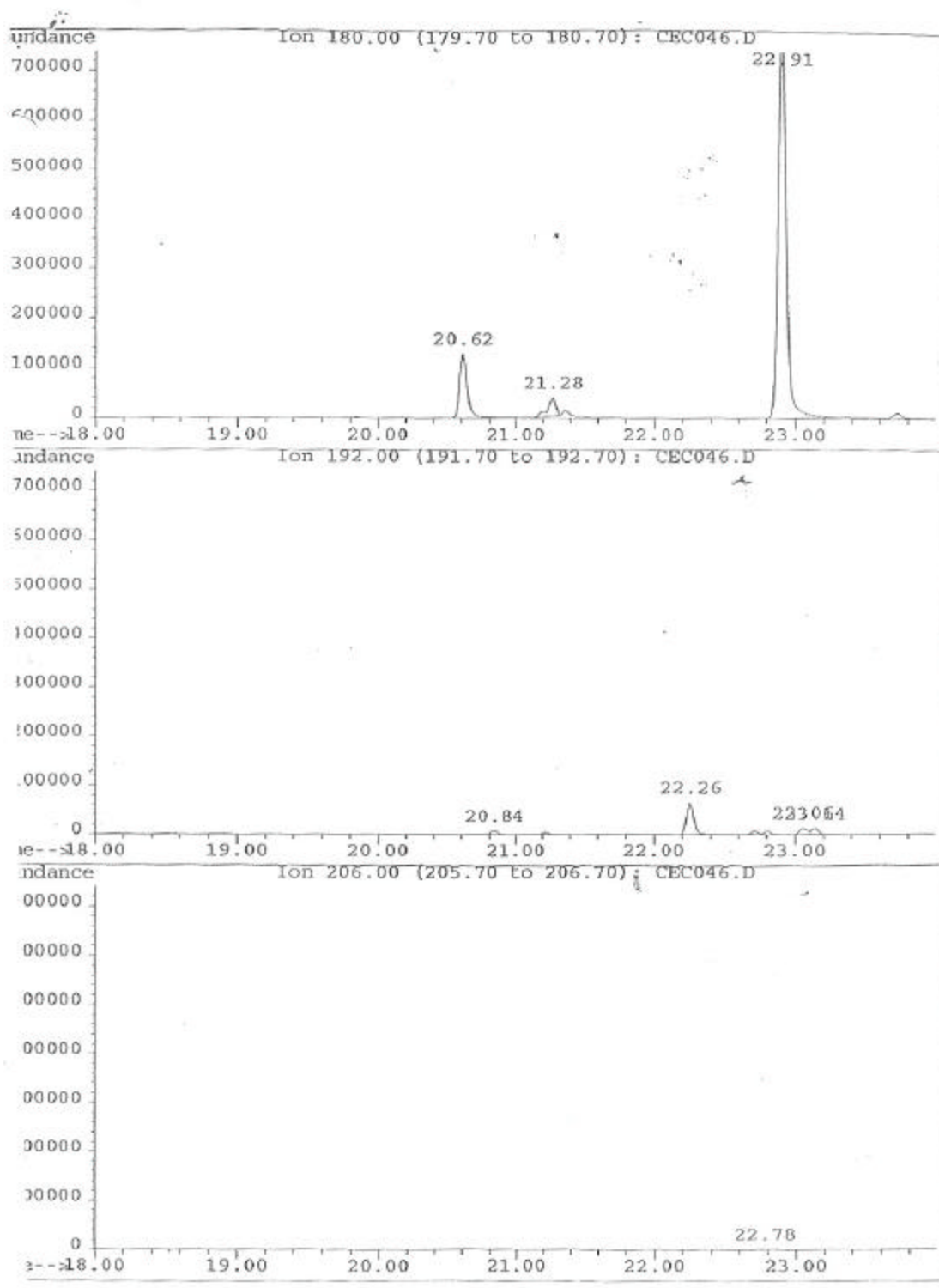
#	Compound	m/z	Ret. Time	Area	Amount	Peak Type
1	Naphthalene-d8	136	12.63	19191708	9.30	*ISTD
2	Naphthalene	128	12.68	12641695	5.20	
3	2-menaphthalene	142	14.28	341657	0.20	
4	1-menaphthalene	142	14.53	414381	0.27	
5	Biphenyl-d10	164	15.35	11913497	6.85	*ISTD = internal standard
6	2,6+2,7-dimenaphthalene	156	15.83	48188	0.03	
7	1,7+1,3+1,6-dimenaphthalene	156	16.02	74640	0.05	
8	2,3+1,4+1,5-dimenaphthalene	156	16.34	23624	0.02	
9	1,2-dimenaphthalene	156	16.56	52667	0.04	
10	1,8-dimenaphthalene	156	16.90	15212	0.01	
11	Biphenyl	154	15.40	208923	0.09	
12	A-Methylbiphenyl	168	0.00	0	0.00	
13	2-Methylbiphenyl	168	15.59	5271	0.00	
14	B-Methylbiphenyl	168	15.59	6777	0.03	
15	3-Methylbiphenyl	168	16.84	31599	0.02	
16	4-Methylbiphenyl	168	17.01	23187	0.02	
17	C-Methylbiphenyl	168	17.01	22565	0.07	
18	A-Trimethylnaphthalene	170	17.20	10824	0.01	
19	1-Ethyl-2-methylnaphthalene	170	17.30	11698	0.01	
20	B-Trimethylnaphthalene	170	17.45	14579	0.02	
21	C-Trimethylnaphthalene	170	17.57	16486	0.02	
22	2-Ethyl-1-methylnaphthalene	170	17.68	245	0.00	
23	E-Trimethylnaphthalene	170	17.77	10498	0.01	
24	F-Trimethylnaphthalene	170	17.85	10199	0.01	
25	G-Trimethylnaphthalene	170	18.03	9077	0.01	
26	H-Trimethylnaphthalene	170	18.29	574	0.00	
27	1,2,8-Trimethylnaphthalene	170	18.77	762	0.00	
28	Acenaphthene-d10	164	16.96	26537437	11.29	*ISTD
29	Acenaphthylene	152	16.59	21066013	4.71	
30	Acenaphthene	154	17.04	72350	0.03	
31	Fluorene	166	18.46	48181	0.02	
32	Phenanthrene-d10	188	21.20	33770442	5.00	*ISTD
33	Phenanthrene	178	21.28	127227445	13.81	
34	A-Methylfluorene	180	19.96	15800	0.00	
35	1-Methylfluorene	180	20.10	7410	0.00	
36	B-Methylfluorene	180	20.25	1550	0.00	
37	C-Methylfluorene	180	20.62	4731032	0.87	
38	A-Methylphenanthrene	192	22.72	177149	0.02	
39	2-Methylphenanthrene	192	22.81	189987	0.02	
40	B-Methylphenanthrene	192	22.96	18559	0.00	
41	C-Methylphenanthrene	192	23.06	439587	0.05	
42	1-Methylphenanthrene	192	23.15	427458	0.05	
43	3,6-Dimethylphenanthrene	206	24.09	18538	0.00	

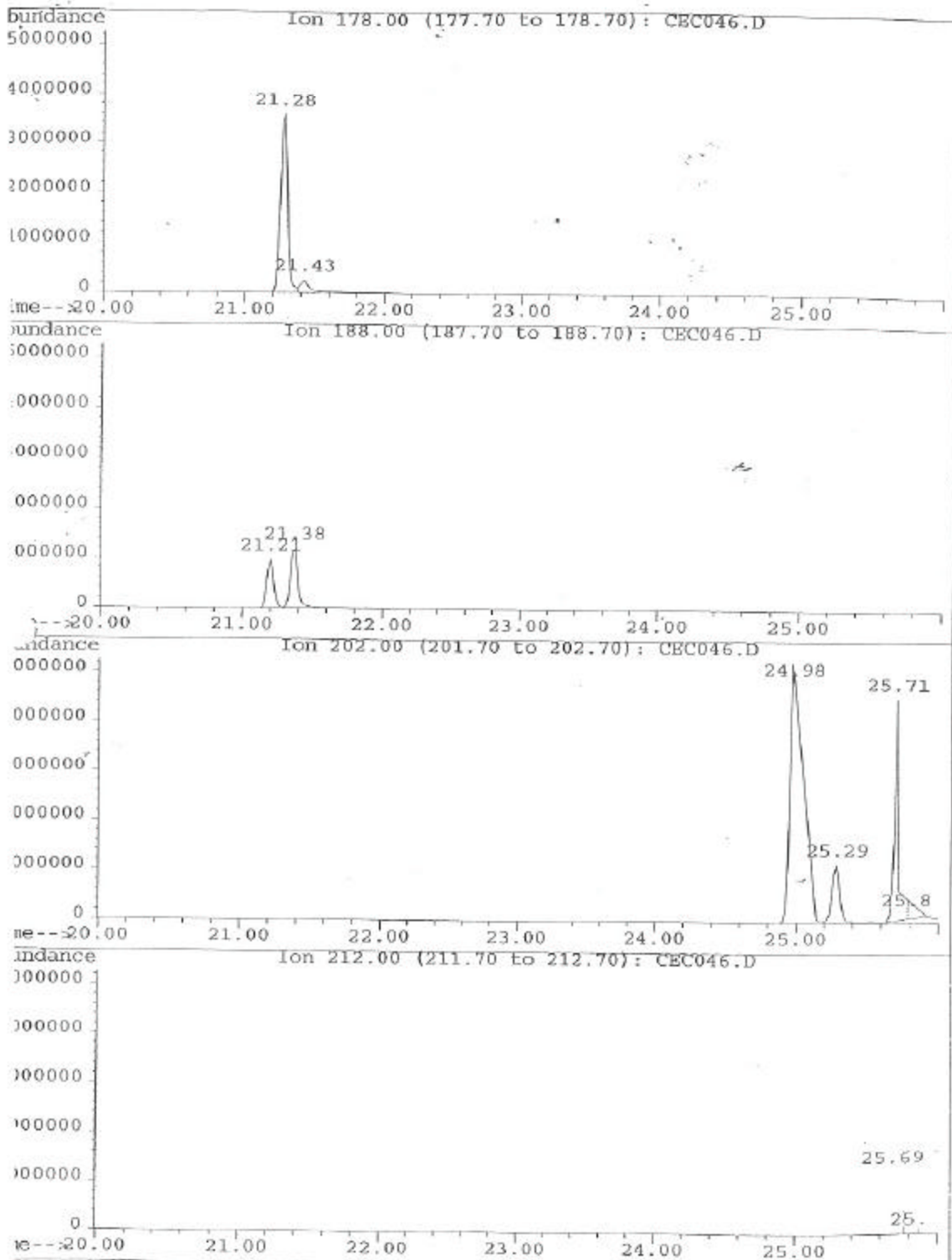


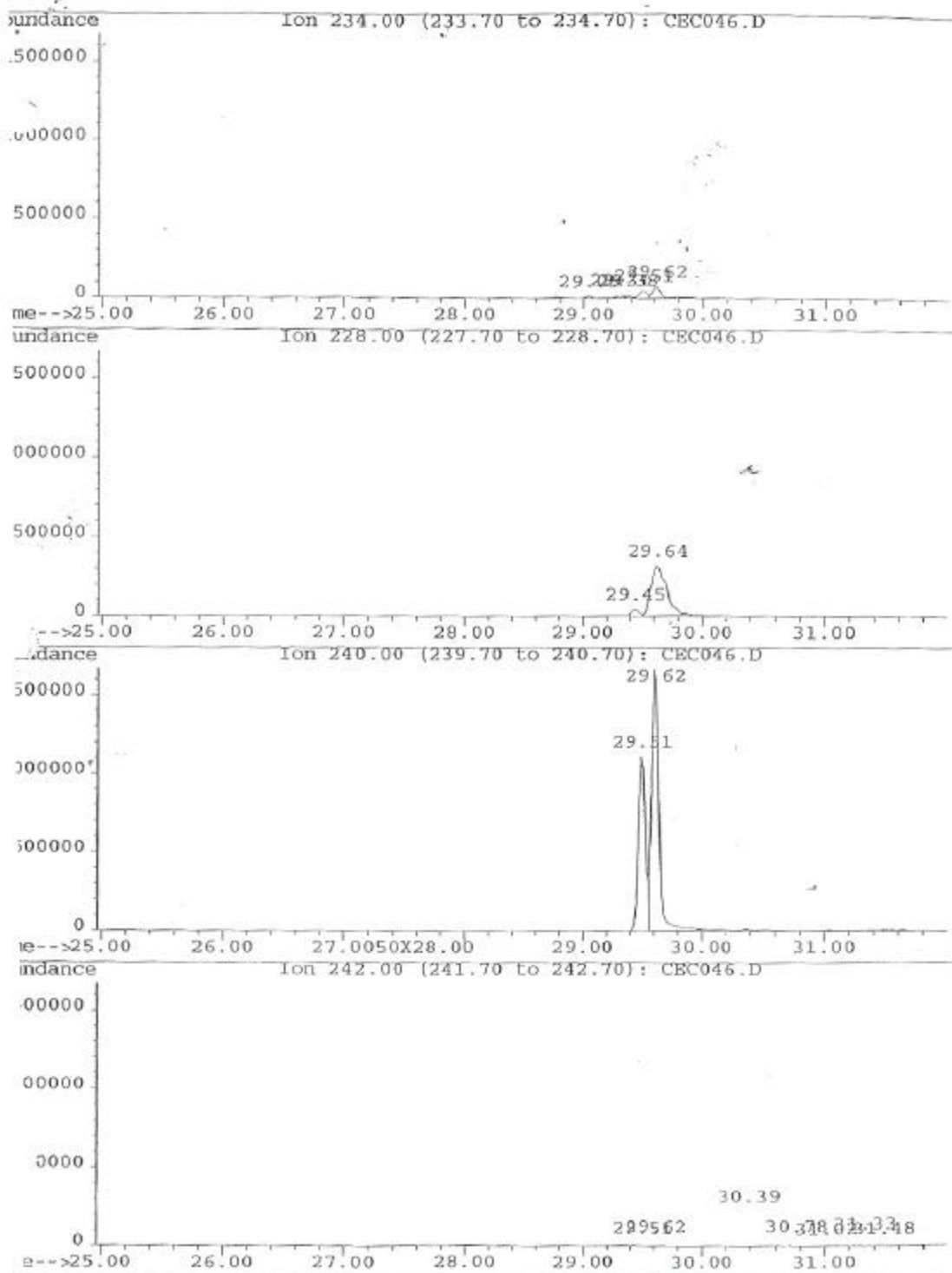
Sheet1

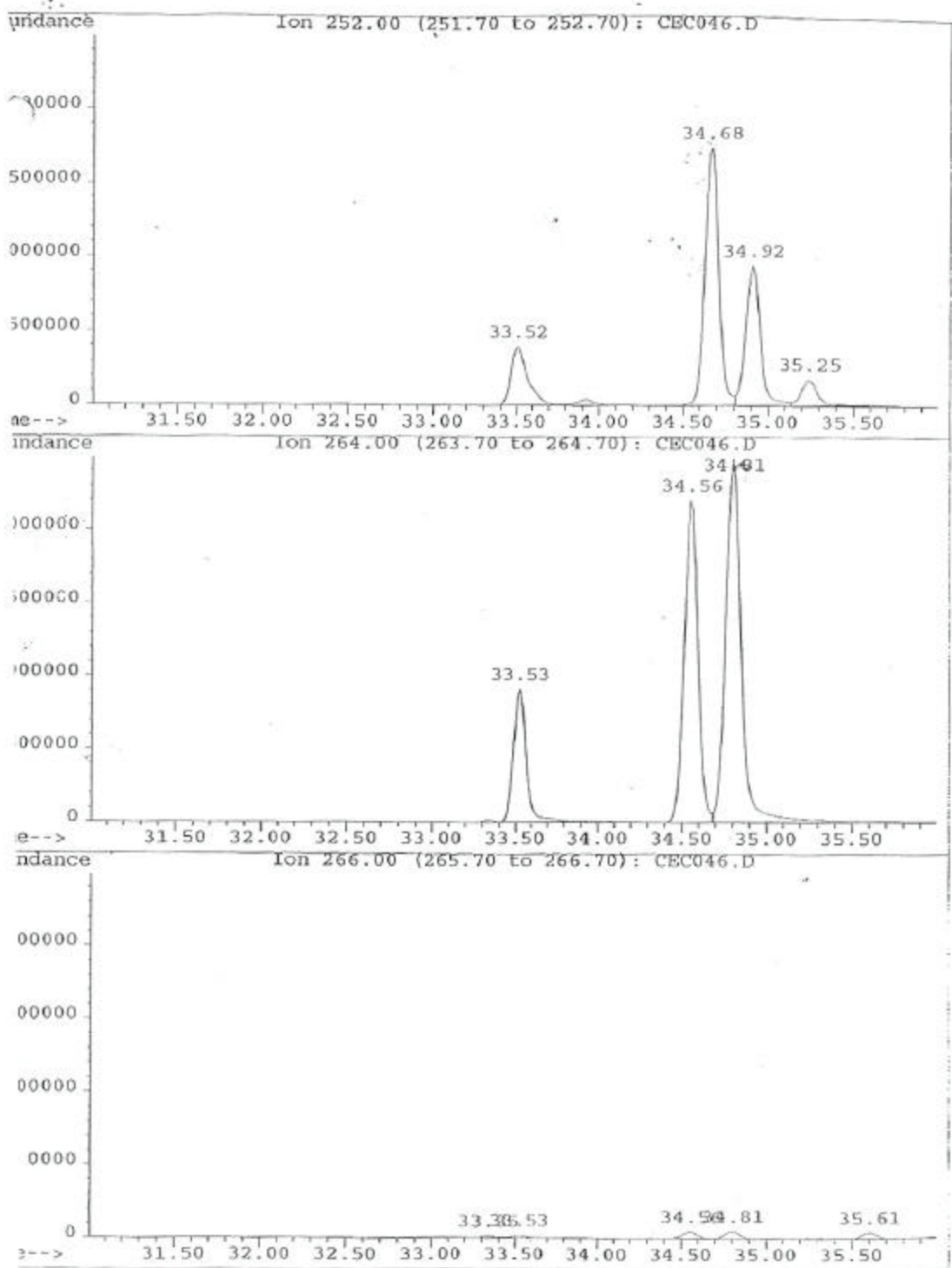
44 A-Dimethylphenanthrene	206	24.18	9843	0.00
45 B-Dimethylphenanthrene	206	24.26	3494	0.00
46 C-Dimethylphenanthrene	206	24.44	9171	0.00
47 1,7-Dimethylphenanthrene	206	24.54	1894	0.00
48 D-Dimethylphenanthrene	206	24.62	2395	0.00
49 E-Dimethylphenanthrene	206	24.74	370402	0.04
50 Anthracene-d10	188	21.38	44456973	6.25 *ISTD
51 Anthracene	178	21.42	9254820	0.94
52 9-Methylanthracene	192	23.60	7914	0.00
53 Pyrene-d12	212	25.68	49498259	5.62 *ISTD
54 Fluoranthene	202	24.98	345137930	34.99 26.45
55 Pyrene	202	25.70	110402797	10.74 10.31
56 Retene	234	26.56	5496	0.00
57 Benzonaphthothiophene	234	28.77	270165	0.02
58 A-Methylpyrene	216	25.45	1207023	0.14
59 B-Methylpyrene	216	26.39	308649	0.03
60 C-Methylpyrene	216	26.68	864326	0.10
61 D-Methylpyrene	216	27.01	38246	0.00
62 E-Methylpyrene	216	27.08	1740533	0.20
63 4-Methylpyrene	216	27.39	5209242	0.59
64 F-Methylpyrene	216	27.49	2237134	0.25
65 Benz(a)anthracene-d12	240	29.50	49394341	1.96 *ISTD
66 Benz(a)anthracene	228	29.63	19270950	0.45
67 7-Methylbenz(a)anthracene	242	31.73	5975	0.00
68 Chrysene-d12	240	29.62	68474726	3.93 *ISTD
69 Chrysene	228	29.75	2047358	0.06
70 Benzo(k)fluoranthene-d12	264	33.53	50471265	2.01 *ISTD
71 Benzo(b+j+k)FL	252	33.51	27814310	1.23
72 Cholestane	217	33.98	210411	0.08
73 7-Methylbenzo(a)pyrene	266	37.22	60740	0.00
74 BeP-d12	264	34.56	123647763	4.60 *ISTD
75 BeP	252	34.67	98152162	3.20
76 BaP-d12	264	34.80	148346584	6.95 *ISTD
77 BaP	252	34.91	53289591	1.42
78 Benzo(ghi)Perylene-d12	288	42.00	80199243	1.10 *ISTD
79 Indeno[123-cd]Pyrene	276	40.54	54284169	0.71
80 Benzo(ghi)Perylene	276	42.19	423253317	6.75
81 Dibenz(ah+ac)anthracene	278	40.53	1468947	0.02
82 Benzo(b)chrysene	278	41.22	2095	0.00
83 Coronene-d12	312	54.57	46003900	0.62 *ISTD
84 Coronene	300	54.83	84913291	1.57

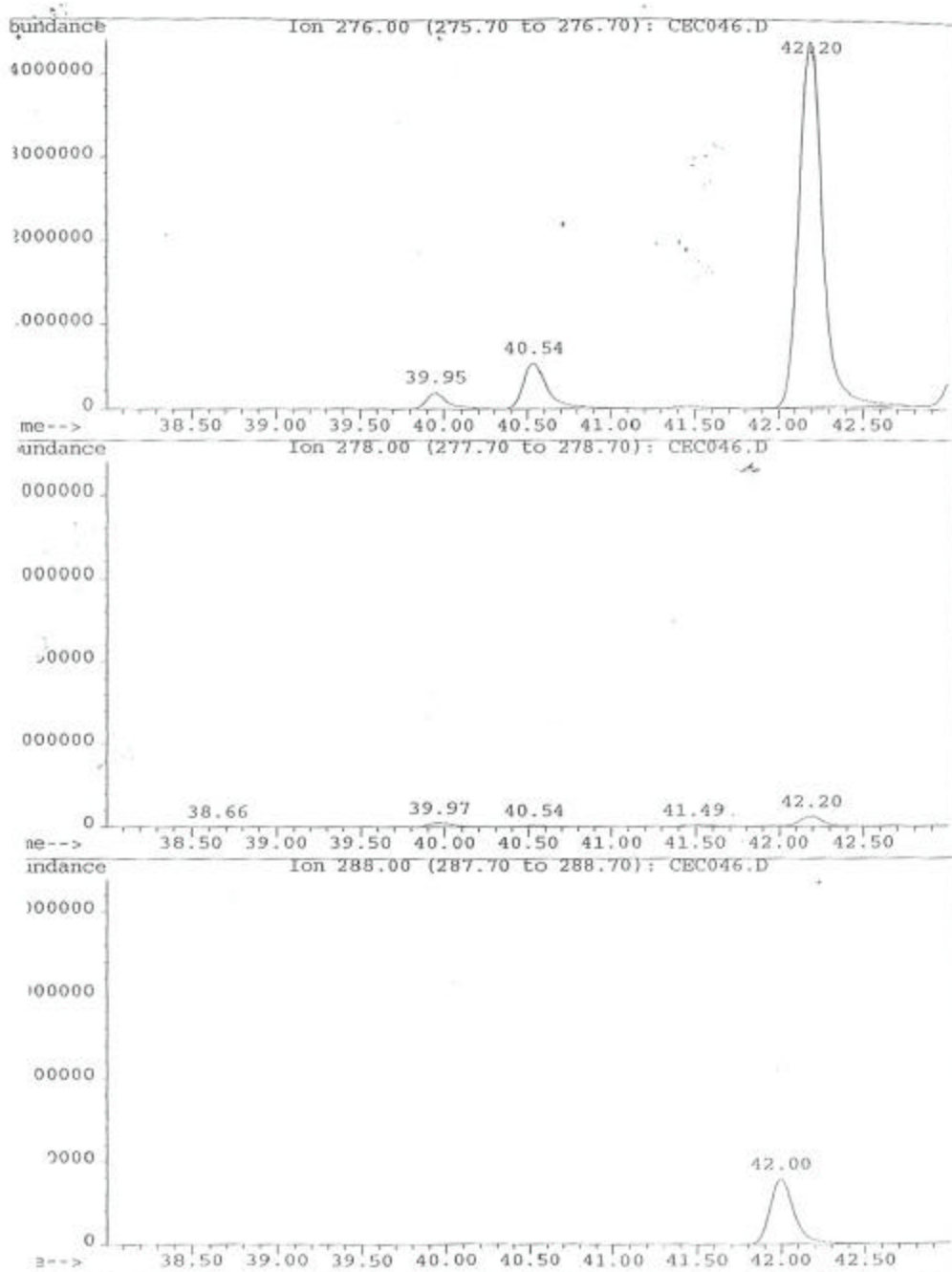


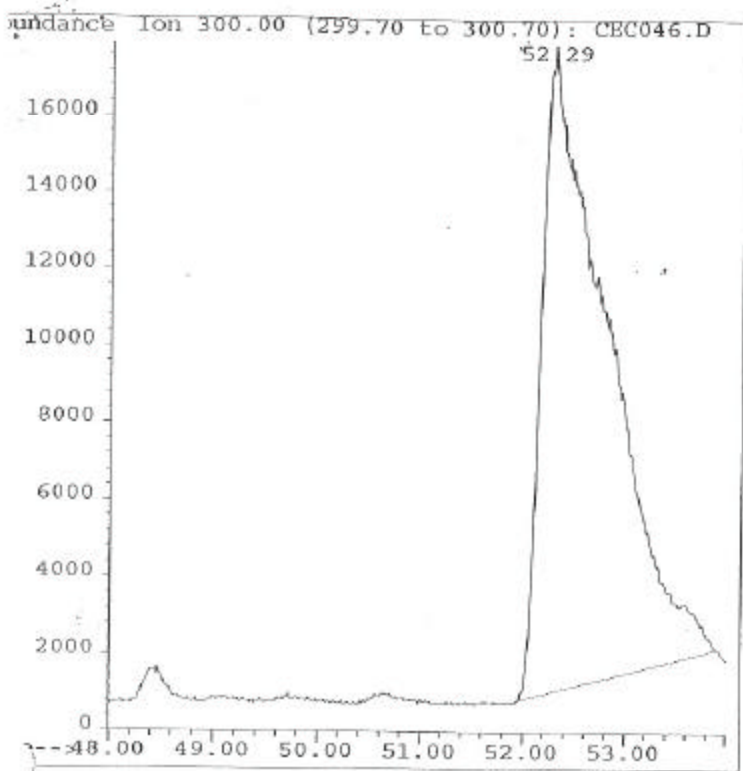












212.00 (211.70 to 212.70): CEC048.D
 carbon, CONT. 6, 20x

CONT. 6 UCI

pk#	Ret Time	Type	Width	Area	Start Time	End Time
	25.723	M	0.172	1421589	25.599	26.378

Pyrene Resp Ratio 1.17

Fluoranthene Resp Ratio 1.15

$$\text{Pyrene} = \frac{31777713}{\cancel{1421589}} \times \frac{5.62}{1.17} = \frac{107.374}{\cancel{1421589}}$$

$$\text{Fluoranthene} = \frac{7707301}{1421589} \times \frac{5.62}{1.15} = \frac{26.455}{\cancel{1421589}}$$



m-202.00 (201.70 to 202.70): CEC048.D
carbon, CONT. 6, 20x

ak#	Ret Time	Type	Width	Area	Start Time	End Time
	25.065	BV	0.189	7707301	24.872	25.650
	25.784	M	0.180	3177713	25.660	26.893

